Australia's National Science Agency

# River model calibration for the Victoria catchment

## A technical report from the CSIRO Victoria River Water Resource Assessment for the National Water Grid

Justin Hughes, Ang Yang, Steve Marvanek, Biao Wang, Matt Gibbs and Cuan Petheram

ISBN 978-1-4863-2089-9 (print)

ISBN 978-1-4863-2090-5 (online)

Citation

Hughes J, Yang A, Marvanek S, Wang B, Gibbs M and Petheram C (2024) River model calibration for the Victoria catchment. A technical report from the CSIRO Victoria River Resource Assessment for the National Water Grid. CSIRO, Australia.





CSIRO Victoria River Water Resource Assessment acknowledgements

This report was funded through the National Water Grid's Science Program, which sits within the Australian Government's Department of Climate Change, Energy, the Environment and Water.

Aspects of the Assessment have been undertaken in conjunction with the NT Government.

The Assessment was guided by two committees:

i. The Assessment's Governance Committee: CRC for Northern Australia/James Cook University; CSIRO; National Water Grid (Department of Climate Change, Energy, the Environment and Water); Northern Land Council; NT Department of Environment, Parks and Water Security; NT Department of Industry, Tourism and Trade; Office of Northern Australia; Queensland Department of Agriculture and Fisheries; Queensland Department of Regional Development, Manufacturing and Water

ii. The Assessment's joint Roper and Victoria River catchments Steering Committee: Amateur Fishermen's Association of the NT; Austrade; Centrefarm; CSIRO; National Water Grid (Department of Climate Change, Energy, the Environment and Water); Northern Land Council; NT Cattlemen's Association; NT Department of Environment, Parks and Water Security; NT Department of Industry, Tourism and Trade; NT Farmers; NT Seafood Council; Office of Northern Australia; Parks Australia; Regional Development Australia; Roper Gulf Regional Council Shire; Watertrust

Responsibility for the Assessment's content lies with CSIRO. The Assessment's committees did not have an opportunity to review the Assessment results or outputs prior to their release.

This report was reviewed by Assoc. Professor Barry Croke, Integrated Catchment Assessment and Management Centre (iCAM) and Institute for Water Futures, The Fenner School of Environment and Society and Mathematical Sciences Institute, ANU College of Science

The authors acknowledge useful conversations and data provided by staff members Simon Cruickshank and Peter Waugh from the Department of Environment, Parks and Water Security, to understand streamflow gauging station history and data quality.

Acknowledgement of Country

CSIRO acknowledges the Traditional Owners of the lands, seas and waters, of the area that we live and work on across Australia. We acknowledge their continuing connection to their culture and pay our respects to their elders past and present.

Photo

Jasper Creek. Source: CSIRO

# Director's foreword

Sustainable development and regional economic prosperity are priorities for the Australian and Northern Territory (NT) governments. However, more comprehensive information on land and water resources across northern Australia is required to complement local information held by Indigenous Peoples and other landholders.

Knowledge of the scale, nature, location and distribution of likely environmental, social, cultural and economic opportunities and the risks of any proposed developments is critical to sustainable development. Especially where resource use is contested, this knowledge informs the consultation and planning that underpin the resource security required to unlock investment, while at the same time protecting the environment and cultural values.

In 2021, the Australian Government commissioned CSIRO to complete the Victoria River Water Resource Assessment. In response, CSIRO accessed expertise and collaborations from across Australia to generate data and provide insight to support consideration of the use of land and water resources in the Victoria catchment. The Assessment focuses mainly on the potential for agricultural development, and the opportunities and constraints that development could experience. It also considers climate change impacts and a range of future development pathways without being prescriptive of what they might be. The detailed information provided on land and water resources, their potential uses and the consequences of those uses are carefully designed to be relevant to a wide range of regional-scale planning considerations by Indigenous Peoples, landholders, citizens, investors, local government, and the Australian and NT governments. By fostering shared understanding of the opportunities and the risks among this wide array of stakeholders and decision makers, better informed conversations about future options will be possible.

Importantly, the Assessment does not recommend one development over another, nor assume any particular development pathway, nor even assume that water resource development will occur. It provides a range of possibilities and the information required to interpret them (including risks that may attend any opportunities), consistent with regional values and aspirations.

All data and reports produced by the Assessment will be publicly available.

C. Chilcott

Chris Chilcott

Project Director

# The Victoria River Water Resource Assessment Team

| | |
|---|---|
| Project Director | Chris Chilcott |
| Project Leaders | Cuan Petheram, Ian Watson |
| Project Support | Caroline Bruce, Seonaid Philip |
| Communications | Emily Brown, Chanel Koeleman, Jo Ashley, Nathan Dyer |

**Activities**

| | |
|---|---|
| Agriculture and socio-economics | Tony Webster, Caroline Bruce, Kaylene Camuti[1], Matt Curnock, Jenny Hayward, Simon Irvin, Shokhrukh Jalilov, Diane Jarvis[1], Adam Liedloff, Stephen McFallan, Yvette Oliver, Di Prestwidge[2], Tiemen Rhebergen, Robert Speed[3], Chris Stokes, Thomas Vanderbyl[3], John Virtue[4] |
| Climate | David McJannet, Lynn Seo |
| Ecology | Danial Stratford, Rik Buckworth, Pascal Castellazzi, Bayley Costin, Roy Aijun Deng, Ruan Gannon, Steve Gao, Sophie Gilbey, Rob Kenyon, Shelly Lachish, Simon Linke, Heather McGinness, Linda Merrin, Katie Motson[5], Rocio Ponce Reyes, Nathan Waltham[5] |
| Groundwater hydrology | Andrew R. Taylor, Karen Barry, Russell Crosbie, Geoff Hodgson, Anthony Knapton[6], Shane Mule, Jodie Pritchard, Steven Tickell[7], Axel Suckow |
| Indigenous water values, rights, interests and development goals | Marcus Barber/Kirsty Wissing, Peta Braedon, Kristina Fisher, Petina Pert |
| Land suitability | Ian Watson, Jenet Austin, Bart Edmeades[7], Linda Gregory, Jason Hill[7], Seonaid Philip, Ross Searle, Uta Stockmann, Mark Thomas, Francis Wait[7], Peter L. Wilson, Peter R. Wilson, Peter Zund |
| Surface water hydrology | Justin Hughes, Matt Gibbs, Fazlul Karim, Steve Marvanek, Catherine Ticehurst, Biao Wang |
| Surface water storage | Cuan Petheram, Giulio Altamura[8], Fred Baynes[9], Kev Devlin[4], Nick Hombsch[8], Peter Hyde[8], Lee Rogers, Ang Yang |

Note: Assessment team as at September, 2024. All contributors are affiliated with CSIRO unless indicated otherwise. Activity Leaders are underlined. For the Indigenous water values, rights, interests and development goals activity, Marcus Barber was Activity Leader for the project duration except August 2022 – July 2023 when Kirsty Wissing (a CSIRO employee at the time) undertook this role.

[1]James Cook University; [2]DBP Consulting; [3]Badu Advisory Pty Ltd; [4]Independent contractor; [5] Centre for Tropical Water and Aquatic Ecosystem Research. James Cook University; [6]CloudGMS; [7]NT Department of Environment, Parks and Water Security; [8]Rider Levett Bucknall; [9]Baynes Geologic

# Shortened forms

| SHORT FORM | FULL FORM |
|---|---|
| **AWRA-L** | Australian Water Resources Assessment – Land |
| **AWRA-R** | Australian Water Resources Assessment – River (a river model) |
| **AWRC** | Australian Water Resources Council |
| **DEPaWS** | Department of Environment, Parks and Water Security (NT) |
| **DS** | downstream |
| **EPD** | error probability difference |
| **ET** | evapotranspiration |
| **ETo** | Morton's wet area potential ET |
| **FAO56** | Food and Agriculture Organization – Irrigation paper 56 |
| **FGARA** | Flinders and Gilbert Agricultural Resource Assessment |
| **GR4J** | modèle du Génie Rural à 4 paramètres Journalier (RR model) |
| **GR7J** | RR model related to GR4J |
| **GR7JFM** | RR model – an adaption of GR7J for drier climates |
| **HRU** | hydrological response unit |
| **IAHS** | International Association of Hydrological Sciences |
| **IQQM** | Integrated Quantity and Quality model |
| **MCMC** | Markov chain Monte Carlo |
| **Mwet** | Morton's wet area potential ET |
| **NASY** | Northern Australia Sustainable Yields |
| **NAWRA** | Northern Australia Water Resource Assessment |
| **netCDF** | Network Common Data Form (a file format for storing multidimensional data) |
| **NN** | nearest neighbour |
| **NSE** | Nash–Sutcliff Efficiency |
| **NT** | Northern Territory |
| **P** | precipitation |
| **Q** | runoff |
| **RR** | rainfall-runoff |
| **RORB** | (a runoff and routing software package) |
| **SILO** | Scientific Information for Land Owners (climate data product) |
| **TOPOG** | (a physically and terrain-based hydrological modelling package) |
| **VRD** | Victoria River Downs |
| **WAVES** | Water And Vegetation Energy Solute – an energy balance model |

# Units

| UNIT | DESCRIPTION |
| --- | --- |
| **DOI** | Digital Object Identifier |
| **GL** | gigalitre |
| **ha** | hectare |
| **km** | kilometre |
| **L** | litre |
| **m** | metre |
| **mAHD** | metres above Australian Height Datum |
| **ML** | megalitre |
| **mm** | millimetre |
| **y** | year |

# Preface

Sustainable development and regional economic prosperity are priorities for the Australian and NT governments and science can play its role. Acknowledging the need for continued research, the NT Government (2023) announced a Territory Water Plan priority action to accelerate the existing water science program 'to support best practice water resource management and sustainable development.'

Governments are actively seeking to diversify regional economies, considering a range of factors. For very remote areas like the Victoria catchment (Preface Figure 1-1), the land, water and other environmental resources or assets will be key in determining how sustainable regional development might occur. Primary questions in any consideration of sustainable regional development relate to the nature and the scale of opportunities, and their risks.

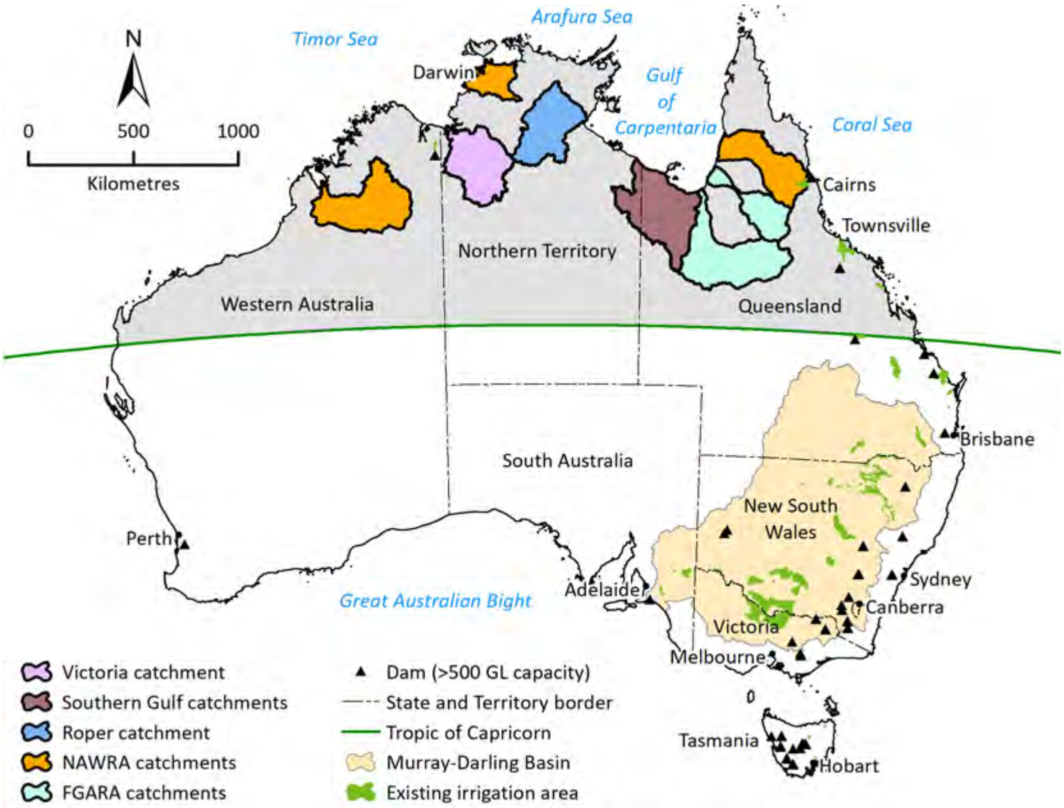


**Preface Figure 1-1 Map of Australia showing Assessment area (Victoria catchment and other recent CSIRO Assessments**

FGARA = Flinders and Gilbert Agricultural Resource Assessment; NAWRA = Northern Australia Water Resource Assessment.

How people perceive those risks is critical, especially in the context of areas such as the Victoria catchment, where approximately 75% of the population is Indigenous (compared to 3.2% for Australia as a whole) and where many Indigenous Peoples still live on the same lands they have inhabited for tens of thousands of years. About 31% of the Victoria catchment is owned by Indigenous Peoples as inalienable freehold.

Access to reliable information about resources enables informed discussion and good decision making. Such information includes the amount and type of a resource or asset, where it is found (including in relation to complementary resources), what commercial uses it might have, how the resource changes within a year and across years, the underlying socio-economic context and the possible impacts of development.

Most of northern Australia's land and water resources have not been mapped in sufficient detail to provide the level of information required for reliable resource allocation, to mitigate investment or environmental risks, or to build policy settings that can support good judgments. The Victoria River Water Resource Assessment aims to partly address this gap by providing data to better inform decisions on private investment and government expenditure, to account for intersections between existing and potential resource users, and to ensure that net development benefits are maximised.

The Assessment differs somewhat from many resource assessments in that it considers a wide range of resources or assets, rather than being a single mapping exercise of, say, soils. It provides a lot of contextual information about the socio-economic profile of the catchment, and the economic possibilities and environmental impacts of development. Further, it considers many of the different resource and asset types in an integrated way, rather than separately. The Assessment has agricultural developments as its primary focus, but it also considers opportunities for and intersections between other types of water-dependent development.

The Assessment was designed to inform consideration of development, not to enable any particular development to occur. The outcome of no change in land use or water resource development is also valid. As such, the Assessment informs – but does not seek to replace – existing planning, regulatory or approval processes. Importantly, the Assessment does not assume a given policy or regulatory environment. Policy and regulations can change, so this flexibility enables the results to be applied to the widest range of uses for the longest possible time frame.

It was not the intention of – and nor was it possible for – the Assessment to generate new information on all topics related to water and irrigation development in northern Australia. Topics not directly examined in the Assessment are discussed with reference to and in the context of the existing literature.

CSIRO has strong organisational commitments to reconciliation with Australia's Indigenous Peoples and to conducting ethical research with the free, prior and informed consent of human participants. The Assessment consulted with Indigenous representative organisations and Traditional Owner groups from the catchment to aid their understanding and potential engagement with its fieldwork requirements. The Assessment conducted significant fieldwork in the catchment, including with Traditional Owners through the activity focused on Indigenous values, rights, interests and development goals. CSIRO created new scientific knowledge about the catchment through direct fieldwork, by synthesising new material from existing information, and by remotely sensed data and numerical modelling.

Functionally, the Assessment adopted an activities-based approach (reflected in the content and structure of the outputs and products), comprising activity groups, each contributing its part to create a cohesive picture of regional development opportunities, costs and benefits, but also risks. Preface Figure 1-2 illustrates the high-level links between the activities and the general flow of information in the Assessment.

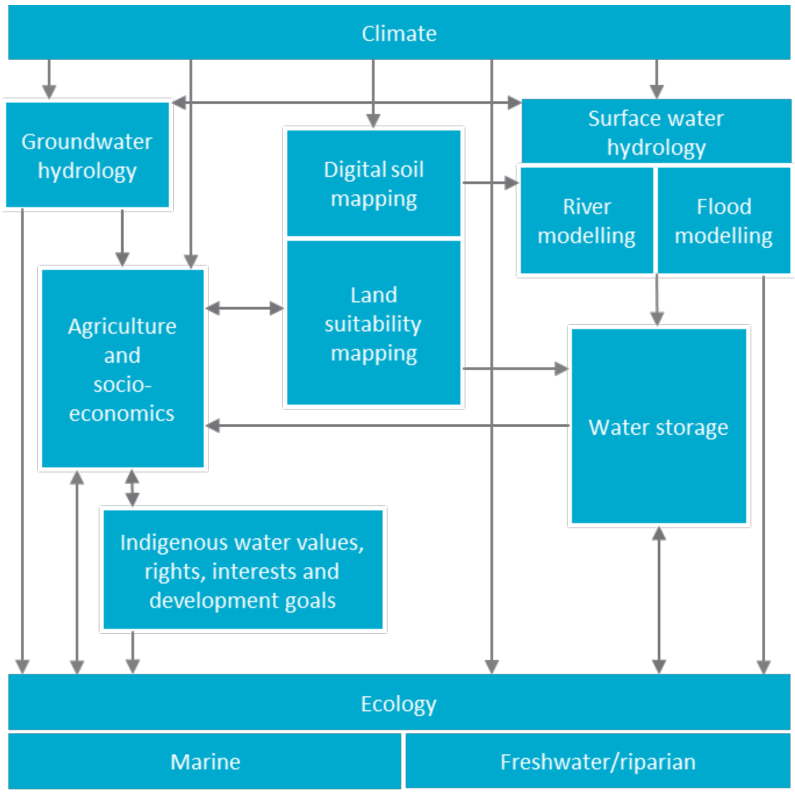


**Preface Figure 1-2 Schematic of the high-level linkages between the eight activity groups and the general flow of information in the Assessment**

*Assessment reporting structure*

Development opportunities and their impacts are frequently highly interdependent and, consequently, so is the research undertaken through this Assessment. While each report may be read as a stand-alone document, the suite of reports for each Assessment most reliably informs discussion and decisions concerning regional development when read as a whole.

The Assessment has produced a series of cascading reports and information products:

- Technical reports present scientific work with sufficient detail for technical and scientific experts to reproduce the work. Each of the activities (Preface Figure 1-2) has one or more corresponding technical reports.
- A catchment report, which synthesises key material from the technical reports, providing well-informed (but not necessarily scientifically trained) users with the information required to inform decisions about the opportunities, costs and benefits, but also risks associated with irrigated agriculture and other development options.
- A summary report provides a shorter summary and narrative for a general public audience in plain English.
- A summary fact sheet provides key findings for a general public audience in the shortest possible format.

The Assessment has also developed online information products to enable users to better access information that is not readily available in print format. All of these reports, information tools and data products are available online at https://www.csiro.au/victoriariver. The webpages give users access to a communications suite including fact sheets, multimedia content, FAQs, reports and links to related sites, particularly about other research in northern Australia.

# Executive summary

At present, surface water allocations within the catchment of the Victoria River are low (0.7 GL) when compared to the median annual streamflow (<0.1%). The development of the surface water resources of this highly seasonal catchment to enable regional economic development, as has occurred in the south of Australia, would in many instances require rivers to be regulated and water stored/diverted. However, an understanding of the size and nature of surface water resources and risks that may attend any development needs to precede any development. This report presents information regarding the construction and calibration of the Victoria River model.

No river model development has been previously undertaken in the Victoria catchment. Hydrological prediction is difficult in northern Australia, and in this instance a lack of data, particularly, but not limited to streamflow observations, contributed to the challenges of model construction and calibration. The lack of data, including a poor spatial coverage of suitable streamflow data, particularly during the dry season, increased model uncertainty and new calibration techniques were used to provide some constraint on model parameters and outputs.

The construction and calibration of the Victoria River model built upon previous model calibration methods used for the Northern Australia Water Resource Assessment and the Roper River Water Resource Assessment. This Assessment used similar techniques as the previous studies, but also included constraints on runoff using a generalised relationship of runoff with climate and regolith depth based on observations from gauged catchments from across northern Australia.

A total of 17 stream gauge sites/stations, have operated or are still operating within the catchment at the time of writing. Of these, nine stream gauges were used within the catchment for calibration. Calibration used a “shingle” approach, which effectively split the catchment into three sections. All parameters within each shingle were calibrated simultaneously for optimal use of limited observational data, and to reduce the chance of over-fitting. Such an approach has advantages when assigning parameter values to ungauged subcatchments. The shingle approach weights long duration, higher flow observations more highly, although their user can modify weightings if needed.

Quality of local streamflow observations were considered generally poor, necessitating a new calibration approach that utilised a further 99, high-quality, long duration, stream gauge datasets from across northern Australia. Mean duration for these sites was 55 years, with mean missing daily observations being less than 5 %. From these data, an empirical relationship predicting runoff coefficient from climate data (specifically mean catchment aridity) and mean catchment regolith depth was derived. These data were used within the calibration algorithm to further constrain streamflow estimates for more robust prediction. Furthermore, two alternate climate inputs with decreased and increased rainfall were used within calibration with the empirical runoff coefficient relationship to constrain model performance in drier and wetter climates. These measures ensured that, for mean streamflow at the least, predictions were in accordance with historical streamflow observations from across northern Australia.

Model goodness of fit was generally good, with, for example, Nash–Sutcliffe Efficiencies ranging from 0.4 to 0.88. The goodness of fit was best at long duration/high-flow sites such as gauges 8110007, 8110113 and 8110006, and parameters based on these sites were used for the majority of ungauged subcatchments. Of the 41 model subcatchments, 32 were ungauged locations. Simulated subcatchment mean runoff coefficient was a close fit to those predicted from the northern Australia empirical relationship for historical, dry and wet climate inputs. This ensures more robust historical prediction, but more notably, future climate estimates of streamflow are more reliable than traditional calibration approaches and constitutes a new innovation in river model calibration.

The mean annual end-of-system flow for the Victoria River at node 81100000 for the reporting period (1890–2021) was estimated to be 6994 GL, while the median annual flow was 5734 GL. Predictive uncertainty was estimated using 1291 other feasible parameter sets identified during the calibration process. Uncertainty analyses suggest a standard deviation of 10% for mean annual streamflow values. Additionally, water harvest yield was tested at a single node as a part of the uncertainty analyses, where standard deviation was 20% of mean annual diversion. This indicates that care should be taken when using diversion estimates. However, it should also be noted that various other sources of uncertainty, such as rainfall and streamflow observation uncertainty or parameter transfer protocol, was not or could not be estimated.

# Contents

# Figures

# Tables

# Part I Main report

# 1 Introduction

The regulation of surface water resources in southern Australia meets about 70% of Australia's 25,000 GL mean annual water use (CSIRO, 2011). With the overallocation of water in southern states, the millennium drought and projections of a drier future climate in southern Australia, there is interest in developing the water resources of northern Australia. However, the extraction of water from rivers, particularly for high water-using industries such as irrigation, can result in large perturbations to streamflow, which can affect existing industries and users and result in ecological change.

To quantify the water resources of a catchment and examine the trade-offs associated with water regulation and extraction, a variety of event-based and continuous hydrological modelling frameworks exist. However, different hydrological modelling frameworks have been developed for different purposes and they have different data requirements and different levels of complexity.

At their simplest, hydrological models can be simple statistical relationships, typically with few input data requirements, but can also have a low predictive capacity. At the more complex end are fully distributed physically based models, for which every parameter has physical meaning and can be assigned by measurement. These include soil–vegetation–atmosphere transfer models such as WAVES (Zhang and Dawes, 1988) and TOPOG (O'Loughlin, 1986) and some landscape models. These models can simulate a wide variety of processes and are useful for exploring scenarios that have not been previously observed in the historical record. However, a key challenge in using physically based models is that they have large data requirements, without which many parameters potentially need to be calibrated, which makes them difficult to apply with confidence, particularly across large areas. In between these two extremes are a wide variety of models of intermediate complexity, including those described in this report:

- lumped conceptual rainfall-runoff (RR) models (e.g. Sacramento, GR4J, RORB), which are particularly adept at modelling runoff
- river system models (e.g. Source, IQQM, AWRA-R), a genre of hydrological model well suited to modelling regulated systems and exploring trade-offs in water use, operation and management rules.

In selecting an appropriate model or suite of models, it is important to understand the modelling objectives and select a model that is commensurate with the level of data available and then to be cognisant of its predictive capacity and model limitations.

## 1.1 Surface water activity objectives

The Victoria River Water Resource Assessment surface water activity seeks to address the following questions:

- How do runoff and key water balance terms vary spatially and temporally across the Assessment area?
- How much water is in the river at different locations and times under current and future climates?
- How much water can be extracted in different reaches and with what degree of reliability, and what is the timing of potential extractions?

- How may water regulation and extraction perturb downstream flow?

This report describes the development of models to assess these items. Simulation based on historical data with historical levels of development are denoted “Scenario A”.

## 1.2 Previous surface water modelling studies in the Victoria catchment

In 1976 the Australian Water Resources Council (AWRC) oversaw an assessment of Australia’s water resources. In that study, each jurisdiction across Australia provided estimates of mean annual flow and the percentage of mean annual flow that could be diverted in each AWRC river basin in Australia. No other information was provided, and the methods used to make these estimates varied from one jurisdiction to another and were not documented.

Thirty years after the AWRC continental assessment of Australia’s water resources the Australian Government commissioned CSIRO to undertake the Northern Australia Sustainable Yields (NASY) project, which was the first hydrological modelling study to examine the water resources of northern Australia (Timor Sea, Gulf of Carpentaria and northern north-east coast drainage divisions), including the assessments of the three study areas, using a consistent set of methods and models (CSIRO, 2009a,b). As part of the NASY project, lumped conceptual RR models were calibrated to streamflow data from 125 gauged catchments in northern Australia and then model parameters were transposed to another 500 ungauged catchments using the nearest neighbour (NN) regionalisation method, extensively informed by expert knowledge (Petheram et al., 2009). The lumped conceptual RR models were calibrated to available observed data up to 31 August 2007. Due to time constraints, no new river system models were developed as part of NASY and at the time of the project only four river system models (IQQM models) existed in the northern-draining drainage divisions. Within the Victoria catchment, RR models were calibrated to a single, reliable stream gauge. This model was then used to estimate streamflow within the Victoria River and simulate streamflow under historical and projected future climates.

Subsequent to the NASY study, CSIRO was commissioned to assess the opportunities for water resource development and associated risks in the Flinders and Gilbert (Queensland) catchments between 2012 and 2013 (Petheram et al., 2013a,b) in an assessment known as the Flinders and Gilbert Agricultural Resource Assessment (FGARA), and then in the Fitzroy (WA), Darwin (NT) and Mitchell (Queensland) catchments in 2016–2018 in an assessment known as the Northern Australia Water Resource Assessment (NAWRA). These Assessments employed river models, landscape models and hydrodynamic models to estimate the effects of development scenarios on water resources. Specific information with regard to river and landscape modelling in FGARA is detailed by Lerat at al. (2013) and in the Northern Australia Water Resource Assessment it is detailed in Hughes et al. (2017) and Hughes et al. (2018). Subsequent to the Northern Australia Water Resource Assessment, CSIRO was commissioned to expand water resource assessment to the Roper catchment in the NT (Hughes et al., 2023). The river model and methods used in this Assessment are largely an evolution of the methods used in the Northern Australia Water Resource Assessment and the Roper River Water Resource Assessment. It should also be noted that there is no jurisdictional or legacy Victoria River model that can be referred to for this Assessment.

# 2 Site characteristics

The physical characteristics of the Victoria catchment are given in detail in Chapter 2 of *Water resource assessment for the Victoria catchment* (Taylor et al., 2024 in Petheram et al. (eds), 2024). To assist the reader, an overview of the site characteristics is included here.

The Victoria catchment has a hot and arid climate. The catchment has a highly seasonal climate with an extended dry season. It receives a mean of 681 mm of rain per year, 95% of which falls during the wet season. Mean daily temperatures and potential evaporation are high relative to other parts of Australia. On average, potential evaporation is approximately 1900 mm/year.

There is a distinct north to south rainfall gradient across the catchment with mean annual rainfall near the coast being 1000 mm near the coast, but less than 500 mm in the far south of the catchment. The area has experienced relatively higher rainfall since about 1970 (Figure 2-1).

The variation in rainfall from one year to the next is moderate compared to elsewhere in northern Australia yet is high compared to other parts of the world with similar mean annual rainfall. The length of consecutive dry years is not unusual in the Victoria catchment and the intensity of the dry years is similar to many centres in the Murray–Darling Basin and east coast of Australia. Since 1969–1970, the Victoria catchment experienced one tropical cyclone in 21% of cyclone seasons and two tropical cyclones in 6% of seasons.

The Victoria River and its tributaries, the most substantial of which being the Baines, the Wickham, the Armstrong, the Camfield and the Angalarri rivers, define a catchment area of 82,400 $km^2$ (Figure 2-2). The Victoria River itself spans approximately 500 km from Entrance Island at its mouth to Kalkarindji in the far south of the catchment. Tidal variation at the mouth of the Victoria River is up to 8 m, and these tides propagate upstream to approximately 5 km downstream of Timber Creek (Power and Water Authority Directorate, 1987). The catchment is relatively flat with maximum elevations around 450 mAHD in the far south-west. The mean annual flow at the catchment outlet is estimated to be around 7000 GL/year.

At the time of writing, there were surface water licences in the river model domain totalling 730 ML/year. There are no substantial structures within the streams themselves across the catchment. The most obvious is the river ford at Dashwood Crossing on the Victoria River which is considered minor.

The northern portion of the catchment area is dominated by escarpments, hills and ridges of sedimentary geology (Figure 2-3). Within this lies a north-east to south-west band of alluvial plain associated with the Baines and Angalarri rivers. Extensive areas of deep cracking clay soils are found on the broad alluvial plains of the major rivers, particularly along the Victoria and Baines rivers. Deep cracking clay soils are also found scattered throughout the eastern, southern and western parts of the upper catchment and are also subject to seasonal wetness. Areas of very friable loams are found along the Victoria and Wickham rivers mainly on narrow levees with broader areas scattered throughout the catchment. These soils are also susceptible to severe sheet and gully erosion and wind erosion. Tertiary level plains and plateaux in the southern catchment contain deep loamy soils that are suitable for a diverse range of irrigated horticulture and spray-irrigated grain, pulse and forage crops, timber crops, sugarcane and cotton. In the southern parts of the catchment where these more versatile soils are located, surface water is relatively less available (Figure 2-4).

Nearly 60% of the catchment is dissected hills, outcrop, plateaux and scarps with rocky and/or shallow soils of little agricultural potential. These higher relief areas give way to lower relief, lower sloping land and alluvial plains. The coastal marine plains are seasonally or permanently wet saline soils with potential acid sulfate risks. These poorly drained soils are unsuitable for cropping but are prospective for aquaculture.

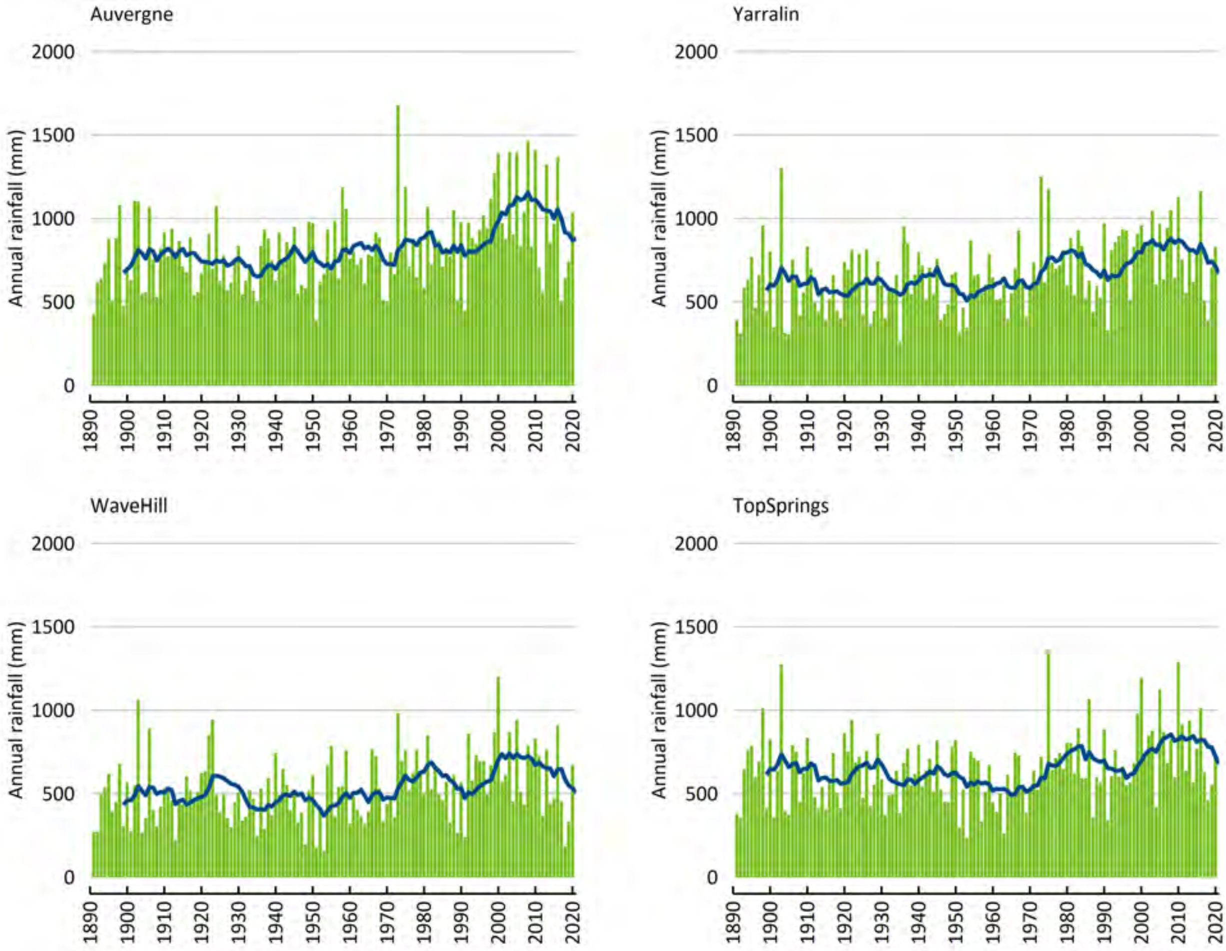


**Figure 2-1 Annual rainfall at four locations in the Victoria catchment under Scenario A: Scenario A is the historical climate (1890 to 2021). The blue line represents the 10-year running mean**

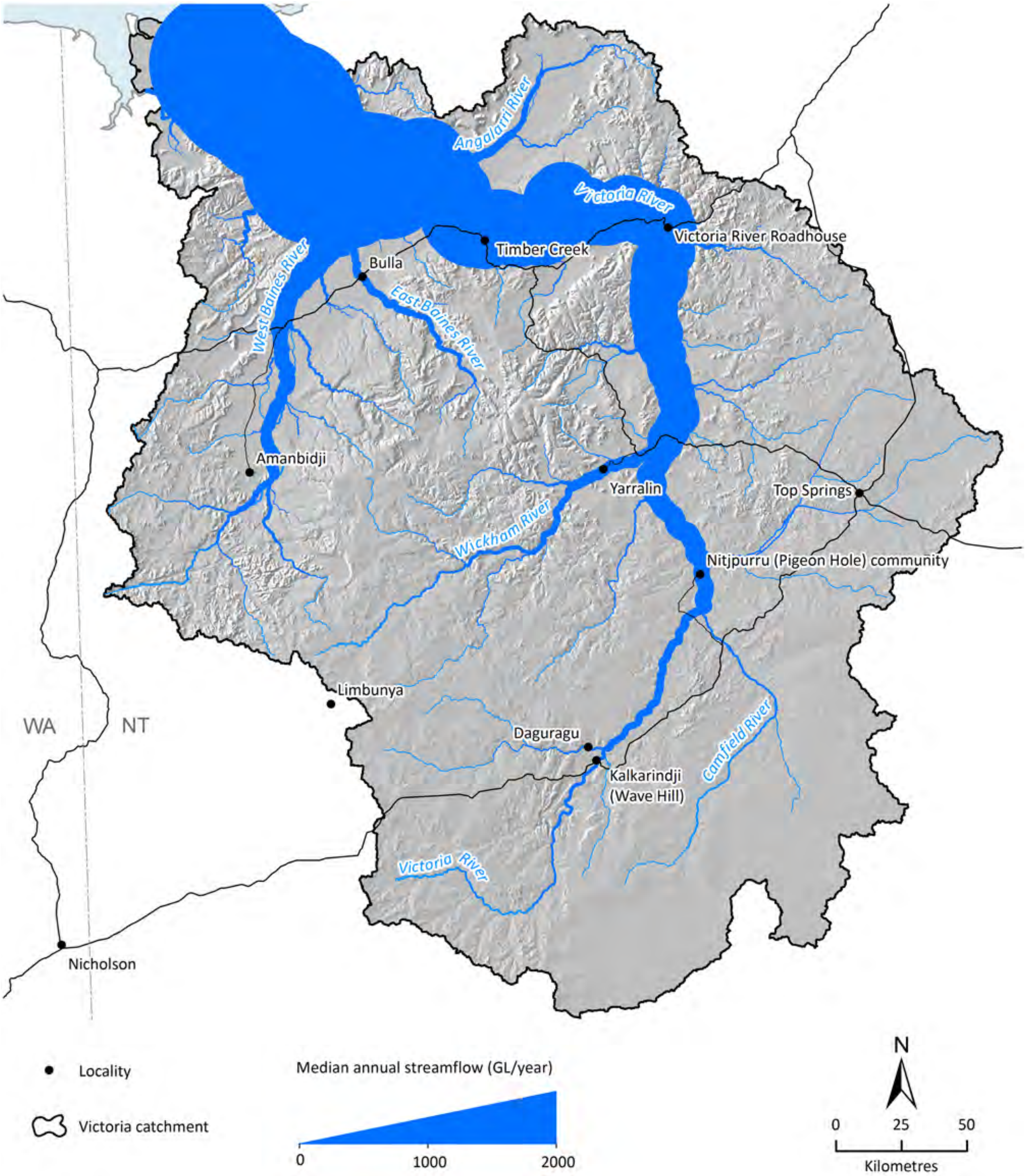


**Figure 2-2 Median annual streamflow (50% exceedance) in the Victoria catchment under Scenario A**

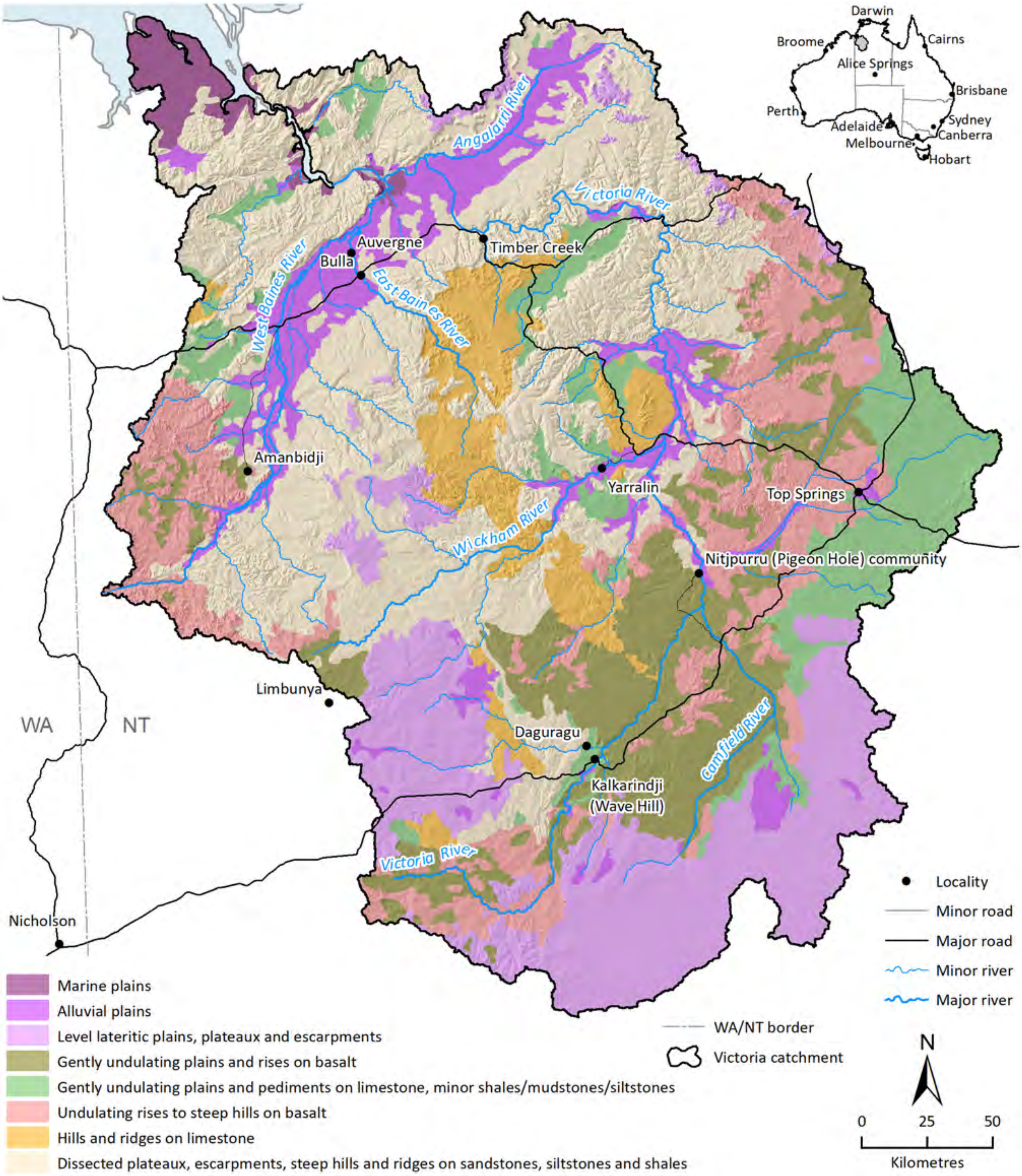


**Figure 2-3 Victoria River Water Resource Assessment area showing the Victoria River and tributaries, physiographic provinces after CSIRO (1970), significant settlements and roads overlaid on hill-shaded terrain relief**

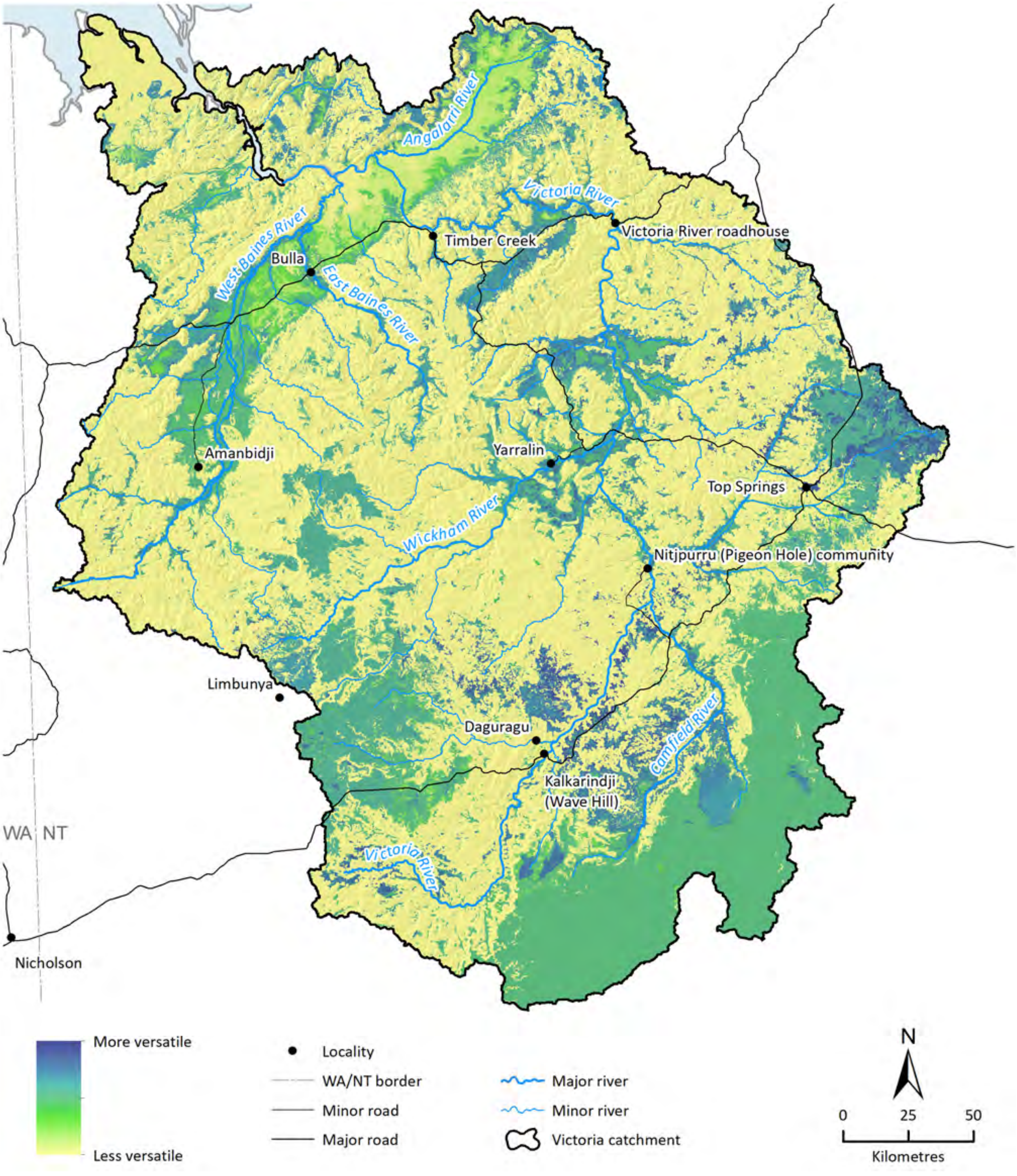


**Figure 2-4 Soil versatility in the Victoria catchment**

# 3 Available data

The quality and quantity of the data available to the modeller have a significant influence on the methods used to estimate streamflow, as well as the potential model applications.

The availability of rainfall gauge data was examined for the catchment area on a decadal basis (McJannet et al., 2023). It can be seen from Figure 3-1 that rain gauge density is quite low relative to a catchment in south-eastern Australia. This has some consequences for hydrological modelling. It should be here noted that, for model simulation, 'patched point' or gauge data are not used as model inputs directly, but rather gridded Data Drill climate data (Jeffery et al., 2001). This is an interpolated product that relies upon the same rainfall data as those shown in Figure 2-1. Data Drill data are a daily product supplied at approximately a 5 × 5 km grid resolution. Where rain gauge data are sparse, for example isolated storm rainfall, it may not be picked up or may be severely underestimated in interpolated products (e.g. SILO). This can result in a substantial observed streamflow event at a stream gauge with, according to SILO data, little to no corresponding rainfall in the catchment area. Conversely, an isolated rainfall event may appear more widespread in gridded inputs than it is in reality, due to interpolation. For these reasons it is difficult to achieve satisfactory goodness of fit in such environments, and of more concern, can contribute to model 'over-fitting', leading to poor predictive performance (Srivastava et al., 2014).

Data from January 1889 until July 2023 were used as model input, although the reporting period begins in 1890. This allows model states to 'warm-up' prior to analysis of model outputs. It should also be noted that errors in the rain gauge observations, the availability of gauges at any point in time and the spatial extent of rainfall will all effect the accuracy of interpolated rainfall products.

Data Drill data were bulk downloaded as spatial layers (netCDF format) and aggregated to daily time series for each grid cell. As a part of this process Morton's wet area (Mwet) potential evapotranspiration (ET) was calculated using other Data Drill variables. Mwet is an estimate of potential ET over a large area, assuming an unlimited supply of water. The model assumes upwind effects are negligible and local variations are ignored, so the estimate is an areal mean (Wang et al., 2001). Chiew and McMahon (1991) found Mwet is similar to Food and Agriculture Organization – Irrigation paper 56 (FAO56) (Allen et al., 1998) in a wet climate but lower than FAO56 in a dry climate. Chiew and Leahy (2003) found that Mwet is similar to FAO56 in the coastal areas of south-eastern and eastern Australia. It is possible, therefore, that the wet-season Morton's ET used in this study is similar to FAO56, but potentially somewhat lower during the dry season. Morton's wet area potential ET calculations are detailed in Appendix A. All gridded data were subsequently spatially averaged according to model subcatchment for use as input in the river models.

Stream gauge data were obtained from theNT Department of Environment, Parks and Water Security (DEPaWS). High-frequency data were aggregated to 9 am for comparison to daily rainfall data. Similarly, stream gauging data were also collected and examined.

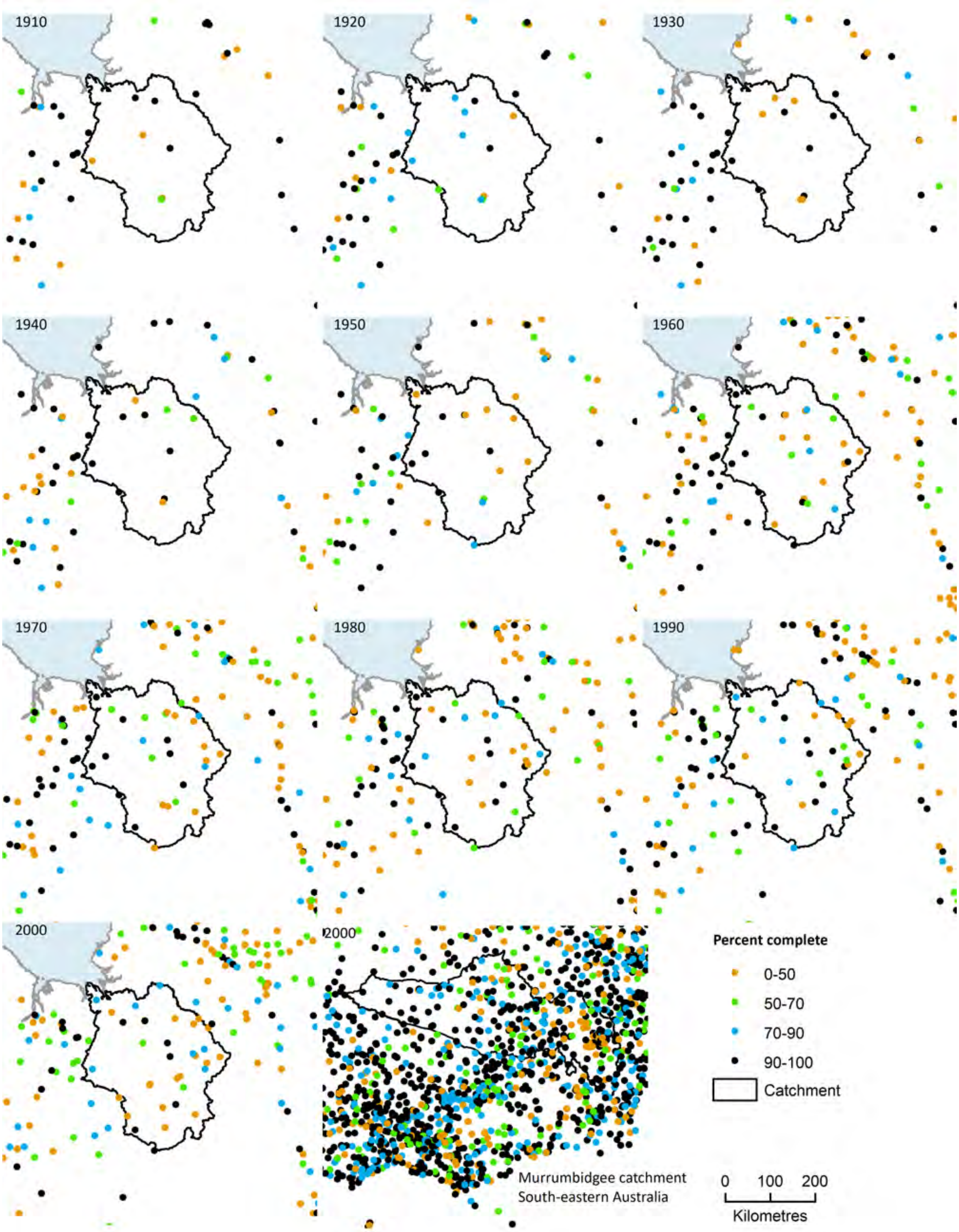


**Figure 3-1 Decadal analysis of the location and completeness of Bureau of Meteorology stations measuring daily rainfall used in the SILO database**

The decade labelled '1910' is defined from 1 January 1910 to 31 December 1919, and so on. At a station, a decade is 100% complete if there are observations for every day in that decade. The last panel shows the availability of rainfall data in the vicinity of the Murrumbidgee catchment in south-eastern Australia for comparison.

## 3.1 Stream gauge data

All stream data, including gaugings and quality codes, were obtained from DEPaWS. These data were examined together to determine the suitability of individual gauges for calibration. Plots illustrating the data are given in Appendix C. An example of these plots is shown in Figure 3-2. These plots assist the hydrologist making judgements of the value of stream gauge data at each site. Gauging period, catchment area and catchment averaged mean annual rainfall are given for Victoria catchment stream gauges in Table 3-1. It should be noted that other gauges, usually of a short duration (typically weeks), or with obvious problems, were not assessed further and not subsequently used for model calibration.

**Table 3-1 Stream gauge observations in the Victoria catchment**

| STATION ID | STATION NAME | CATCHMENT AREA ($km^2$) | DAYS OF OBSERVATION | OBSERVATION START | OBSERVATION END | MISSING DAYS | DRY-SEASON % OF ALL OBSERVATIONS |
|---|---|---|---|---|---|---|---|
| **8110004** | East Baines River - U/S Victoria Hwy | 2444 | 11442 | 1963-01-08 | 2023-07-05 | 10652 | 35 |
| **8110006** | West Baines River - Victoria Hwy | 8695 | 12956 | 1961-11-24 | 2023-07-05 | 9548 | 41 |
| **8110007** | Victoria River - Coolibah Homestead | 52192 | 13056 | 1953-01-01 | 2022-04-18 | 12254 | 33 |
| **8110012** | Timber Crk - U/S Victoria Hwy | 164 | 10699 | 1968-12-25 | 2022-05-28 | 8814 | 42 |
| **8110014** | Sullivans Crk - U/S Fig Tree Yard | 156 | 3232 | 1970-11-27 | 1993-04-01 | 4930 | 24 |
| **8110016** | Upper Victoria River - Wave Hill Police Station | 4584 | 11636 | 1973-12-20 | 2022-06-02 | 6061 | 40 |
| **8110018** | Victoria River - Victoria Hwy | 50891 | 6626 | 1972-11-09 | 2022-06-02 | 11477 | 41 |
| **8110073** | Armstrong River - Top Springs | 601 | 1839 | 1971-11-18 | 1986-07-03 | 3503 | 34 |
| **8110074** | Montejinnie Crk - Montejinnie Homestead | 141 | 3971 | 1973-11-10 | 1986-09-09 | 716 | 50 |
| **8110101** | Dick Crk - Victoria Hwy | 507 | 1046 | 1968-11-25 | 1978-04-13 | 2381 | 10 |
| **8110107** | Saddle Crk - Victoria Hwy | 221 | 5759 | 1968-11-19 | 2022-06-02 | 13795 | 34 |
| **8110110** | Surprise Crk - VRD Road Xng | 350 | 4654 | 1959-11-23 | 2004-06-29 | 11637 | 9 |
| **8110113** | Victoria River - Dashwood Xng | 40723 | 13412 | 1962-12-22 | 2023-06-26 | 8690 | 42 |
| **8110232** | Wickham River - Williams Xng | 5525 | 15452 | 1965-12-31 | 2022-06-15 | 5169 | 45 |
| **8110238** | Delamere Crk – Delamere Homestead | 681 | 1849 | 1971-11-27 | 1987-06-20 | 3836 | 16 |
| **8110251** | West Baines River - Brumby Hill | 161 | 1508 | 1965-11-03 | 1986-02-26 | 5913 | 12 |
| **8110253** | Gibble Crk - Wagon Wheel W/Hole | 490 | 1912 | 1971-11-20 | 1992-02-29 | 5495 | 11 |

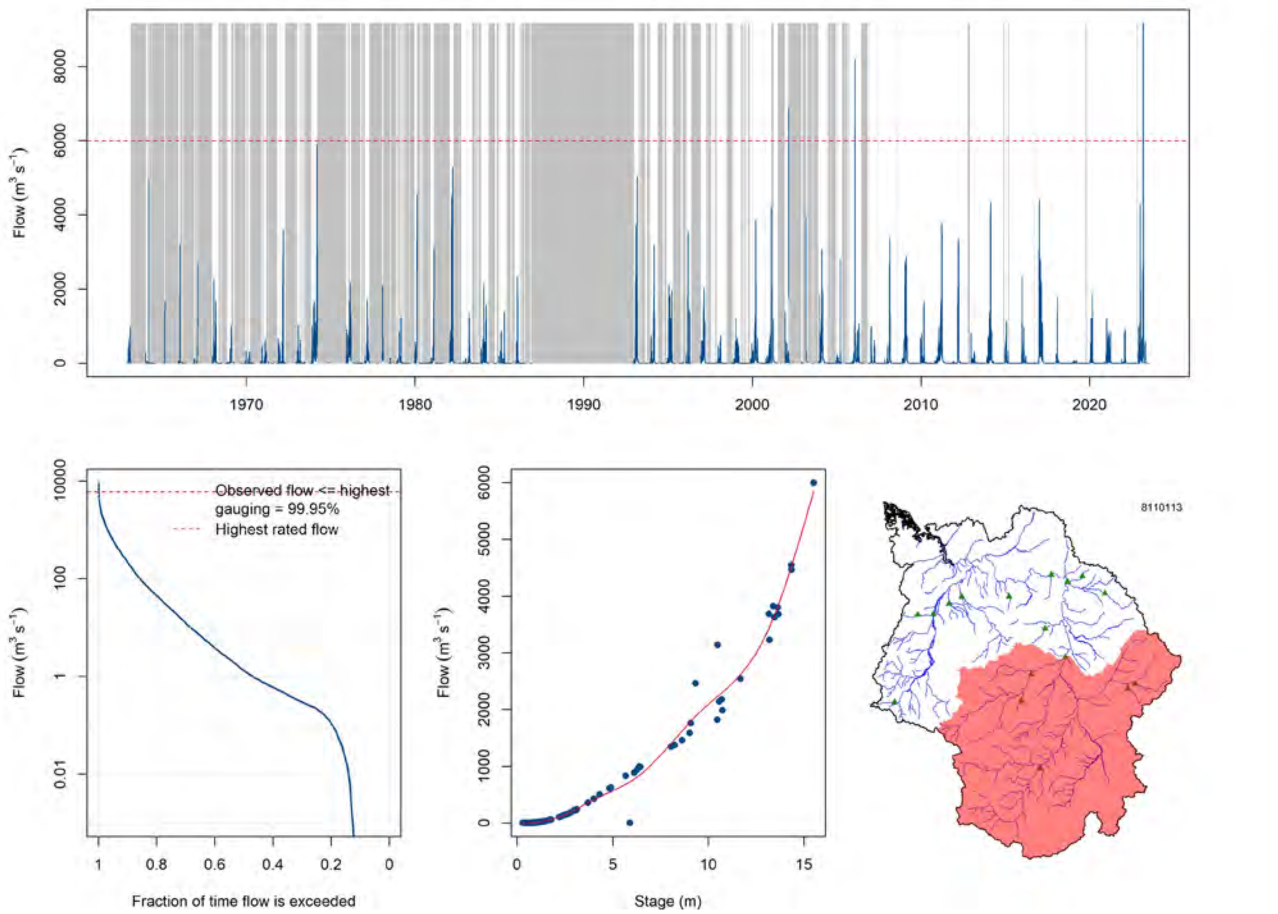


**Figure 3-2 Stream gauge data for site 8110113 (Victoria River at Dashwood Crossing)**

The dashed red line in the top and bottom left panel indicates highest gauged flow. Grey vertical lines indicate missing data.

Some aspects of gauge quality are not easily quantified and require more intuition/judgement. For example, a sudden increase in baseflow that is not noted in other gauges at a similar time can increase doubt on the veracity of the observations. Another example is where the peak flows are unusually consistent, or more obviously, where the rating data are poor.

It is worth noting here the case of the gauge at Wave Hill Police Station (8110016). This gauge has a long record and what appears to be reasonable rating data. However, the apparent runoff coefficient for these data is greater than 18% (even after patching mostly dry-season missing data with simulated flow). This is roughly twice what may be expected in such an environment (see Appendix B). Attempts were made to model gridded runoff across the catchment with a single parameter set (regionalisation), and use of this gauge in calibration resulted in higher than observed streamflow at other gauges. Such high runoff in such an arid area is possible, although unlikely, so the decision was made not to use these data jointly with other gauge data in river model calibration, but rather as a stand-alone calibration. With more time the apparent behaviour of this gauge could be investigated further.

Ultimately, stream gauge data are used to derive model parameters and assess the veracity of simulation based on these parameters. Stream gauge data context is an additional consideration here, particularly the climate during observation in relation to the simulation period. These data can be seen in Figure 3-3. The catchment annual rainfall is shown against the climate of the stream gauge contributing area for each gauge during each respective observation period. What is most obvious is that stream gauge data have been collected in a relatively wet period, and there is no data regarding hydrological response in the pre-1960 period. This situation is further exacerbated for gauges 8110016, 8110113 and 8110074 where stream gauging is of a relatively short duration or bridges a relatively wet period in the 1970s.

The Victoria catchment is relatively remote and is a considerable distance from Darwin where hydrographers servicing the catchment are based. The priority for hydrographic measurement in the catchment is river stage to serve as a source of information for flood warnings. As such, relatively less effort goes into gauging and streamflow estimates.

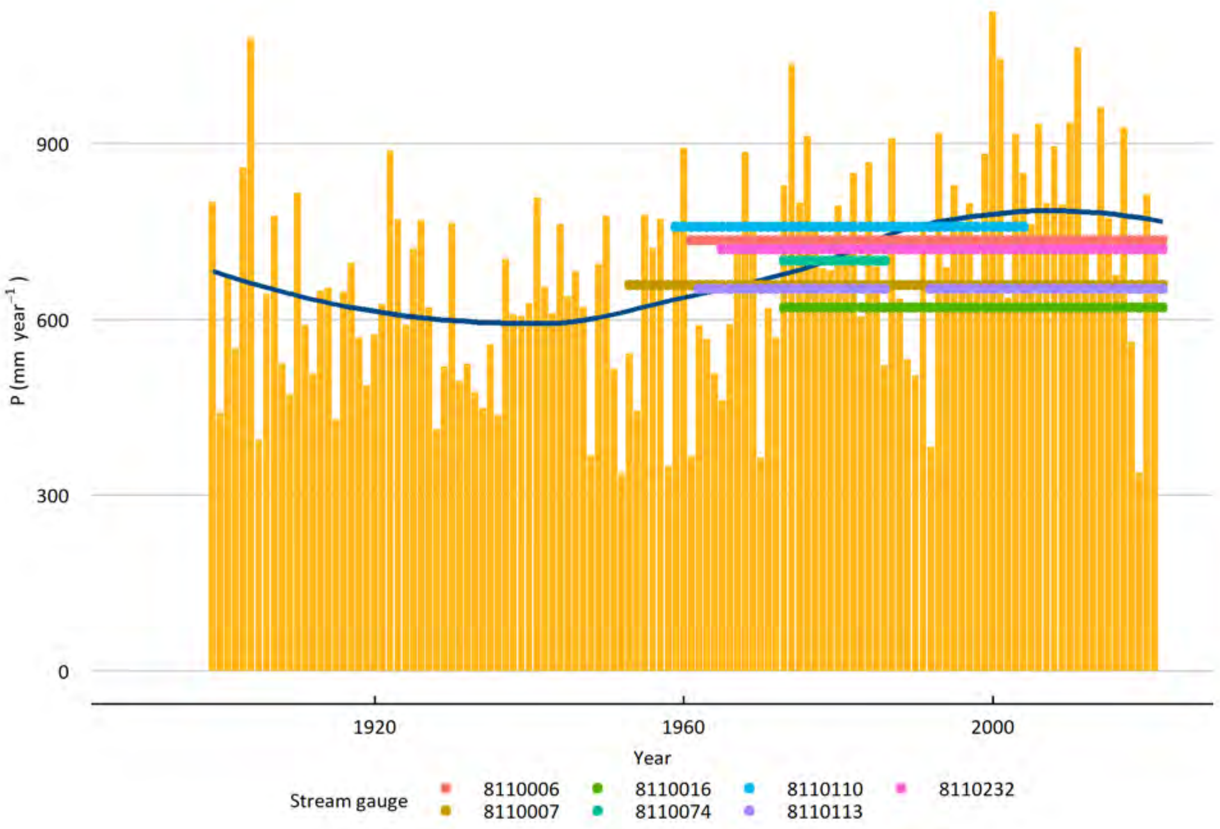


**Figure 3-3 Victoria catchment annual rainfall (yellow columns) and stream gauge observation period expressed as mean contributing area rainfall in the respective years of observation**

The blue line is the smoothed catchment annual rainfall data.

## 3.2 Topographic data and catchment delineation

Accurate delineation of contributing area to any point, including the catchment outlet is vital for hydrological applications and can be a source of considerable uncertainty in hydrological prediction (Gan et al., 1990). For the estimation of Victoria River catchment (including model subcatchments), one arc-second Shuttle Radar Topography Mission (SRTM) data was used (Gallant et al., 2012). Based on these data the Victoria catchment is predicted to extend further south beyond the present AWRC catchment boundary, well into the Wiso basin. The Wiso basin is particularly dry, and examination of aerial imagery indicates that surface water flow is unlikely from the vaguely defined open depressions that cross the southern edge of the of the Victoria AWRC catchment. Accordingly, the catchment boundary was truncated at these points, resulting in a catchment that is similar in size and shape to the present Victoria River AWRC catchment. A large storm event in March 2023 flooded large parts of the southern Victoria River catchment, resulting in the evacuation of many residents. Surface water extent was evaluated during this event using radar data from the Sentinel 1 satellite to ascertain if any surface flow may have moved across the current AWRC boundary in the south of the catchment.

Sentinel-1 Synthetic Aperture Radar (SAR) data were used to map floods due to the sensor's ability to penetrate through cloud. Sentinel-1 data, available from the European Space Agency, was downloaded for the Victoria River catchment for the flood dates as well as a dry period. It was processed to an analysis-ready format (through applying a radiometric and geometric terrain correction as well as calibrating the pixel values to normalised radar backscatter). A low threshold value, as well as the difference in backscatter between the dry and flooded images, was used to extract flood water. Small 'clumps' of water pixels, which were incorrectly identified as water due to confusion with other low backscatter landcover as well as data speckle, were removed using a sieve filter. A DEM was also used to remove erroneous pixels classified as water on steep terrain.

These images showed no indication of water movement across the proposed catchment boundary, and there was no evidence of concentrated surface water flow in that region. This increased the confidence that the truncated SRTM derived catchment was fit for purpose.

# 4 Model software and structure

## 4.1 River model

The AWRA-R model has been selected as the river modelling platform for the Assessment. It was selected over 'Source' (a commonly used platform by jurisdictions) largely since it is flexible and has very short run times. AWRA-R is not designed to incorporate complicated operations rules as Source might, although for relatively undeveloped areas such as northern Australia this presents few, if any, simulation difficulties. Rather, the flexibility and short run times allow for extensive sensitivity analyses of development scenarios, automated model optimisation and an ability to make the model available to users via a website where simulations can be run 'live' with development parameters of their choosing and accompanying ecosystem analyses.

The AWRA-R model is based upon a series of connected subcatchments that can receive streamflow from upstream nodes, perform various processes within each subcatchment, and, using a water balance approach, calculate various fluxes including subcatchment outflow, which may be used as an input to a downstream subcatchment. Outflow points for each subcatchment are generally denoted as a 'node'. Model parameters and inputs are required for each subcatchment.

The AWRA-R model framework used for the Victoria River is written in the C language and is used in conjunction with the R language for ease of data processing and access to various functions such as optimisers, goodness-of-fit measures and plotting functions via R packages.

A brief summary is provided here, otherwise the reader is directed to the original references of Dutta et al. (2015) and Dutta et al. (2017). Each node in the model requires a configuration vector, a parameter vector, and a time series array as inputs. The standard model output is a time series of model states, including outflow. Where irrigation sub-models are used, these require additional irrigation parameters and configuration vectors, as well as additional time series inputs (e.g. crop coefficient values).

### 4.1.1 Routing routine

Routing represents the transport of water down a river reach from upstream to downstream. A river channel has capacity to store water in varying degrees, which induces a time lag from inflow to outflow, as well some attenuation and dampening of the hydrograph peak across the reach. These effects were simulated using a Muskingum procedure (Koussis, 1980):

$$\frac{dV}{dt} = I - O \tag{1}$$

and

$$V = K[x * I - O(1 - x)] \tag{2}$$

where $V$ is the routing volume ($L^3$), $I$ and $O$ are the reach inflow and outflow respectively ($L^3$), and $x$ and $K$ are calibrated routing parameters.

### 4.1.2 Loss model

Physically, as water moves along a channel it may experience losses due to exchanges with groundwater or soil water. Transmission losses are very difficult to measure directly, so any loss function that is calibrated jointly with other states (against observed flow) will also implicitly account for gauge error, poor system representation, or overestimates in other model states (e.g. unaccounted runoff). Most model estimates of loss are flow-based on:

$$L(t) = f(Q(t)) \tag{3}$$

where $L$ is the loss and $f$ is a function describing the flow-based loss. For the Assessment, the loss estimation method developed by Doble et al. (2012) was used. This method is dependent on physical properties of the river bed material, river stage, river length, river width, depth to groundwater and specific water yield of the aquifer. This method is denoted as 'Doble loss' subsequently. The river hydraulic conductivity parameter is calibrated jointly with the RR and routing parameters for each reach. Optimal parameter sets are then used for subsequent simulation. The equations for the Doble loss calculations are given below:

$$Q_{gw} = \min(I_{riv}, \Delta S_{riv} + Q_{riv}) * \Lambda \tag{4}$$

$$I_{riv} = Ks_{riv} w_{riv} \left(\frac{h_{riv}}{d_c} + 1\right) \tag{5}$$

$$\Delta S_{riv} = d_{gw} S_y x_w \tag{6}$$

$$Q_{riv} = K_{aq} d_{aq} \frac{2h_{riv}}{x_w} \tag{7}$$

where $I_{riv}$ is potential infiltration rate from river per unit length of the river ($m^2$/second), $\Delta S_{riv}$ is total storage per unit length of the reach ($m^2$/second) within the regolith beneath the streambed, $Q_{riv}$ is maximum volume of water discharging from the aquifer ($m^2$/second), $\Lambda$ is the reach length (m), $Ks_{riv}$ is river bed hydraulic conductivity (m/second), $w_{riv}$ is width of the river (m) obtained from flow-area relationship, $h_{riv}$ is depth of river water (m) obtained from a flow–depth relationship, $d_{gw}$ is depth to groundwater (m), $d_c$ is the thickness of the river bed material (m), $S_y$ is the aquifer-specific water yield (dimensionless), $x_w$ is the width of the river (m) derived from a flow–width relationship, $K_{aq}$ is the aquifer hydraulic conductivity (m/second) and $d_{aq}$ is the aquifer thickness. In all cases, depth to groundwater information was not available at appropriate spatial and temporal resolution. Accordingly, depth to watertable was assumed static at 5.0 m.

The river bed conductivity was calibrated jointly with runoff and routing parameters. Effectively, the $Q_{gw}$ calculations are simplified to an estimation of $I_{riv}$ that is at least partly controlled by the calibrated parameter $Ks_{riv}$, since $Q_{qw}$ is taken as the minimum of the two terms $I_{riv}$ and $\Delta S_{riv} + Q_{riv}$, and the final two states $\Delta S_{riv} + Q_{riv}$, are likely to be higher than $I_{riv}$ due to depth to groundwater assumptions. This method was favoured partly since it is more physically based than other methods, but also since it requires only one calibrated parameter and can be applied easily to ungauged locations, requiring an estimate of reach length and assuming the parameters from donor catchments.

### 4.1.3 Rainfall-runoff model

RR models take a ‘top-down’ approach to estimating runoff, viz., model parameters are adjusted until the model simulation matches streamflow observations to the satisfaction of the hydrologist. This model can then be used to estimate flow at a time outside of the calibration period (assuming inputs, usually daily precipitation and potential ET, are available). In many situations, no streamflow observations are available at a desired location, and parameters have to be estimated or assumed using other methods.

The calculations within the RR models are influenced by observations of hydrological processes, and hence these models are often termed ‘conceptual models’. The ease of use and modest data requirements of these models has seen their widespread application, so much so that these models are applied in a vast array of environments not anticipated (presumably) by the original model authors. Given this, the modeller must take care in their application, especially in environments such as northern Australia. Furthermore, these models are prone to ‘over-fitting’ (i.e. poor predictive performance despite satisfactory representation of observed streamflow during calibration). This is related to the inability of the model to implicitly represent all processes, and fitting to any error in model input and streamflow observations.

The river model used for the Assessment relies on RR models to generate runoff in each model subcatchment. The Assessment builds upon some previous assessments of RR models in other northern Australian catchments (Petheram et al., 2012; Hughes et al., 2017, 2021a, 2023). More information regarding these models and choices for this Assessment can be found in Section 5.

### 4.1.4 Node-link structure

The number and position of river model nodes across a study area are determined by the study’s modelling objectives. Increasing the number of nodes increases the flexibility of the model in relation to the number and degree of detail possible within model scenarios; however, increasing the number of nodes also increases the computational burden and model run times. For the Assessment, nodes were assigned to:

1. represent stream gauge positions, allowing for model calibration
2. divide the catchment into reasonably evenly distributed subcatchments
3. represent communities such as Yarralin and Pigeon Hole where estimates of water availability may be needed
4. potential dam sites (identified using the DamSite model (Yang et al., 2023)) and areas of soil suitable for irrigated agriculture (identified using land suitability data generated by the companion technical report on land suitability (Thomas et al., 2024))
5. based on the location of ecological assets and where reporting on changes to ecological assets may be desired.

In addition to these influences, nodes were placed in topographic positions that may, at some future time, be suitable for stream gauging, for example, where a stream moves through a narrow gap in a rocky ridge. The final node and subcatchment structure are shown in Figure 4-1 .

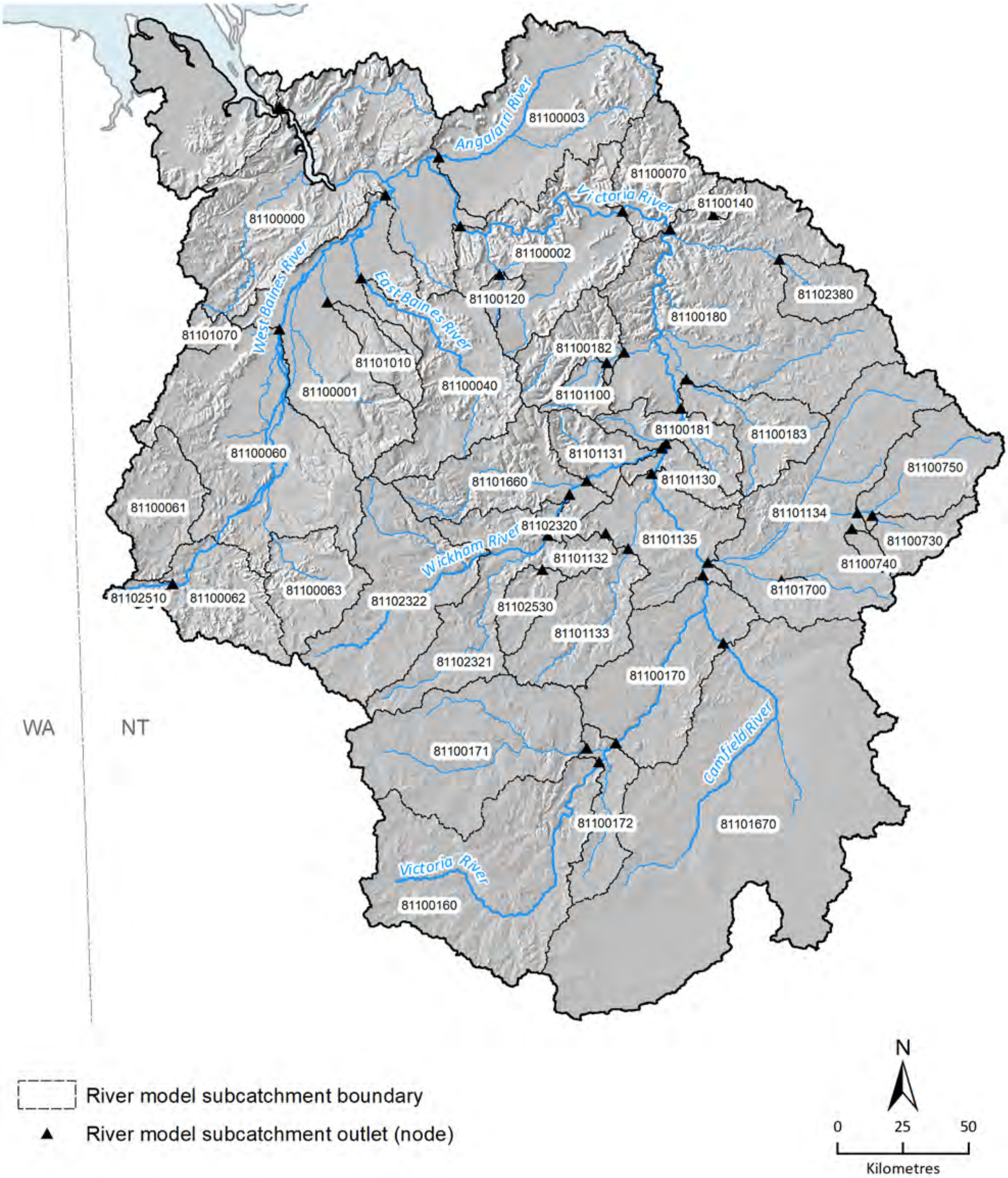


**Figure 4-1 River model nodes and subcatchment areas**

Note that calibration gauge sites were used as simulation nodes and simulation node ID is the same as calibration gauge ID with the addition of a '0'.

# 5 River model calibration

This section relates to the calibration of the Victoria River model. Unlike in the Northern Australia Water Resource Assessment, no independent calibration of a landscape model was conducted in the Assessment. Rather, the Sacramento RR model and parameters used in the final river mode version were used to generate gridded runoff data for use in other components of this Assessment.

River system models consist of a series of linked nodes or reaches in which the processes of losses and gains are modelled. These nodes are linked in an upstream to downstream chain, enabling representation of the river-related states in time and space. In this regard, river system models are semi-distributed, with the outputs of upstream nodes acting as inputs to downstream nodes.

RR models are the primary way of estimating runoff/streamflow generated within each river model subcatchment. They utilise subcatchment mean daily precipitation and potential ET time series as inputs, without the need for inputs other than model parameters. There are many options in terms of RR models and the selection of RR models for this Assessment builds on investigation of RR models used within river models in northern Australia by Hughes et al. (2017). The Hughes et al. (2017) study also tested a range of objective functions, loss models and calibration methods. These investigations were continued in the Roper River Water Resource Assessment (Hughes et al., 2023).

Hughes et al. (2017) tested the GR4J model (Perrin et al., 2003) and compared it to both Sacramento (Burnash, 1995) and AWRA-L (Viney et al., 2015), noting that AWRA-L is not, strictly speaking, a RR model since it is more ‘physically based’ and has a number of spatially explicit input parameters that are not calibrated. However, AWRA-L can be calibrated to observed streamflow and generate runoff estimates as a RR model might. While results varied with location, they suggested that the Sacramento RR model had better overall performance. This was particularly the case for low-flow representation, and general performance in arid areas. GR4J has only four parameters, which in isolation of performance, makes it attractive for system calibration. Given this, Hughes et al. (2023) included adaptions of the GR4J model intended to improve low-flow performance. The GR7J model (Hughes et al., 2013a; Grigg and Hughes, 2018) is an adaption to GR4J that was designed to cope with long-term changes in storage and climate change better than the GR4J model. GR7J has also been shown to give better performance in drier climates (Hughes et al., 2021a). However, low-flow performance of this model, while improved somewhat, was still inadequate for many applications, most notably ecological assessment. Ideally a model should be able to represent zero-flow days since this is an important ecological metric. To that end adjustments to the GR7J model formulation were attempted and tested. This model was denoted GR7JFM and while reasonably successful, Sacramento was favoured since its performance was similar and the model well known to most hydrologists.

Typically, river system models are calibrated on a ‘reach-by-reach’ basis in which each node is calibrated against an observed gauge in isolation from upstream outputs other than inflows and downstream performance is not considered until that reach is calibrated in turn (e.g. Hughes et al., 2014a, 2017). However, this method suffers from problems since the method for calibration, and simulation for prediction, are quite different (Lerat et al., 2013). An obvious alternative to this is the ‘system-calibration’ method where all parameters for all reaches are calibrated simultaneously, running the model in the same way in calibration as it would be used for predictive modelling. This has benefits (Hughes et al., 2016), but high dimensionality in optimisation becomes a problem depending upon the number of reaches and types of RR models used. Hughes et al. (2023) used a new method which, mechanistically, lies between reach-by-reach and system-calibration methods.

Shingle calibration divides the catchment, and available stream gauge locations, into overlapping sections or ‘shingles’. At its most simple, each shingle consists of three gauges in serial order in which the uppermost gauge has already been calibrated and a time series of simulations are available. The second gauge and third gauge are then calibrated simultaneously (i.e. the goodness of fit for the second and third gauge are both utilised in the optimising function). Once calibration is complete, the time series of the second gauge is saved and is used as an input to the subsequent shingle where it is the first gauge. This process is illustrated in Figure 5-1, where a hypothetical river system of five nodes is represented. Blue nodes in each calibration shingle have been calibrated in a previous shingle, while simulation performance of both the green and red nodes is optimised simultaneously in the current shingle. Parameters estimated for the green node are saved and a time series of simulated flow is used as an input in the following calibration shingle. This is a highly simplified example and, in practice, some modifications to this process are required (e.g. for headwater nodes and final nodes), although the same principles apply. The intention of this process was to constrain parameters in each reach by performance at the calibration gauge (green nodes in Figure 5-1) and its effect on at least one downstream node (red nodes in Figure 5-1). This allows many of the benefits of system calibration to be realised, while reducing problems associated with high dimensionality.

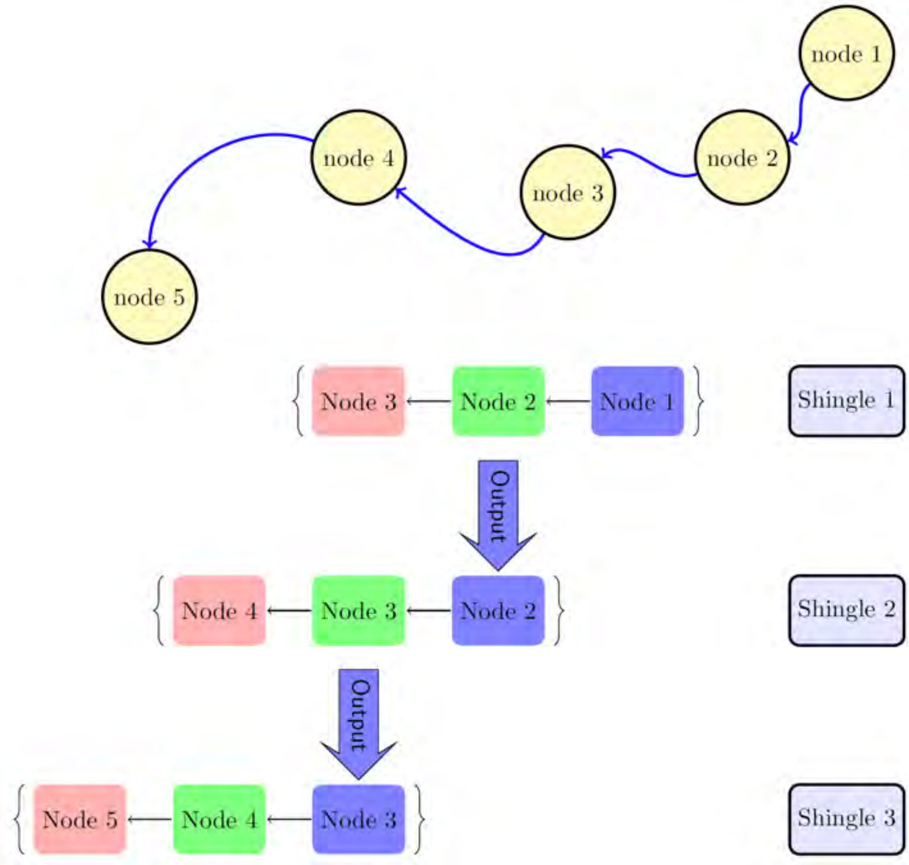


**Figure 5-1 Shingle calibration conceptual diagram for a section of five nodes of a river system model**

Each calibration shingle has a pre-calibrated input time series (blue), a calibration node (green), and an auxiliary calibration node (red) that is jointly calibrated with green nodes.

In most river modelling situations, there will be at least some ungauged nodes (i.e. nodes for which streamflow simulations are required, but there are no available gauge data at that location). In these situations, model parameters must be obtained in another way. Prediction in ungauged areas is an area of ongoing research in hydrology and there have been many publications relating to this situation. Indeed, the International Association of Hydrological Sciences (IAHS) initiated the Prediction in Ungauged Basins program in 2003 (Sivapalan, 2003) to address these needs. During and since this initiative, there have been many publications that aimed to examine various methods of transferring parameters to or estimating parameters for ungauged catchments. This process is termed ‘regionalisation’ and was reviewed by Bloschl et al. (2013).

Regionalisation falls into two broad groups, NN and hydrological response unit (HRU) approaches respectively. The HRU approach aims to use various catchment physical descriptors to classify catchments of similar type. The physical descriptors may be related to catchment climate, topography, vegetation and regolith/geological characteristics. Parameters are transferred to the ungauged catchments either as a set or individually (often ignoring parameter correlation), based on similarity with gauged catchments. The NN approach simply takes parameters from the nearest gauged catchment(s). For more information see the review of Parajka et al. (2013). Examination of the relative success of these methods is inconclusive, although the most relevant study in the context of this Assessment is that of Petheram et al. (2012), who concluded that NN methods were the most successful in northern Australia.

The shingle calibration method was adapted so that parameters could be 'shared' between gauged subcatchments and ungauged subcatchments within a calibration shingle and/or parameters could be 'borrowed' from pre-existing calibrations (usually from preceding shingles). Since all gauges within a shingle are jointly calibrated, and any simulation at a gauged location will be affected by upstream and downstream goodness of fit, as well as its own location, a measure of constraint is applied to shared parameters, at least greater than consideration at a single gauge. It should be noted that the protocol in terms of donor and receiver catchments is a decision made by the hydrologist a priori, rather than any automated procedure, and hence there is scope for various parameter sharing possibilities for any single location. For example, if a conceptual calibration shingle has three gauged nodes and three ungauged nodes, parameters must be assigned to the three ungauged nodes (Figure 5-2). Even if it is assumed that no parameters are 'borrowed' from outside the shingle, and only parameters from within the shingle are used, there are still 27 different parameter combinations that could be used across the three ungauged sites. Considering that there will generally be multiple shingles used for any river model, the possibilities for parameter transfer increase exponentially, and as such, the judgement of the hydrologist is required to eliminate most of these permutations. Despite the NN method of parameter transfer being generally favoured, judgement based on physical factors (i.e. a HRU approach) are sometimes warranted.

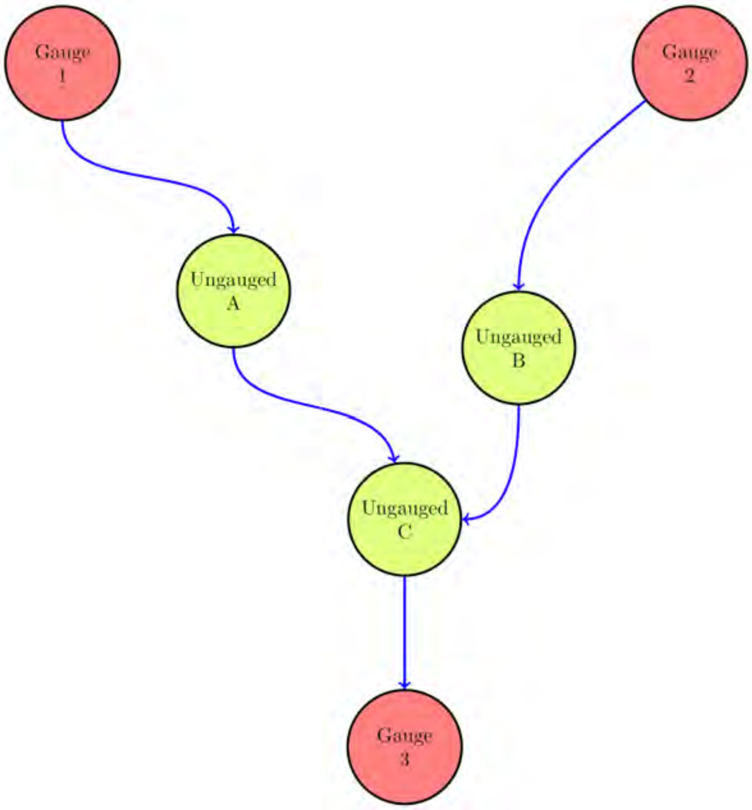


Figure 5-2 Conceptual diagram of a six-node calibration shingle, of which three nodes are ungauged

## 5.1 Constraining ungauged runoff estimates

For this Assessment, the availability of stream gauge observations and the quality of these data required a new approach in which constraints on expected runoff coefficient were used in the calibration process. Similar approaches have been used in other studies using pre-existing empirical relationships (Zhang et al., 2001; Croke and Norton, 2004: Yadav et al., 2007). Where there are no gauge data available, or the gauge data are poor, other estimates of likely rates of runoff or streamflow may be used to help guide the selection of more robust parameters. The approach taken in this Assessment is to use streamflow observations from across northern Australia to act as a guide as to what mean runoff volumes may be expected from various environmental conditions.

Runoff coefficient/actual evaporation has been shown to be influenced by climate in various empirical studies (e.g. Choudhury, 1999; Zhang et al., 2001). A similar approach has been taken here by utilising climate and streamflow records from across northern Australia in a similar way to the quoted studies, but also including catchment regolith depth estimates to generate mean runoff coefficient estimates for any catchments where such data are available. In a similar way, mean runoff coefficient estimates can be derived for future climates given assumptions or estimates of possible future climates.

Details of the method and results for ungauged catchment mean runoff coefficient estimation are given in Appendix B. Briefly, the method uses Bayesian regression to generate ensembles of parameters and estimates of mean runoff coefficient for any location. These can be used to estimate a mean and standard deviation of estimated runoff coefficient in each ungauged (or gauged) subcatchment. Such a facility also allows for estimates of future runoff coefficient in each subcatchment given some assumptions regarding future climates. These can be utilised in the model optimisation process to ensure that, for historical, and both future wet and future dry climates, runoff coefficients are what may be expected (or are acceptably close) given the generalised relationship from Appendix B. Future dry climate was represented by a 15% reduction to historical rainfall. Similarly wet climate was represented by a 15% increase to historical rainfall. These estimates are given in Table 5-1.

**Table 5-1 Estimated mean runoff coefficient and standard deviation for model subcatchments given dry future, historical and wet future climates**

| NODE ID | DRY CLIMATE† | | HISTORICAL CLIMATE | | WET CLIMATE‡ | |
|---|---|---|---|---|---|---|
| | **Mean** | **σ** | **Mean** | **σ** | **Mean** | **σ** |
| **81101670** | 0.03 | 0.0104 | 0.04 | 0.0128 | 0.06 | 0.0150 |
| **81100171** | 0.06 | 0.0083 | 0.09 | 0.0087 | 0.11 | 0.0091 |
| **81100160** | 0.06 | 0.0088 | 0.09 | 0.0089 | 0.11 | 0.0087 |
| **81100172** | 0.06 | 0.0079 | 0.08 | 0.0083 | 0.10 | 0.0085 |
| **81101700** | 0.09 | 0.0109 | 0.12 | 0.0109 | 0.15 | 0.0106 |
| **81100740** | 0.08 | 0.0084 | 0.10 | 0.0087 | 0.12 | 0.0090 |
| **81100730** | 0.08 | 0.0083 | 0.10 | 0.0085 | 0.13 | 0.0088 |
| **81100750** | 0.08 | 0.0097 | 0.10 | 0.0107 | 0.12 | 0.0117 |
| **81101134** | 0.09 | 0.0084 | 0.12 | 0.0082 | 0.14 | 0.0080 |

| NODE ID | DRY CLIMATE† | | HISTORICAL CLIMATE | | WET CLIMATE‡ | |
|---|---|---|---|---|---|---|
| **81100170** | 0.08 | 0.0088 | 0.10 | 0.0088 | 0.12 | 0.0085 |
| **81101133** | 0.09 | 0.0112 | 0.12 | 0.0112 | 0.15 | 0.0110 |
| **81101132** | 0.11 | 0.0123 | 0.13 | 0.0124 | 0.16 | 0.0123 |
| **81101135** | 0.09 | 0.0098 | 0.12 | 0.0096 | 0.15 | 0.0092 |
| **81102322** | 0.09 | 0.0083 | 0.12 | 0.0081 | 0.14 | 0.0080 |
| **81102530** | 0.10 | 0.0114 | 0.13 | 0.0114 | 0.15 | 0.0112 |
| **81102321** | 0.09 | 0.0090 | 0.12 | 0.0087 | 0.15 | 0.0084 |
| **81102320** | 0.11 | 0.0108 | 0.13 | 0.0106 | 0.16 | 0.0103 |
| **81101660** | 0.12 | 0.0108 | 0.15 | 0.0106 | 0.18 | 0.0103 |
| **81101131** | 0.11 | 0.0092 | 0.14 | 0.0088 | 0.17 | 0.0084 |
| **81101130** | 0.10 | 0.0091 | 0.13 | 0.0088 | 0.15 | 0.0085 |
| **81100181** | 0.10 | 0.0094 | 0.13 | 0.0091 | 0.16 | 0.0087 |
| **81100183** | 0.10 | 0.0085 | 0.12 | 0.0082 | 0.15 | 0.0080 |
| **81101100** | 0.11 | 0.0084 | 0.14 | 0.0081 | 0.17 | 0.0079 |
| **81100182** | 0.13 | 0.0101 | 0.16 | 0.0097 | 0.19 | 0.0094 |
| **81102380** | 0.11 | 0.0082 | 0.14 | 0.0081 | 0.16 | 0.0082 |
| **81100140** | 0.14 | 0.0123 | 0.18 | 0.0121 | 0.21 | 0.0120 |
| **81100180** | 0.12 | 0.0091 | 0.15 | 0.0087 | 0.17 | 0.0083 |
| **81100070** | 0.15 | 0.0099 | 0.18 | 0.0095 | 0.21 | 0.0093 |
| **81100120** | 0.15 | 0.0114 | 0.18 | 0.0112 | 0.22 | 0.0110 |
| **81100002** | 0.14 | 0.0088 | 0.17 | 0.0084 | 0.20 | 0.0081 |
| **81102510** | 0.11 | 0.0136 | 0.14 | 0.0137 | 0.17 | 0.0137 |
| **81100062** | 0.11 | 0.0132 | 0.14 | 0.0134 | 0.16 | 0.0134 |
| **81100061** | 0.11 | 0.0118 | 0.14 | 0.0117 | 0.17 | 0.0115 |
| **81100063** | 0.10 | 0.0101 | 0.13 | 0.0098 | 0.16 | 0.0095 |
| **81101070** | 0.13 | 0.0088 | 0.16 | 0.0084 | 0.19 | 0.0081 |
| **81100060** | 0.10 | 0.0085 | 0.13 | 0.0082 | 0.16 | 0.0079 |
| **81101010** | 0.13 | 0.0085 | 0.16 | 0.0081 | 0.19 | 0.0079 |
| **81100040** | 0.14 | 0.0107 | 0.17 | 0.0104 | 0.20 | 0.0101 |
| **81100001** | 0.11 | 0.0092 | 0.13 | 0.0099 | 0.16 | 0.0106 |
| **81100003** | 0.13 | 0.0100 | 0.16 | 0.0110 | 0.19 | 0.0122 |
| **81100000** | 0.16 | 0.0084 | 0.20 | 0.0081 | 0.23 | 0.0082 |

†Historical rainfall was decreased by 15%.
‡Historical rainfall was increased by 15%
σ Standard deviation

The calibration approach was to combine the 'shingle' approach outlined above with consideration also given to how well simulated runoff coefficient matched those expected in all model subcatchments for historical, dry and wet climates. The standard deviation of estimates can be used to calculate the probability that simulated mean runoff coefficient within a subcatchment agrees with those estimated using the generalised relationship.

Consider the following example where, for a hypothetical subcatchment, the generalised relationship predicts mean runoff coefficient to be 0.2, with a standard deviation of 0.04 (Figure 5-3).

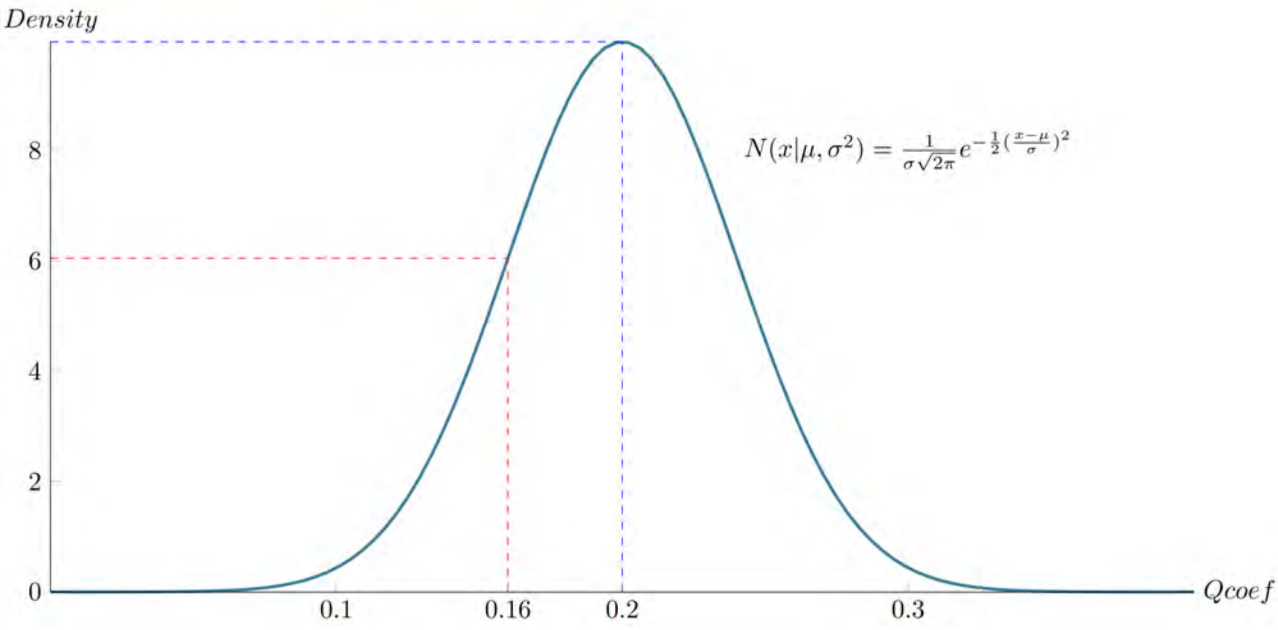


**Figure 5-3 An example of a normal probability distribution function with a mean of 0.2 and a standard deviation of 0.04**

The maximum density occurs at the mean value, 0.2. The closer a value is to the mean, the higher the density. For this example, if a simulated value in the subcatchment had a runoff coefficient of 0.16 (shown by the dashed red lines in Figure 5-3), it returns a much lower density. For use in calibration, a ratio or score can be calculated using the simulated (red dashed lines) and maximum density (blue dashed lines). In this example, the maximum density at a runoff coefficient of 0.2 is 9.97, while the density at the simulated value of 0.16 is 6.05. As a proportion of the maximum density, this is 6.05/9.97, which is 0.61. In this way, the 'goodness of fit' for any subcatchment can be calculated based on expected and simulated runoff coefficient. Mathematically the density for any normal distribution is given by:

$$N(x|\mu,\sigma^2) = \frac{1}{\sigma\sqrt{2\pi}}e^{-\frac{1}{2}\left(\frac{x-\mu}{\sigma}\right)^2} \quad (8)$$

where $x$ is the value of interest (simulated runoff coefficient for this example), $\mu$ is the mean of the normal distribution and $\sigma$ is the standard deviation. The goodness of fit for a single location can be expressed as:

$$\omega_i = \frac{N(x_i|\mu_i,{\sigma_i}^2)}{N(\mu_i|\mu_i,{\sigma_i}^2)} \quad (9)$$

where $x_i$ is the simulated mean runoff coefficient for the node $i$, while $\mu_i$ and ${\sigma_i}^2$ are the expected mean and variance of runoff coefficient for the node $i$.

The procedure for determining the goodness of fit for simulated runoff coefficient across all model nodes in a calibration shingle is similar, using the mean of all individual node values:

$$\overline{\omega} = \frac{\sum_{i=1}^{n} \omega_i}{n} \tag{10}$$

In a similar way, the suitability of ungauged runoff can be tested in drier or wetter climates. Here a reduction of annual rainfall of 15% and an increase of mean rainfall of 15% were used to test parameter suitability in future climates.

## 5.2 Calibration procedure

In each calibration shingle, the protocol for sharing parameters between gauged and ungauged nodes was pre-determined. It was considered desirable to share parameters within a shingle where possible, since this means that the shared parameter set is subject to performance constraints (i.e. goodness-of-fit measures in ungauged nodes and objective function scores at downstream gauges within the shingle). Occasionally some parameters were borrowed from nodes outside of the calibration shingle and these were read in from saved values. Calibration proceeded in three shingles. These are shown in Table 5-2.

**Table 5-2 Donor parameter and shingle information for all model nodes**

| NODE ID | DONOR ID | CALIBRATION SHINGLE |
|---|---|---|
| **81101670** | 81101670 | † |
| **81100171** | 81100160 | 1 |
| **81100160** | 81100160 | † |
| **81100172** | 81100160 | 1 |
| **81101700** | 81101130 | 1 |
| **81100740** | 81101130 | 1 |
| **81100730** | 81101130 | 1 |
| **81100750** | 81101130 | 1 |
| **81101134** | 81101130 | 1 |
| **81100170** | 81101130 | 1 |
| **81101133** | 81101130 | 1 |
| **81101132** | 81101130 | 1 |
| **81101135** | 81101130 | 1 |
| **81102322** | 81101130 | 1 |
| **81102530** | 81101130 | 1 |
| **81102321** | 81101130 | 1 |
| **81102320** | 81101130 | 1 |
| **81101660** | 81101130 | 1 |
| **81101131** | 81101130 | 1 |

| NODE ID | DONOR ID | CALIBRATION SHINGLE |
|---|---|---|
| **81101130** | 81101130 | 1 |
| **81100181** | 81100180 | 2 |
| **81100183** | 81100180 | 2 |
| **81101100** | 81100180 | 2 |
| **81100182** | 81100180 | 2 |
| **81102380** | 81100140 | 2 |
| **81100140** | 81100140 | 2 |
| **81100180** | 81100180 | 2 |
| **81100070** | 81100070 | 2 |
| **81100120** | 81100120 | 2 |
| **81100002** | 81100070 | 2 |
| **81102510** | 81100060 | 3 |
| **81100062** | 81100060 | 3 |
| **81100061** | 81100060 | 3 |
| **81100063** | 81100060 | 3 |
| **81101070** | 81101070 | 3 |
| **81100060** | 81100060 | 3 |
| **81101010** | 81100040 | 3 |
| **81100040** | 81100040 | 3 |
| **81100001** | 81100060 | 3 |
| **81100003** | 81100060 | 3 |
| **81100000** | 81100070 | 3 |

†These gauges were pre-calibrated individually.

The exceptions here are nodes 81101670 and 81100160 in the far south of the catchment. As stated previously, the gauge at node location 81100160 had a suspiciously high runoff coefficient. Calibration here utilised the predicted runoff coefficient (Table 5-2) as per other node locations, but rather than direct calibration to the gauge data, parameters were selected from a pre-calibrated library of Sacramento RR model parameters. These were calibrated at each of the gauges listed in Appendix B ($n$ = 99). Donor parameters were ranked in terms of goodness of fit to expected ungauged runoff and Nash–Sutcliffe efficiency (NSE) (Nash and Sutcliffe, 1970), and low-flow fit at gauge 8110016. Of the ten best performing donor gauges, one was selected after inspection of its hydrographs and flow duration curve. A similar procedure was conducted for gauge 81101670, only in that case, no streamflow data were available at the site, rather, the parameter set was jointly assessed at node 81101130, where a gauge was available (downstream of node 81101670) and using expected runoff coefficient for node 81101670.

Objective functions provide an opportunity for the hydrologist to influence the nature of the simulations that the model will produce. Goodness-of-fit metrics commonly used such as bias and NSE, may not be adequate to produce simulations to the satisfaction of the hydrologist. With some knowledge of how the simulations may be used, the hydrologist may require more emphasis on various components of streamflow. For example, flood studies require more emphasis on accurate peak flow representation, while some ecological studies may require more accurate low-flow representation. It should be noted that in this context the 'objective function' is used in conjunction with goodness-of-fit scores for ungauged runoff to obtain an acceptable parameter set.

In this Assessment, a series of model/objective function/parameter transfer combinations were tested in an iterative process with the aim of exploring and producing a more satisfactory collection of simulations. Broadly, these were all judged on the basis of goodness of fit at gauge locations. This Assessment builds upon the various investigations of objective functions previously used in northern Australian studies (Hughes et al., 2018; Hughes et al., 2023).

The objective function used in this Assessment is as follows:

$$OF = (2 - NSE(\sqrt{Q}) * (2 - NSE\left(FDC(Q_{hf})\right) * \left(1 + EPD(Q_{q90})\right) * \left(1 + EPD(Q_{q98})\right) * \left(1 + EPD(Q_{200})\right) * (1 + |bias|) \quad (11)$$

where EPD or error probability difference of a given flow value $x$ is defined as:

$$EPD_x = |P_x(Q_{obs} - Q_{sim})| \quad (12)$$

where $x$ is a user defined flow rate and $q_{90}$was the 90% exceedance non-zero flow (based on observed flows), $q_{98}$ was the 98% exceedance non-zero flow, and $Q_{200}$ is 200 ML/day (nominally a value below which it may be difficult to extract water via a pump). These terms are intended to place some weighting on low-flow values.

$FDC(Q_{hf})$ compares the quantile values from simulated and observed flows for exceedance values of 0, 0.001, 0.005, 0.01, 0.0115 and 0.02%. This is intended to place some calibration weighting on high flows.

The objective function returned value is minimised during optimisation and a perfect fit would have a value of 1.0. However, the final 'score' returned to the optimiser also incorporated the goodness-of-fit metric based upon expected ungauged runoff for each subcatchment for historical, dry and wet climates.

$$Score = OF * (1 + \overline{\omega}_{hist}) * (1 + \overline{\omega}_{dry}) * (1 + \overline{\omega}_{wet}) \quad (13)$$

where $\overline{\omega}_{hist}$, $\overline{\omega}_{dry}$ and $\overline{\omega}_{wet}$ are goodness-of-fit scores for ungauged runoff in historical, dry and wet climates respectively. It should be noted that the standard deviation used for calculation of ungauged runoff goodness of fit was increased to 0.03 in all cases, which is higher than the calculated values in Table 5-1. This effectively reduced the weighting of the final optimisation score on ungauged runoff scores, allowing for a better balance of performance at streamflow gauges and expected ungauged runoff.

Optimisation used the differential evolution algorithm (Ardia et al., 2010), within the R platform. The models were run for 300 iterations. The best parameter sets were selected. An additional optimisation was designed to examine parameter uncertainty within the river model. This run combined the entire catchment into a single shingle and was run for 100 iterations. Computationally, this was a costly process due to the model size and total number of parameters.

All model iterations were recorded and all parameter sets within 10% of the final calibration score of the accepted model were saved. It is acknowledged that the parameter uncertainty is only a component of the total uncertainty in streamflow estimation. Uncertainty in model inputs (particularly gridded rainfall inputs), observed streamflow (including rating curve uncertainty), catchment contributing area estimates, parameter sharing protocols, and model structure all contribute to uncertainty and are not quantified here.

# 6 Calibration results

The calibration goodness-of-fit scores at all gauges used are given in Table 6-1. Scores indicate that NSE values are acceptable, and in almost all cases the error probability distance values for low flows are also good. The exception to this is at gauge 81100180, where observations indicate that flow ceases for approximately 40% of all observations. Upstream at gauge 81101130, and just downstream at 81100070, flows are either perennial or near perennial. Simulation bias values are beyond 10% for three gauges, although these are generally where gauge confidence is lower. It must be remembered that expected ungauged runoff values also provide some constraint on simulated mean flow volumes, and in some cases, these differ substantially from apparent runoff coefficients calculated from observed flows (e.g. 81100160). Further goodness-of-fit information is available in Appendix D.

**Table 6-1 Goodness-of-fit statistics for the Victoria River model**

| NODE ID | $NSE^{0.5}$ | EPD98 | EPD90 | EPD200 | EPD500 | BIAS (%) | NSEHF |
|---|---|---|---|---|---|---|---|
| **81100160** | 0.64 | 0.04 | 0.00 | 0.01 | 0.00 | -35.1 | 0.65 |
| **81101130** | 0.85 | 0.00 | 0.05 | 0.08 | 0.05 | 10.2 | 0.99 |
| **81100140** | 0.54 | 0.31 | 0.28 | 0.05 | 0.00 | -4.5 | 0.83 |
| **81100180** | 0.88 | 0.39 | 0.35 | 0.19 | 0.14 | 0.6 | 0.93 |
| **81100070** | 0.87 | 0.00 | 0.00 | 0.04 | 0.05 | -1.1 | 0.96 |
| **81100120** | 0.40 | 0.20 | 0.17 | 0.02 | 0.01 | -16.3 | 0.25 |
| **81101070** | 0.45 | 0.04 | 0.08 | 0.01 | 0.01 | -6 | 0.91 |
| **81100060** | 0.68 | 0.00 | 0.01 | 0.01 | 0.02 | -0.1 | 0.91 |
| **Suggested good score** | >0.7 | <0.1 | <0.1 | <0.1 | <0.1 | <\|10\| | >0.9 |

Expected runoff coefficient values were a substantial part of the optimisation process and these values are presented in Figure 6-1. As can be seen, the simulated runoff coefficients were similar to the expected runoff coefficient for all subcatchments and climates. The $R^2$ of the correlation for these data was 0.88. Historical simulated mean subcatchment runoff values are plotted in Figure 6-2. The data indicate that catchment mean aridity is the major influence on simulated mean runoff coefficient, with the exception of subcatchment 811001670. At this location, expected and simulated runoff coefficient were, when adjusting for climate, lower than other subcatchments. This is because estimated subcatchment mean regolith depth at 27 m is greater than the mean value for all other subcatchments (~8 m). For more information on the calculation of expected runoff coefficient values see Appendix B.

Further to this, mean subcatchment runoff coefficient was plotted to see how consistent the spatial pattern of runoff coefficient was (Figure 6-3). In general, one would expect the spatial variation to be consistent without any abrupt changes across subcatchment boundaries, and that changes are broadly consistent with the spatial distribution of mean annual rainfall.

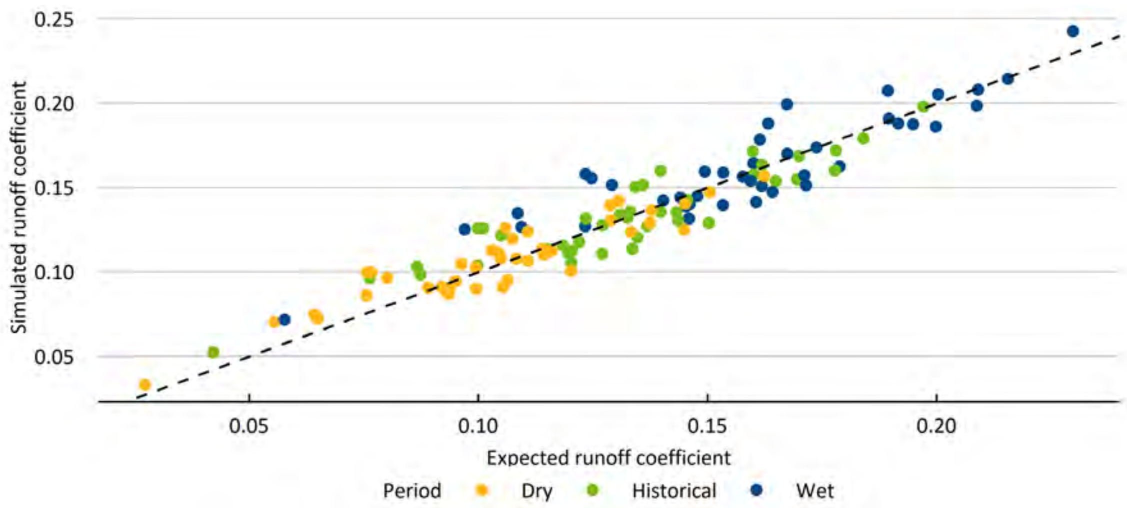


**Figure 6-1 Expected and simulated runoff coefficient for all model subcatchments for historical, dry and wet climates**

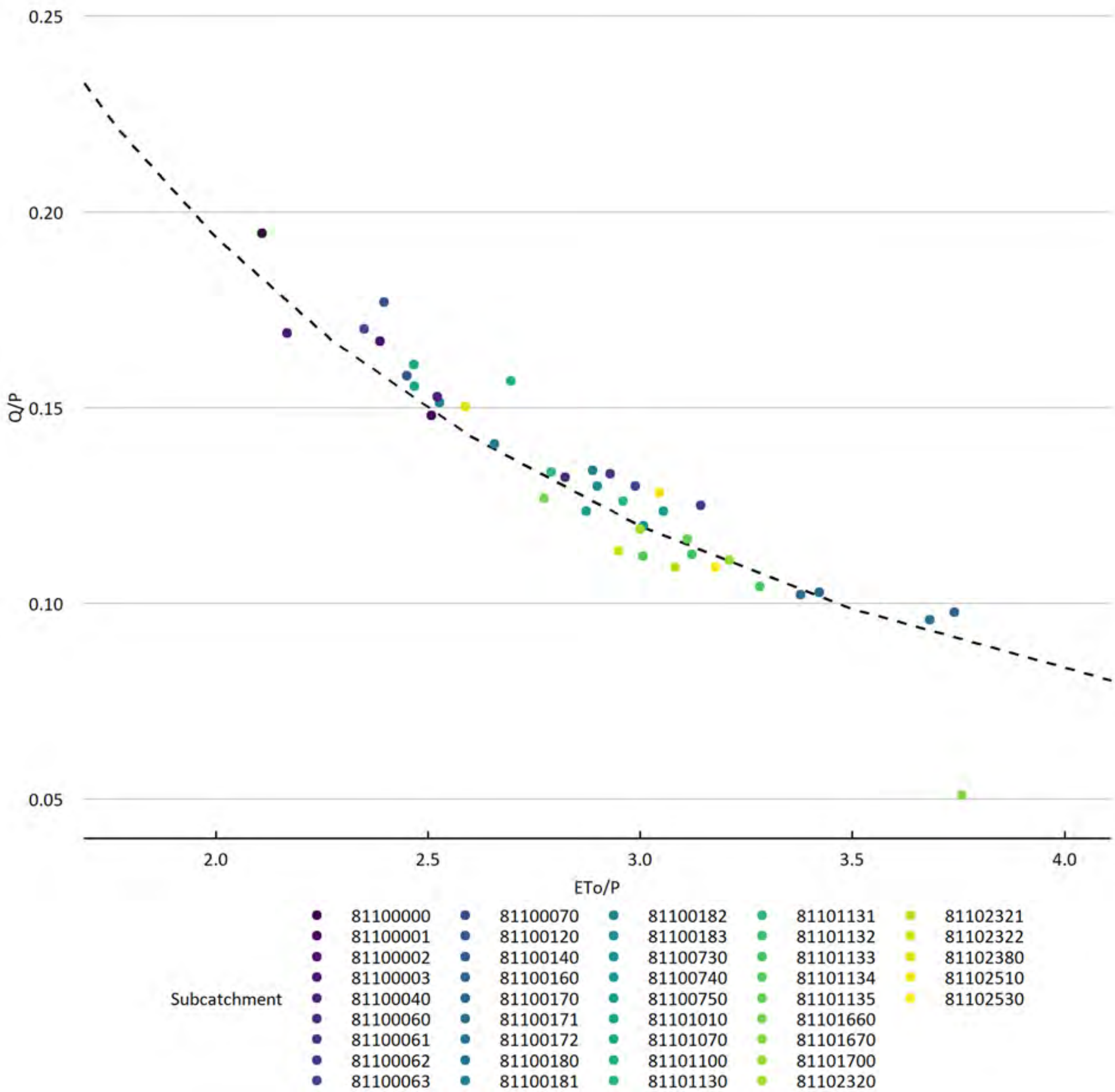


**Figure 6-2 Simulated historical mean runoff coefficient by subcatchment**

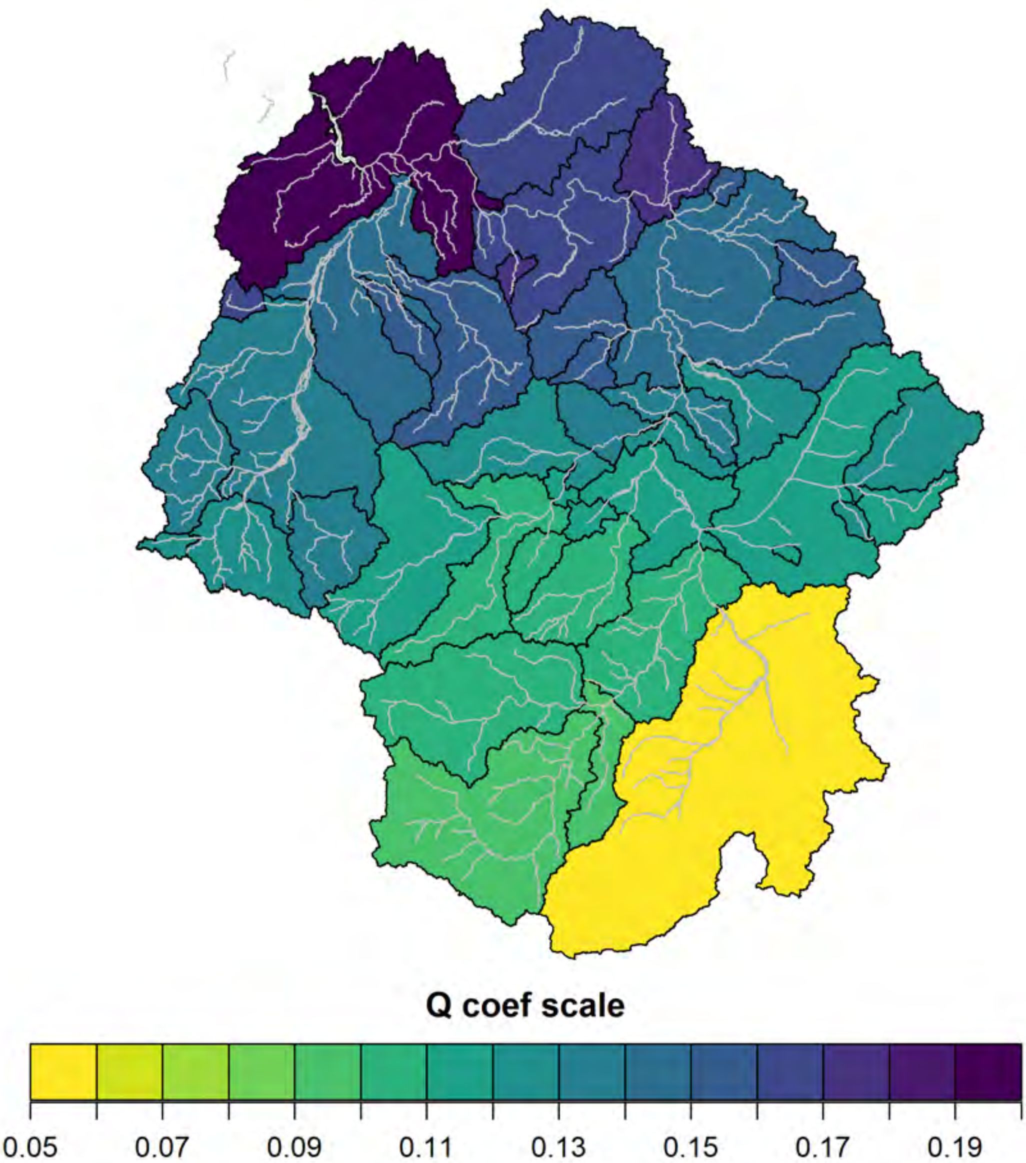


Figure 6-3 Spatial distribution of simulated mean runoff coefficient by subcatchment

Mean annual end-of-system flow from the selected calibrated model was 6990 GL. This was very similar to the end-of-system flow estimated by Petheram et al. (2009) at 6710 GL and well within one standard deviation calculated by parameter uncertainty estimates of 680 GL (Figure 6-4). System objective function scores were substantially poorer than the final optimised model score since the computational burden was high and optimisation was terminated before system objective scores could stabilise. However, it does indicate that the end-of-system flows can be reasonably variable and still regarded as 'acceptable'. Additionally, water harvest yield was tested at a single node as a part of the uncertainty analyses (node 81100060). Uncertainty analysis simulations predicted a mean yield of around 80 GL/year at this site using a pump start threshold of 500 ML/day and pump capacity of 1000 ML/day. This is much higher than the value calculated from the final accepted model of 53 GL/year. Standard deviation of the water harvest uncertainty estimates was 16 GL/year.

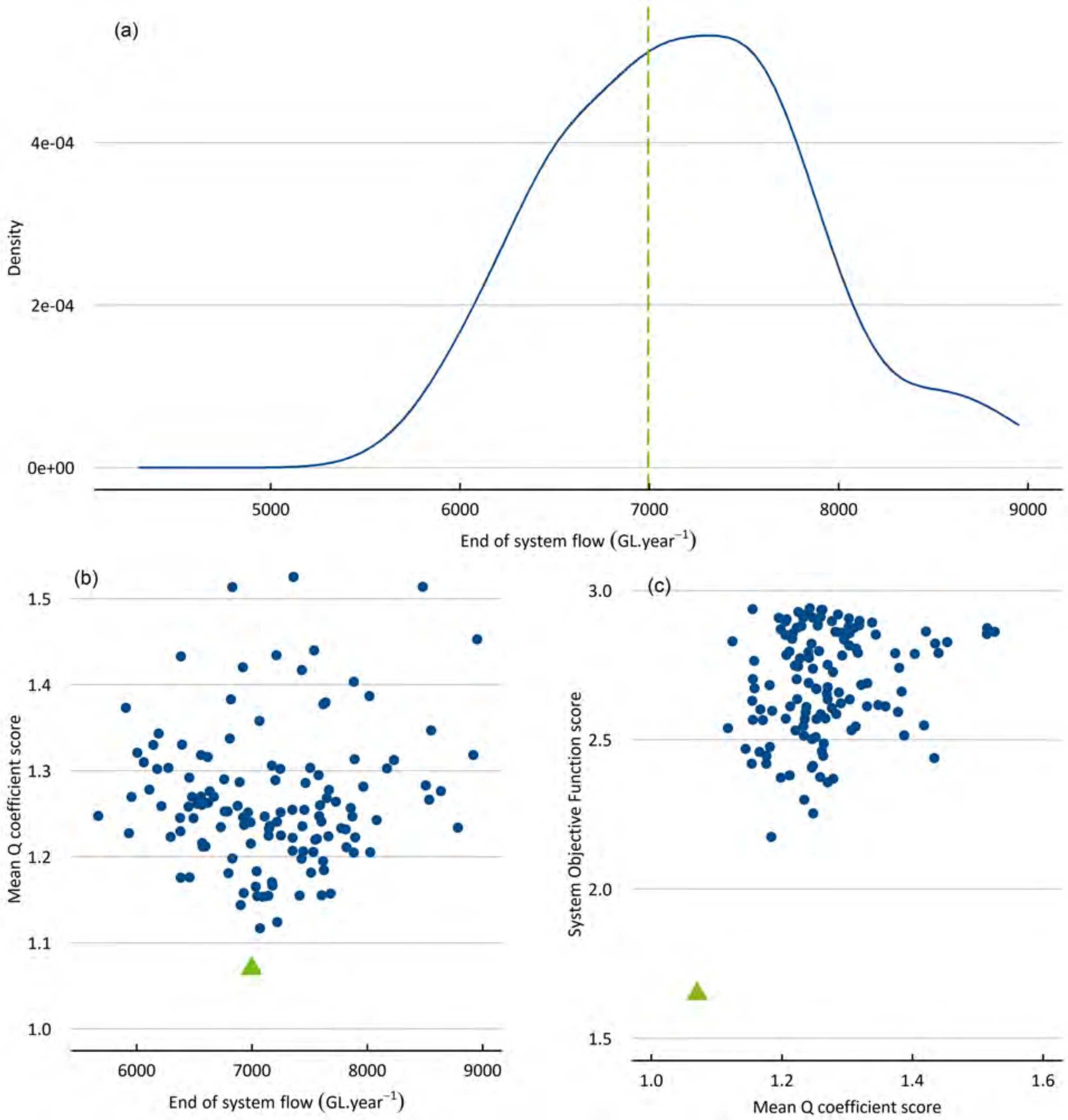


**Figure 6-4 The impact of parameter uncertainty estimates of (a) mean end-of-system flow, (b) end-of-system flow vs mean runoff coefficient score and (c) mean runoff coefficient score vs system objective function score**

Green lines and points indicate values for the selected river model parameter set.

# 7 Discussion and conclusion

The river model outlined in this report is the first of its kind to be attempted in the Victoria catchment. Previous estimates have been made for streamflow at the catchment outlet (e.g. Petheram et al., 2009), and the mean annual end-of-system flow calculated here of 6990 GL was very similar to the Petheram et al. (2009) study. Parameter uncertainty analyses suggest that alternative 'acceptable' parameter sets will generate end-of-system mean annual flow estimates that vary somewhat from those estimates (having a standard deviation of 680 GL). Internal model states for all parameter sets (flow at other nodes) were not examined, however, water harvest yields at one site were recorded and summarised. These had a coefficient of variation of around 0.3, which is substantially higher than the variation in end-of-system flow (coefficient of variation of around 0.1). This suggests that estimated water harvest yields are relatively sensitive to the magnitude and nature of flows that may be part of an acceptable river system model.

The Victoria River model was structured and calibrated to perform a wide range of water resource scenarios including diversions and future climates and estimate how these may affect the behaviour of the river system for each scenario considered. It is capable of fast simulation allowing for extensive sensitivity analyses. These requirements differ somewhat from typical jurisdictional river models that are generally designed to represent individual water licences and allocations and test water management policies.

Stream gauge data in the Victoria catchment was of limited availability and often of poor quality. This reflects the jurisdictional priority placed on flood warning as opposed to volumetric measurement within the catchment as well as the remoteness/inaccessibility of the area, particularly during the wet season. As a result, a novel technique was required to constrain model parameters. A relationship between climate, regolith depth and runoff coefficient was derived using long duration, high-quality gauged sites from across northern Australia. This was used to estimate the runoff coefficient in model subcatchments for historical and future climates. These estimates were used in the model optimisation process. While this technique was useful, there is no substitute for more and higher quality stream gauge data for more robust predictions.

Gauging data with which to estimate flow rates from stage data already available in the catchment could be collected to obtain better estimates of streamflow across the site. This is a labour intensive, expensive and often dangerous proposition, however, new technologies such as velocimetry from video footage and remotely piloted airborne and waterborne craft with various sensors may help expedite further hydrographic data collection.

# References

Allen RG, Pereira LS, Raes D and Smith M (1998), Crop evapotranspiration - Guidelines for computing crop water requirements, FAO Irrigation and drainage paper 56, FAO - Food and Agriculture Organization of the United Nations.

Ardia D, Boudt K, Carl P, Mullen KM and Peterson BG (2010) Differential evolution with 'DEoptim': an application to non-convex portfolio optimization. R Journal 3(1), 27–34. DOI:10.32614/RJ-2011-005.

Bloschl G, Sivapalan M, Wagener T, Vigliione A and Savenjie H (eds) (2013) Runoff prediction in ungauged basins: synthesis across processes, places and scales. Cambridge University Press, Cambridge.

Burnash RJC (1995) The NWS River Forecast System – Catchment Modeling. In: Vijay P Singh (ed) Computer models of watershed hydrology. Revised edition. Water Resources Publications, Highlands Ranch, Colo.

Chiew FHS and McMahon TA (1991) Applicability of Morton's and Penman's evapotranspiration estimates in rainfall-runoff modeling. Water Resources Bulletin 27, 611–620.

Chiew FHS and Leahy CP (2003) Comparison of evapotranspiration variables in evapotranspiration maps for Australia with commonly used evapotranspiration variables. Australian Journal of Water Resources 7, 111.

Choudhury B (1999) Evaluation of an empirical equation for annual evaporation using field observations and results from a biophysical model. Journal of Hydrology 216(1–2), 99–110. DOI:10.1016/S0022-1694(98)00293-5.

CSIRO (1970) Lands of the Ord-Victoria area, Western Australia and Northern Territory. Land Research Series No. 28. Commonwealth Scientific and Industrial Research Organisation, Melbourne.

CSIRO (2009a) Water in the Fitzroy region. In: CSIRO (ed) Water in the Timor Sea Drainage Division. A report to the Australian Government from the CSIRO Northern Australia Sustainable Yields Project. CSIRO Water for a Healthy Country Flagship, Australia, 61–128.

CSIRO (2009b) Water in the Gulf of Carpentaria drainage division. A Report to the Australian Government from the CSIRO Northern Australia Sustainable Yields Project. CSIRO Water for Healthy Country Flagship, Australia, xi + 479.

CSIRO (2011) Water: science and solutions for Australia. Ed. Ian Prosser. CSIRO Land and Water.

Croke BFW. and Norton JP (2004) Regionalisation of Rainfall-Runoff models, In Pahl, C., Schmidt, S., Rizzoli, A.E. and Jakeman, A.J. (eds.) Complexity and Integrated Resources Management, Transactions of the 2nd Biennial Meeting of the International Environmental Modelling and Software Society, Volume 3 pp. 1201-1207. iEMSs, June 2004.

Doble RC, Crosbie RS, Smerdon BD, Peeters L and Cook FJ (2012) Groundwater recharge from overbank floods. Water Resources Research 48.

Dutta D, Kim S, Hughes J, Vaze J and Yang A (2015) AWRA-R v5.0 Technical Report. CSIRO Land and Water.

Dutta D, Kim S, Hughes J, Vaze J, Yang A, Teng J and Lerat J (2017) Development and application of a large scale river system model for national water accounting in Australia. Journal of Hydrology 547, 124–142.

Gallant J, Read A and Dowling T. (2012) Building the national one-second digital elevation model for Australia. In: Water Information Research and Development Alliance: Science Symposium Proceedings; Melbourne. CSIRO; 2012. 250-256. csiro:EP116771. http://hdl.handle.net/102.100.100/100794?index=1.

Gan KC, McMahon TA and O'Neil IC (1990). Errors in estimated streamflow parameters and storages for ungauged catchments. Water Resources Bulletin, 36(3), 443 – 450.

Grigg AH and Hughes JD (2018) Non-stationarity driven by multidecadal change in catchment groundwater storage. A test of modifications to a common rainfall–run-off model. Hydrological Processes 32, 3675–3688.

Hughes JD, Silberstein RP and Grigg AH (2013a) Extending rainfall-runoff models for use in environments with long–term catchment storage and forest cover. Proceeding of 20th International Congress on Modelling and Simulation, Adelaide, Australia, 1–6 December 2013.

Hughes JD, Mainuddin M, Lerat J, Dutta D and Kim SSH (2013b) An irrigation model for use in river systems modelling. 20th International Congress on Modelling and Simulation, Modelling and Simulation Society of Australia and New Zealand, Adelaide.

Hughes JD, Dutta D, Vaze J, Kim SSH and Podger G (2014a) An automated multi-step calibration procedure for a river system model. Environmental Modelling and Software 51, 173–183. Viewed 4December 2023, https://doi.org/10.1016/j.envsoft.2013.09.024.

Hughes J, Dutta D, Yang A, Marvanek S, Vaze J and Mainuddin M (2014b) Improvement of AWRA-R Irrigation Model and its applications in the Murray-Darling Basin. Technical Report. CSIRO, Land and Water.

Hughes JD, Kim SSH, Dutta D and Vaze J (2016), Optimization of a multiple gauge, regulated river-system model. A system approach, Hydrological Processes, 30(12), 1955–1967, https://doi.org/10.1002/hyp.10752.

Hughes J, Yang A, Wang B, Marvanek S, Carlin L, Seo L, Petheram C and Vaze J (2017) Calibration of river system and landscape models for the Fitzroy, Darwin and Mitchell catchments. A technical report to the Australian Government from the CSIRO Northern Australia Water Resource Assessment, part of the National Water Infrastructure Development Fund: Water Resource Assessments. CSIRO, Australia.

Hughes J, Yang A, Wang B, Marvanek S, Seo L, Petheram C and Vaze J (2018) River model simulation for the Fitzroy, Darwin and Mitchell catchments. A technical report to the Australian Government from the CSIRO Northern Australia Water Resource Assessment, part of the National Water Infrastructure Development Fund: Water Resource Assessments. CSIRO, Australia.

Hughes J, Yang A, Wang B, Marvanek M, Read A, Petheram C and Vaze J (2021a) River model calibration and scenario analysis for the De Grey catchment. A report from the Transforming Agriculture in the Pilbara Project for the Western Australian Department of Primary industries and Regional Development.

Hughes JD, Potter N, Zhang L and Bridgart R (2021b) Conceptual model modification and the millennium drought of southeastern Australia. Water 13, 669. Viewed 11 January 2023, https://doi.org/10.3390/w13050669.

Hughes JD, Yang A, Marvanek S, Wang B, Petheram C and Philip S (2023) River model calibration and scenario analysis for the Roper catchment. A report from the Roper River Water Resource Assessment to the Government of Australia. CSIRO, Australia.

Jeffery SJ, Carter JO, Moodie KB and Beswick AR (2001) Using spatial interpolation to construct a comprehensive archive of Australian climatic data. Environmental Modelling and Software 16, 309–330.

Koussis AD (1980) Comparison of Muskingum method difference scheme. Journal of the Hydraulic Division ASCE 106, 925–929.

Lerat J, Egan C, Kim S, Gooda M, Loy A and Petheram C. (2013), Calibration of river models for the Flinders and Gilbert catchments. A technical report to the Australian Government from the CSIRO Flinders and Gilbert Agricultural Resource Assessment, part of the North Queensland Irrigated Agriculture Strategy. Canberra, A.C.T.: CSIRO; 2013. csiro:EP132648. https://doi.org/10.4225/08/584d96511fb59.

McJannet D, Yang A and Seo L (2023) Climate data characterisation for hydrological and agricultural scenario modelling across the Victoria, Roper and Southern Gulf catchments. A technical report from the CSIRO Victoria River and Southern Gulf Water Resource Assessments for the National Water Grid. CSIRO, Australia.

Morton FI (1983) Operational estimates of areal evapotranspiration and their significance to the science and practice of hydrology. Journal of Hydrology 66, 1–76.

Nash JE and Sutcliffe JV (1970) River flow forecasting through conceptual models part I–A discussion of principles. Journal of Hydrology 10(3), 282–290. Viewed 11 January 2023, https://doi.org/10.1016/0022-1694(70)90255-6.

NT Government (2023) Territory Water Plan: A plan to deliver water security for all Territorians, now and into the future. Office of Water Security. Viewed 17 September 2024, https://watersecurity.nt.gov.au/territory-water-plan#:~:text=Priority%20actions%20in%20the%20plan,and%20productivity%20in%20water%20use.

O'Loughlin EM (1986) Prediction of surface saturation zones in natural catchments by topographic analysis. Water Resour. Res. 22(5), 794– 804. DOI:10.1029/WR022i005p00794.

Parajka J, Viglione A, Rogger M, Salinas JL, Sivapalan M and Blöschl G (2013) Comparative assessment of predictions in ungauged basins – Part 1: Runoff-hydrograph studies. Hydrology and Earth System Sciences 17, 1783–1795. Viewed 11 January 2023, https://doi.org/10.5194/hess-17-1783-2013.

Petheram C, Philip S, Watson I, Bruce C and Chilcott C (eds) (2024) Water resource assessment for the Victoria catchment. A report from the CSIRO Victoria River Water Resource Assessment for the National Water Grid. CSIRO, Australia.

Petheram C, Rustomji P and Vleeshouwer J (2009) Rainfall-runoff modelling across northern Australia. CSIRO, Australia. Viewed 4December 2023, https://doi.org/10.4225/08/584af30de743b.

Petheram C, Rustomji P, Chiew FHS and Vleeshouwer J (2012) Rainfall–runoff modelling in northern Australia: a guide to modelling strategies in the tropics. Journal of Hydrology 462–463, 28–41. Viewed 11 January 2023, https://www.sciencedirect.com/science/article/abs/pii/S0022169412000418.

Petheram C, Watson I and Stone P (2013a) Agricultural resource assessment for the Flinders catchment. A report to the Australian Government from the CSIRO Flinders and Gilbert Agricultural Resource Assessment, part of the North Queensland Irrigated Agriculture Strategy. CSIRO Water for Healthy Country and Sustainable Agriculture flagships, Australia.

Petheram C, Watson I and Stone P (2013b) Agricultural resource assessment for the Gilbert catchment. A report to the Australian Government from the CSIRO Flinders and Gilbert Agricultural Resource Assessment, part of the North Queensland Irrigated Agriculture Strategy. CSIRO Water for Healthy Country and Sustainable Agriculture flagships, Australia.

Perrin C, Michael C and Andréassian V (2003) Improvement of a parsimonious model for streamflow simulations. Journal of Hydrology 279, 275–289.

Power and Water Authority (1987). Baseflow water quality surveys in the Northern Territory. Volume 5, Fitzmaurice and Victoria Rivers. Report 10/1987. Water Quality Section, Water Resources Group. Darwin.

Sivapalan M (2003) Prediction in ungauged basins: a grand challenge for theoretical hydrology. Hydrological Processes 17, 3163–3170. Viewed 11 January 2023, https://doi.org/10.1002/hyp.5155.

Srivastava PK, Han D, Rico-Ramirez MA and Islam T (2014) Sensitivity and uncertainty analysis of mesoscale model downscaled hydro-meteorological variables for discharge prediction. Hydrological Processes 28, 4419–4432. https://doi.org/10.1002/hyp.9946.

Taylor AR, Hughes J, Philip S, Pritchard J, Marvanek S, Wilson PR, McJannet, D, Karim F, Want B, Petheram C and Crosbie R (2024). Chapter 2: Physical environment of the Victoria catchment. In: Petheram C, Philip S, Watson I, Bruce C and Chilcott C (eds) (2024) Water resource assessment for the Victoria catchment. A report from the CSIRO Victoria River Water Resource Assessment for the National Water Grid. CSIRO, Australia.

Thomas M, Philip S, Stockmann U, Wilson PR, Searle R, Hill J, Gregory L, Watson I and Wilson PL (2024) Soils and land suitability for the Victoria catchment, Northern Territory. A technical report from the CSIRO Victoria River Water Resource Assessment for the National Water Grid. CSIRO, Australia.

Viney N, Vaze J, Crosbie R, Wang B, Dawes W and Frost A (2015) AWRA-L v5.0: Technical description of model algorithms and inputs.

Wang QJ, McConachy FLN, Chiew FHS, James R, de Hoedt GC and Wright WJ (2001) Climatic atlas of Australia, maps of evapotranspiration.

Yadav M, Wagener T and Gupta H (2007) Regionalization of constraints on expected watershed response behaviour for improved predictions in ungauged basins. Advances in Water Resources, 30, 1756–1774, DOI:10.1016/j.advwatres.2007.01.005.

Yang A, Petheram C, Marvanek S, Baynes F, Rogers L, Ponce Reyes R, Zund P, Seo L, Hughes J, Gibbs M, Wilson PR, Philip S and Barber M (2024) Assessment of surface water storage options in the Victoria and Southern Gulf catchments. A technical report from the CSIRO Victoria River and Southern Gulf Water Resource Assessments for the National Water Grid. CSIRO Australia

Zhang Z and Dawes W (1998) WAVES – an integrated energy and water balance model. CSIRO Land and Water Technical Report No. 31/98. CSIRO Land and Water, Canberra.

Zhang L, Dawes W and Walker G (2001) Response of mean annual ET to vegetation changes at catchment scale. Water Resources Research 37(3), 701–708.

Page deliberately left blank

# Part II Appendices

# Appendix A Morton's wet area potential ET calculation

```
static double CalculateETwp(DateTime today, double Elevation, double Latitude, double tmax,
            double tmin, double eact, double radin, out double RH)
        {
            double height, lat, tavg, esat, pratio, gammap, pdelta,
                   pi, psai, dr, delta, omega, radextra, radinnet, radout, radnet,
                   nNratio, _as, bs, albedo, sigma, term1, term2, term3, fz, ediff, stabfac,
                   Dpfact, vptc, htc, xesat, xtemp, xdelta, tempinc, radnetx, ETpp, ETppx, ETwp,
                   tdiff, esatMax, esatMin, esatMean, ea;

            int julday;

            //psea = 101.3;       //kPa
            pi = 3.1415927;
            _as = 0.25;         // Angstorm formula, regression constant
            bs = 0.50;          // Angstorm formula, regression constant
            albedo = 0.23;
            sigma = 4.903E-9;   // Stefan-Boltzmann constant

            height = Elevation;
            lat = Latitude;

            if (tmax <= -99.0 || tmin <= -99.0 || eact <= -99.0 || radin <= -99.0) // ||  esat <= -99.0 ||
radin == 0 ) //|| sunhrs <= -99.0)
            {
                ETpp = -99.0;
                ETwp = -99.0;
                ea = -99.0;
                RH = -99.0;
                tavg = -99.0;
            }
            else
            {
                tavg = (tmax + tmin) / 2.0;

                //calculate esat

                //formula 35
                esatMax = 0.6108 * Math.Exp(17.27 * tmax / (tmax + 237.3));
                esatMin = 0.6108 * Math.Exp(17.27 * tmin / (tmin + 237.3));
                esatMean = 0.6108 * Math.Exp(17.27 * tavg / (tavg + 237.3));
```

```
//formula 43
ea = 0.25 * esatMax + 0.5 * esatMean + 0.25 * esatMin;
esat = ea;

if (esat <= 0.0) esat = 0.0001;
if (eact <= 0.0) eact = 0.0001;
if (eact > esat) eact = esat;

RH = eact / esat;

//     Calculate ratio of atmospheric at the station to that at the sea level (Pstn/Psea)
pratio = Math.Pow((293.0 - 0.0065 * height) / 293.0, 5.26);

//     Calculate psychrometric constant (kPa/C)
if (tavg >= 0.0)
    gammap = 0.066 * pratio;
else
    gammap = 0.0574 * pratio;


//     Calculate slope of saturation vapour pressure/temperature curve (kPa/C)

if (tavg >= 0.0)
    pdelta = (4098.0 * esat) / Math.Pow((tavg + 237.3), 2);
else
    pdelta = (5809.0 * esat) / Math.Pow((tavg + 265.5), 2);


//     Calculate extraterrestrial radiation (Ra=radextra)   (MJ/m2/day)

psai = (lat / 180.0) * pi;

julday = today.DayOfYear;
dr = 1.0 + 0.033 * Math.Cos(0.0172 * Convert.ToDouble(julday));
delta = 0.409 * Math.Sin(0.0172 * Convert.ToDouble(julday) - 1.39);
omega = Math.Acos(-1.0 * Math.Tan(psai) * Math.Tan(delta));
radextra = (118.1 / pi) * dr * (omega * Math.Sin(psai) * Math.Sin(delta) + Math.Cos(psai)
* Math.Cos(delta) *Math.Sin(omega));

// Calculate nNratio based on radin

nNratio = (radin / radextra - _as) / bs;

//     Calculate NET incoming solar radiation (Rns=radinnet)

radinnet = (1.0 - albedo) * radin;

//     Calculate net outgoing longwave radiation (Rnl=radout)
```

```
            term1 = (Math.Pow((tmax + 273.16), 4) + Math.Pow((tmin + 273.16), 4)) / 2.0;
            term2 = (0.34 - 0.14 * Math.Sqrt(eact)) * (0.10 + 0.9 * nNratio);
            radout = sigma * term1 * term2;
            if (radout < 0.0) radout = 0.0;

            //     Calculate net radiation (Rn) : if negative set it to zero

            radnet = radinnet - radout;
            if (radnet < 0.0) radnet = 0.0;

            //     Calculate stability factor(stabfac), vapour pressure transfer
            //    coefficient(fa=vptc)and heat transfer coeffieient(lamda=htc)

            if (tavg >= 0.0)
                fz = 24.19;
            else
                fz = 27.82;



            ediff = esat - eact;
            if (ediff <= 0.0) ediff = 0.0001;
            term3 = gammap * (Math.Sqrt(1.0 / pratio)) * fz * ediff; //
term3=gammap*((1.0/pratio)**0.5)*fz*ediff !!!can be wrong because of Jai
            stabfac = 1.0 / (0.28 * (1.0 + eact / esat) + pdelta * radnet / term3);
            if (stabfac < 1.0) stabfac = 1.0;               //!!!!! MODIFICATION

            vptc = (Math.Sqrt(1.0 / pratio)) * fz / stabfac;  //vptc=((1.0/pratio)**0.5)*fz/stabfac
            htc = gammap + (1.804E-8 * Math.Pow((tavg + 273.0), 3)) / vptc; //htc=gammap+(1.804E-
8*(tavg+273.0)**3)/vptc;

            //     Carryout iterative procedure to satisfy the energy balance and obtain
            //     equlibrium quantities

            xesat = esat;
            xtemp = tavg;
            xdelta = pdelta;

            do
            {
                tempinc = (radnet / vptc + eact + htc * (tavg - xtemp) - xesat) / (xdelta + htc);
                tdiff = Math.Abs(tempinc);
                if (tdiff < 0.01)
                    break;
                else
                {
                    xtemp = xtemp + tempinc;
                    if (xtemp >= 0.0)
```

```
                xesat = 0.6108 * Math.Exp((17.27 * xtemp) / (xtemp + 237.3));
            else
                xesat = 0.6108 * Math.Exp((21.88 * xtemp) / (xtemp + 265.5));


            if (xtemp >= 0.0)
                xdelta = (4098.0 * xesat) / Math.Pow((xtemp + 237.3), 2);
            else
                xdelta = (5809.0 * xesat) / Math.Pow((xtemp + 265.5), 2);
        }

    } while (true);


    ETppx = radnet - htc * vptc * (xtemp - tavg);
    ETpp = ETppx * 0.408;
    if (ETpp < 0.0) ETpp = 0.0;

    //     Calculate Morton Wet Environment Areal Potential Evapotranspiration. ETwp

    radnetx = ETppx + gammap * vptc * (xtemp - tavg);
    Dpfact = xdelta / (gammap + xdelta);
    ETwp = 0.408 * (1.2096 + 1.2 * Dpfact * radnetx);
}

return ETwp;
}
```

# Appendix B Constraining ungauged runoff estimates with space for time substitution

## B.1 Introduction

Hydrological prediction relies on the use of models to estimate hydrological response from a given set of inputs (usually climate). The nature of the model used will vary with the model context and the nature of products or information required from it. Regardless, even the simplest models require parameters of some form. For physically based models, parameters may be a measurable, real physical property, whereas for 'conceptual' models or empirical models, the parameters themselves will have no physical meaning. Conceptual models require 'calibration' (i.e. parameters are adjusted with reference to some observation of interest until the model can reproduce the observed behaviour). The assumption is that the calibrated parameters and the model itself implicitly capture the system behaviour allowing prediction outside of the calibration conditions.

The ability of a model to simulate outputs that are closely matched to observations may be thought to validate the model and its hypothesis of catchment processes. However, it is recognised that this is not the case for both conceptual and physically based models due to problems associated with parameter identifiability (Ibbit and O'Donnell, 1971; Sorooshian and Gupta, 1983; Hooper et al., 1988; Beven 1889; Jakeman and Hornberger, 1993), viz. many different parameter sets can provide a reasonably good agreement between observations and model simulation. Of the various acceptable parameter sets, model behaviour for an independent period or location can be highly variable.

Improvement in model identifiability generally relies upon the use of new or additional information in the model calibration process (Kuczera and Mroczkowski, 1998), and/or multiple objectives used in calibration (Booij and Krol, 2010). Furthermore, longer calibration time series can improve model predictive performance (Razavi and Tolson, 2013; Yang et al., 2022). While calibration issues related to equifinality have provided difficulties, the parameter selection process for ungauged catchments is more difficult again since the actual hydrological response is unknown. In these instances, parameters must be estimated by other means. The difficulties and strategies related to predicting hydrological response in ungauged catchments triggered the 'Prediction in Ungauged Basins' initiative by the IAHS in 2003 (Sivapalan, 2003). Subsequently, there have been numerous studies that have examined methods of estimating parameter values in ungauged catchments (see Bloschl, 2013; Parajka, 2013). The process of parameter estimation in this context is generally termed 'regionalisation', and the two most common techniques are:

1. nearest neighbour (NN)

2. hydrological response unit (HRU).

NN relies on a nearby catchment/gauge to derive parameters that are then used in the ungauged catchment, while HRU approaches use various physical descriptors to find 'similar' catchments from which parameters are received. Typically, factors such as slope, geology, land use and climate are used as physical descriptors. While many studies have compared regionalisation methods (Nathan and McMahon, 1990; Oudin et al., 2006; Post, 2009; Petheram et al., 2012), there has been no consistency in the reported results. Context and model requirements will generally heavily influence the suitability of any methods used for parameter estimation. For example, future climate studies may require a hydrological model to predict hydrological response to conditions quite unlike those used for calibration. These will generally result in poor prediction (Vaze et al., 2010). How then can parameters be selected for ungauged areas that can also be used for future climate studies with confidence?

For any predicted future climate, the possibility exists that, for a given location, a similar climate exists in the present at another location. If this is true, then the system behaviour at another location may be a reasonable indicator of the future climate response in the location of interest. This is sometimes called a 'space for time substitute' and is often used in ecological studies where simulation of future climate effects is very difficult (Koltermann, 1992; Blois et al., 2013). Space for time substitution is common in hydrology, and while the phrase is not used in such examples, the concept nonetheless is applied in generalised relationships between climate and either runoff or actual evaporation. These relationships use data from many observations/locations for their derivation (Budyko, 1974; Choudhury, 1999; Zhang et al., 2001), and act as a general guide for the effect of climate on water balance.

The thesis in this Assessment is that where no streamflow data exists or it is of limited duration and quality, a space for time approach based on observations from northern Australia may be able to provide some constraint with regard to parameter selection, viz, parameter sets that substantially deviate from generalised relationships between climate and runoff can be eliminated. Similarly, the same relationships can be used to gauge the veracity of parameter sets for future climates, thereby providing for more robust future climate estimates of hydrological response. An empirical approach based on observed data was used as means for predicting long-term runoff (Q) in areas where no streamflow data exists.

## B.2 Method

Northern Australia has some unique hydrological properties that make prediction difficult. Intensity, inter-annual and intra-annual variability of rainfall is very high (Petheram et al., 2008, 2012). For these reasons observations from northern Australia were used to construct generalised 'space for time' relationships. Catchments were selected in the region that had long records, had a low proportion of missing data, and were of good quality according to gauging data/rating curves. Sites were selected to cover a range of climates, of which the more arid areas were less numerous (Apx Figure B-1 and Apx Table B-1). Climate data was obtained from SILO (http://www.longpaddock.qld.gov.au/silo/; Jeffrey et al., 2001) and mean daily climate variables were calculated for each stream gauge using grids that were coincident with gauge contributing area.

For each SILO grid, for each day, Morton's wet area potential ET (ETo) was calculated (Morton, 1983). Mean catchment aridity was calculated by dividing mean catchment ETo by mean catchment precipitation (P), while runoff coefficient was calculated by dividing mean catchment runoff (Q) by mean catchment P.

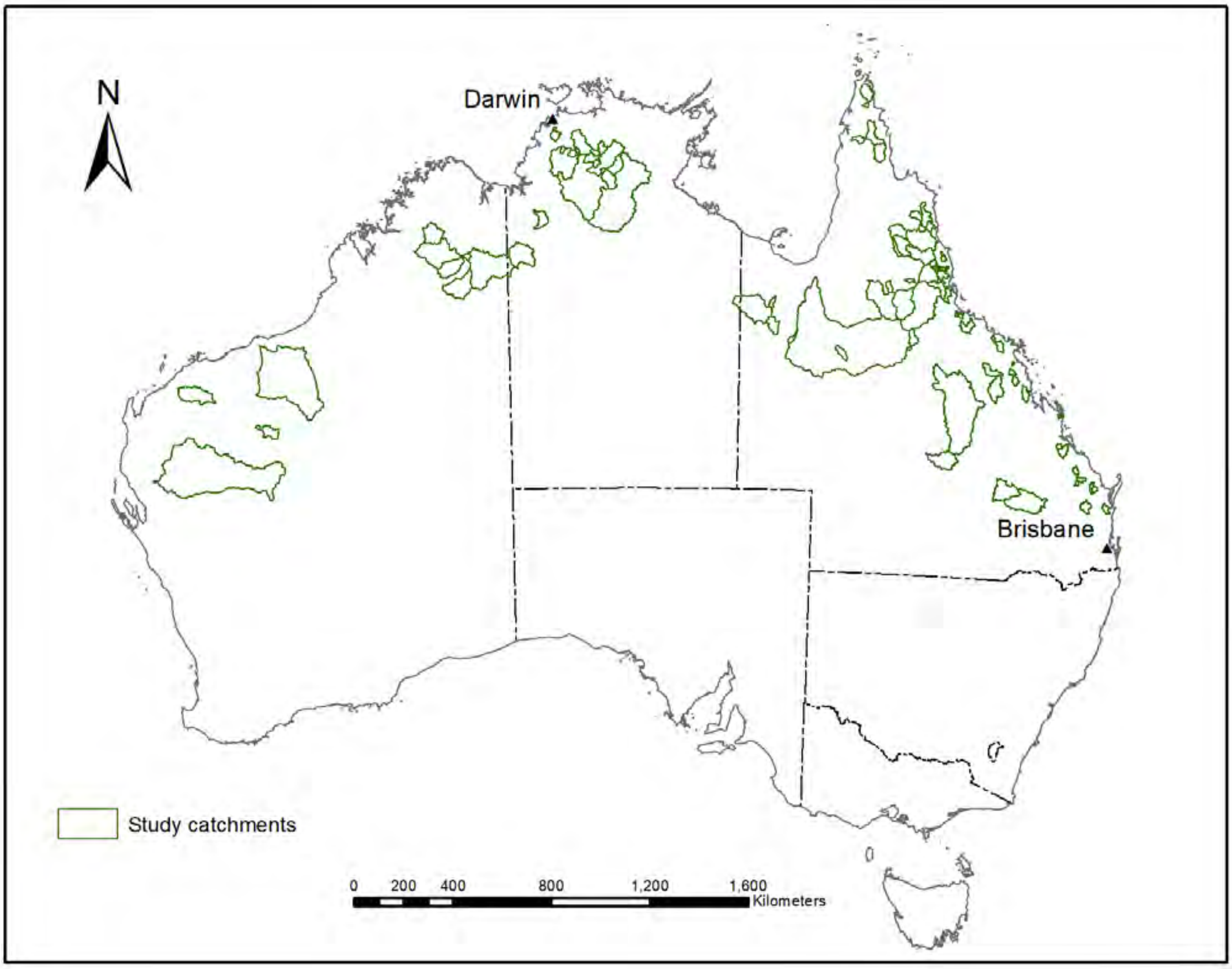


**Apx Figure B-1 Surface water catchments (*n* = 99) used to derive relationships between runoff, climate and regolith depth**

Initial regression testing between climate data and catchment runoff suggested that catchments in ‘rockier’ areas, as judged from aerial images, appeared to have higher runoff than others after accounting for climate. To explore this relationship more thoroughly, we sought to include data for ‘rockiness’ that was able to test these observations. Accordingly, The Soil Landscape Grid of Australia (Grundy et al., 2015) data were used to obtain estimates of regolith depth for each catchment. More specifically, mean estimated regolith depth (Wilford et al., 2015) for each 30 × 30 m grid cell was aggregated to derive a mean catchment regolith depth for further analyses. Regolith depth across the study area is shown in Apx Figure B-2. While study catchments covered a wide range of regolith depths, most catchments were clustered around regions of shallower regolith. This may be partly due to the favourability of rocky, constricted areas for stream gauging. To test the effect of both regolith depth and climate on hydrological response, a linear mixed model was utilised as a means of examining these factors, but also accounting for possible regional differences across northern Australia.

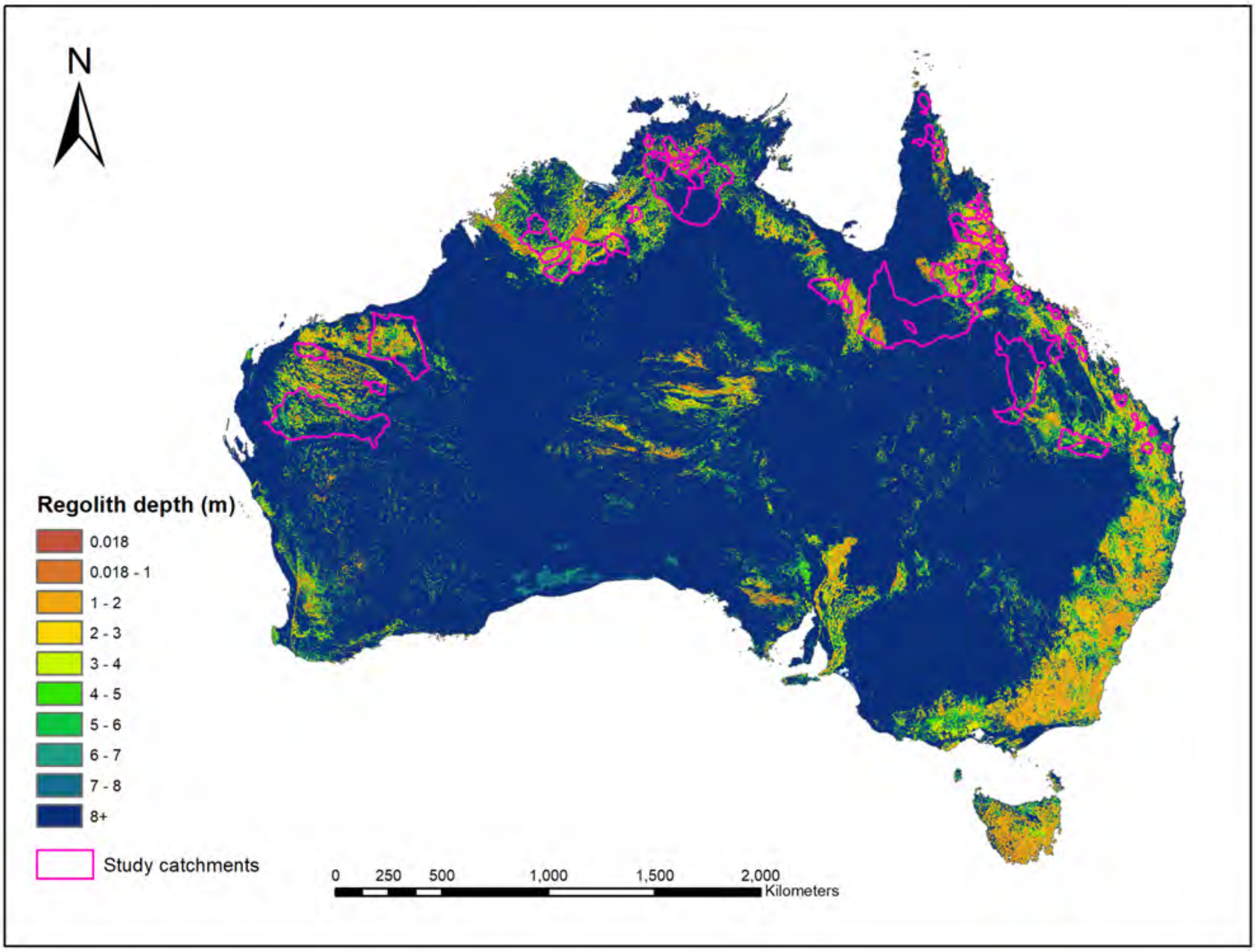


Apx Figure B-2 Mean regolith depth (Soil Landscape Grid of Australia) and study catchments

### B.2.1 Linear mixed model

The generalised form of a linear model with two covariates is as follows:

$$y_i = \beta_0 + \beta_1 x_{i1} + \beta_2 x_{i2} + \epsilon_i \tag{14}$$

where $\beta_0$ is the population *y*-intercept (value of $y$ when all partial slopes equal zero), $\beta_1$, $\beta_2$, are the partial population slopes of $Y$ on $X_1$ and $X_2$, respectively holding the other *X* constant. $\epsilon_i$ is the random unexplained error or residual component. Re-writing this in matrix notation (for a generalised case):

$$\mathbf{y} = \mathbf{X\beta} + \boldsymbol{\epsilon} \tag{15}$$

$$\boldsymbol{\epsilon} \sim N_{\mathrm{n}}(\mathbf{0}, \sigma^2 \mathbf{I_n}) \tag{16}$$

where $\mathbf{y} = (y_1, y_2, \dots, y_n)$ is the response vector; $\mathbf{X}$ is the model matrix (of $n * p$ dimensions), $\boldsymbol{\beta} = (\beta_1, \beta_2, \dots, \beta_p)$ is the vector of regression coefficients; $\boldsymbol{\epsilon} = (\epsilon_1, \epsilon_2, \dots, \epsilon_n)$ is the vector of errors; $N_{\mathrm{n}}$ represents the *n*-variable multivariate-normal distribution; $\mathbf{0}$ is an $(n * 1)$ vector of zeroes; and $\mathbf{I_n}$ is the order-*n* identity matrix. The error term in this generalised format is a 'random' effect, in that its value is not a single number (it varies randomly with each value of *i*), unlike those in the coefficient vector, which are fixed. In this way, the coefficients may be thought of as 'fixed' terms.

Mixed models, or 'mixed effects' models are similar to the model above, but include additional random effects terms, and are appropriate for representing clustered or dependent data (such as some categorical classification). For example, if some data has three levels of categorical data, rather than expressing a linear model for each of the three categories, these data are combined within the one model with random effects for those categories.

Using matrix notation, a generalised form of a mixed effects model is as follows:

$$\mathbf{y}_i = \mathbf{X_i}\boldsymbol{\beta} + \mathbf{Z}_{\boldsymbol{i}}\mathrm{b}_{\boldsymbol{i}} + \boldsymbol{\epsilon}_{\boldsymbol{i}} \tag{17}$$

$$\mathrm{b}_{\boldsymbol{i}} \sim \boldsymbol{N_q}(\mathbf{0}, \boldsymbol{\Psi}) \tag{18}$$

$$\boldsymbol{\epsilon}_{\boldsymbol{i}} \sim \boldsymbol{N_n}(\mathbf{0}, \boldsymbol{\sigma}^{\mathbf{2}}\Lambda_{\boldsymbol{i}}) \tag{19}$$

where,

$\mathbf{y}_i$ is the $n_i * 1$ response vector for observations in the *i*th group

$\mathbf{X_i}$ is the $n_i * p$ model matrix for the fixed effects for observations in group *i*

$\boldsymbol{\beta}$ is the $p * 1$ model matrix for the fixed effects for observations in group *i*

$\mathbf{Z}_{\boldsymbol{i}}$ is the $n_i * q$ model matrix for the random effects for observations in group *i*

$\mathrm{b}_{\boldsymbol{i}}$ is the $q * 1$ vector of random-effect coefficients for group *i*

$\boldsymbol{\epsilon}_{\boldsymbol{i}}$ is the $n_i * 1$ vector of random-effect coefficients for group *i*

$\boldsymbol{\Psi}$ is the $q * q$ covariance matrix for the random effects

$\boldsymbol{\sigma}^{\mathbf{2}}\Lambda_{\boldsymbol{i}}$ is the $n_i * n_i$ covariance matrix for the errors in group *i*.

For this Assessment the mean runoff coefficient (Q/P) was calculated for 99 catchments across northern Australia. This was the response vector used for subsequent modelling. In each catchment, for the concurrent period of streamflow observation, mean aridity (ETo/P) was also calculated along with the mean regolith depth as the model matrix (fixed effects). Author defined 'zones' were also included as the grouping for random effects (Apx Figure B-3).

These groupings were included since there may be unknown regional influences on catchment hydrological response, including the jurisdiction responsible for collection of stream data. In Australia, state governments are the jurisdictions responsible for stream data collection and the state boundaries can be seen in Apx Figure B-1.

The distribution of data was skewed in most cases, and relationships between dependent and independent data were nonlinear. Accordingly, data were transformed and rescaled prior to model fitting.

Linear mixed models were fitted using R software (R Core Team, 2021) and the 'lme4' package (Bates et al., 2015). Noting that transformed and scaled independent variables for aridity and regolith depth were denoted 'scaleArid' and 'scaleRocky' respectively, while transformed and scaled runoff coefficient was denoted 'scaleQcoef'. A linear model without any consideration of region (i.e. without random effects) was also considered for comparison. This model was denoted 'multiple linear regression', and results are shown for the two model versions in Apx Figure B-4.

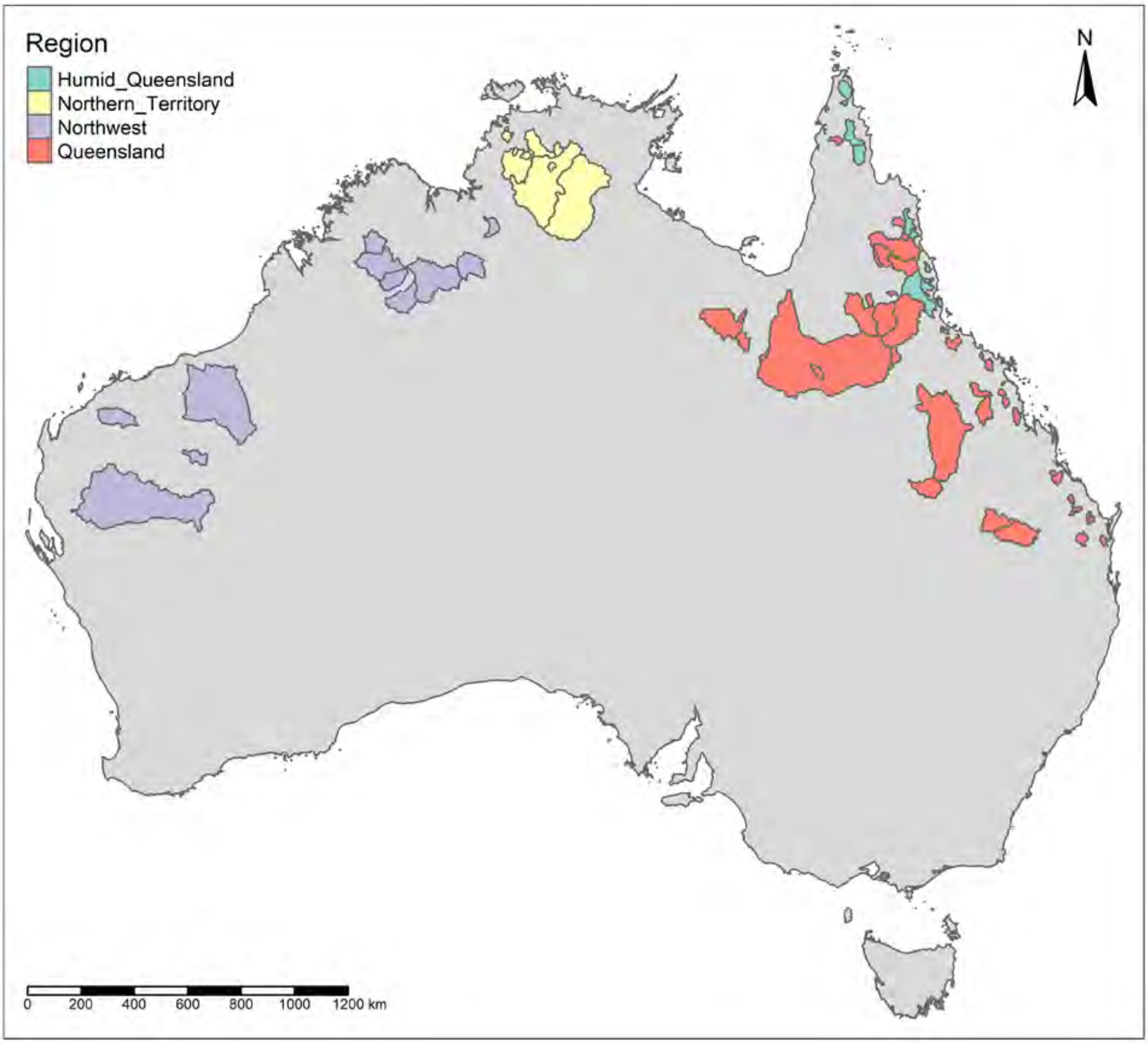


**Apx Figure B-3 Regional classification assigned to study catchments**

Comparison of the two models is not entirely simple since the methods use different measures of performance. Calculation of $R^2$ for mixed effect predictions, at 0.80, is very similar to those from the multiple linear regression model (0.76). Further, the magnitude of random-effect category 'regions' variance is only 20% of the residual variance and is therefore of marginal benefit. The predicted and observed data from the linear mixed model can be seen in Apx Figure B-5. These data indicate that the general pattern of predicted runoff coefficient is good, although observed variance is obviously higher. An inconvenience of the linear mixed effects predictions is how difficult it is to understand the model uncertainty/confidence interval. For this reason, a Bayesian approach to prediction was also tested. This has the advantage of conveniently generating prediction ensembles that can be used to estimate uncertainty for each prediction.

| | Multiple linear regression | Linear mixed model |
|---|---|---|
| R code | `lm(scaleQcoef ~ scaleArid + scaleRocky, data = ...)` | `lmer(scaleQcoef ~ scaleArid + scaleRocky + (1\|region), data = ...)` |

**Results – Multiple linear regression**

| | Dependent variable: Runoff coefficient |
|---|---|
| Aridity | -0.810*** |
| | (0.053) |
| Regolith depth | -0.150*** |
| | (0.053) |
| Constant | 0.000 |
| | (0.049) |
| Observations | 99 |
| R2 | 0.763 |
| Adjusted R2 | 0.758 |
| Residual Std. Error | 0.492 (df = 96) |
| F Statistic | 154.302*** (df = 2; 96) |
| Note: | *p<0.1; **p<0.05; ***p<0.01 |

**Results – Linear mixed model**

| | Dependent variable: Runoff coefficient |
|---|---|
| Aridity | -0.742*** |
| | (0.068) |
| Regolith depth | -0.153*** |
| | (0.054) |
| Constant | 0.043 |
| | (0.124) |
| Observations | 99 |
| Log Likelihood | -69.760 |
| Akaike Inf. Crit. | 149.521 |
| Bayesian Inf. Crit. | 162.497 |
| Note: | *p<0.1; **p<0.05; ***p<0.01 |

**Apx Figure B-4 A comparison of a multiple linear regression model and a linear mixed effects model of the catchment data**

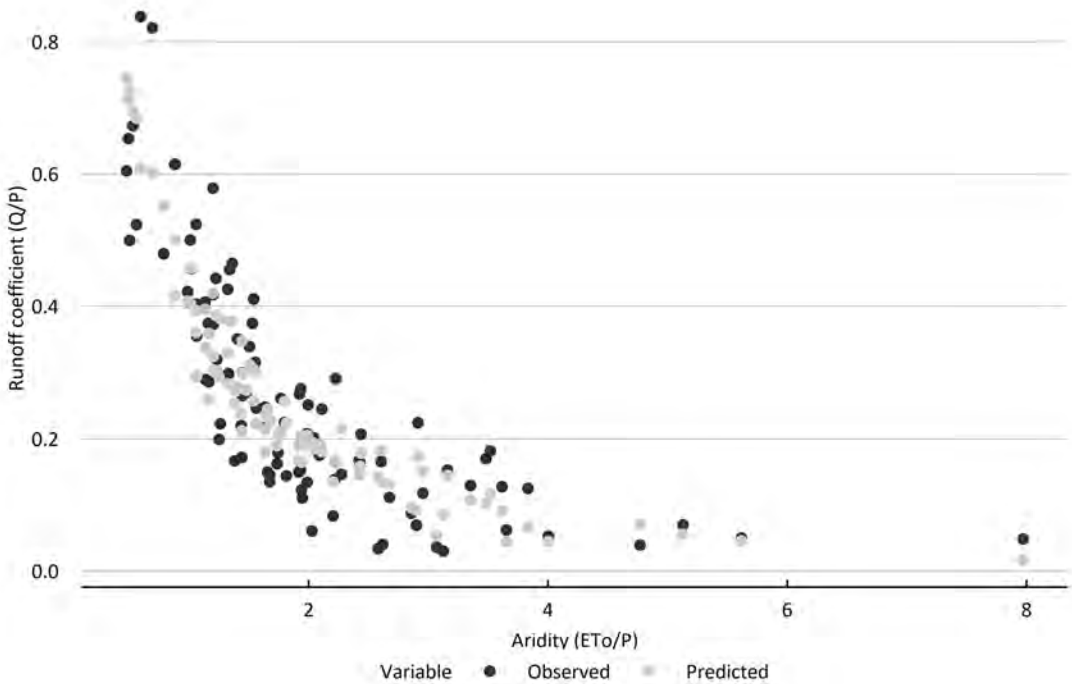


**Apx Figure B-5 Observed and predicted runoff coefficient for study catchments using a linear mixed effects model**

### B.2.2 Bayesian regression

A Bayesian model of runoff coefficient was run and compiled in R software using the 'rjags' package (Plummer, 2022). R code to build the model using rjags format is shown in Apx Figure B-6.

```
multi_model <- "model{
    # Likelihood model for Y[i]
    for(i in 1:length(Y)) {
    Y[i] ~ dnorm(m[i], s^(-2))
    m[i] <- a + b * X[i] + b2 * X2[i]
    }
    # Prior models for a, b, s
    a ~ dnorm(0.0, 1.5^(-2))
    b ~ dnorm(0, 0.5^(-2))
    b2 ~ dnorm(0, 0.5^(-2))
    s ~ dunif(0, 1.2)
    }"
```

Apx Figure B-6 R code to build the model using rjags

This regression uses the same data and model terms as the multiple linear regression, with the exception being that the Bayesian method includes an error estimate for which parameter distributions are estimated. Similarly, distributions are derived for model covariates which enables for posterior prediction estimates, one of the strengths of the method. The rjags method uses a Gibbs sampler to generate the posterior estimates. The Markov chain Monte Carlo (MCMC) chains were run for 5000 iterations after a burn in of 1000 iterations. These exhibited good mixing properties and posterior parameter values at peak density were similar to the estimates obtained by the linear mixed effects model (Apx Figure C-7). Using the model and ensemble of posterior parameter estimates, an estimate of mean runoff coefficient could be made for any location in northern Australia where climate and regolith depth data were available (Apx Table B-2). An example of this can be seen in Apx Figure B-8.

The method allows predictions of mean runoff coefficient to be made in ungauged locations and can also be used to estimate future climate runoff coefficient (where the future climate is within range of calibration data) and provides uncertainty estimates for each of those predictions.

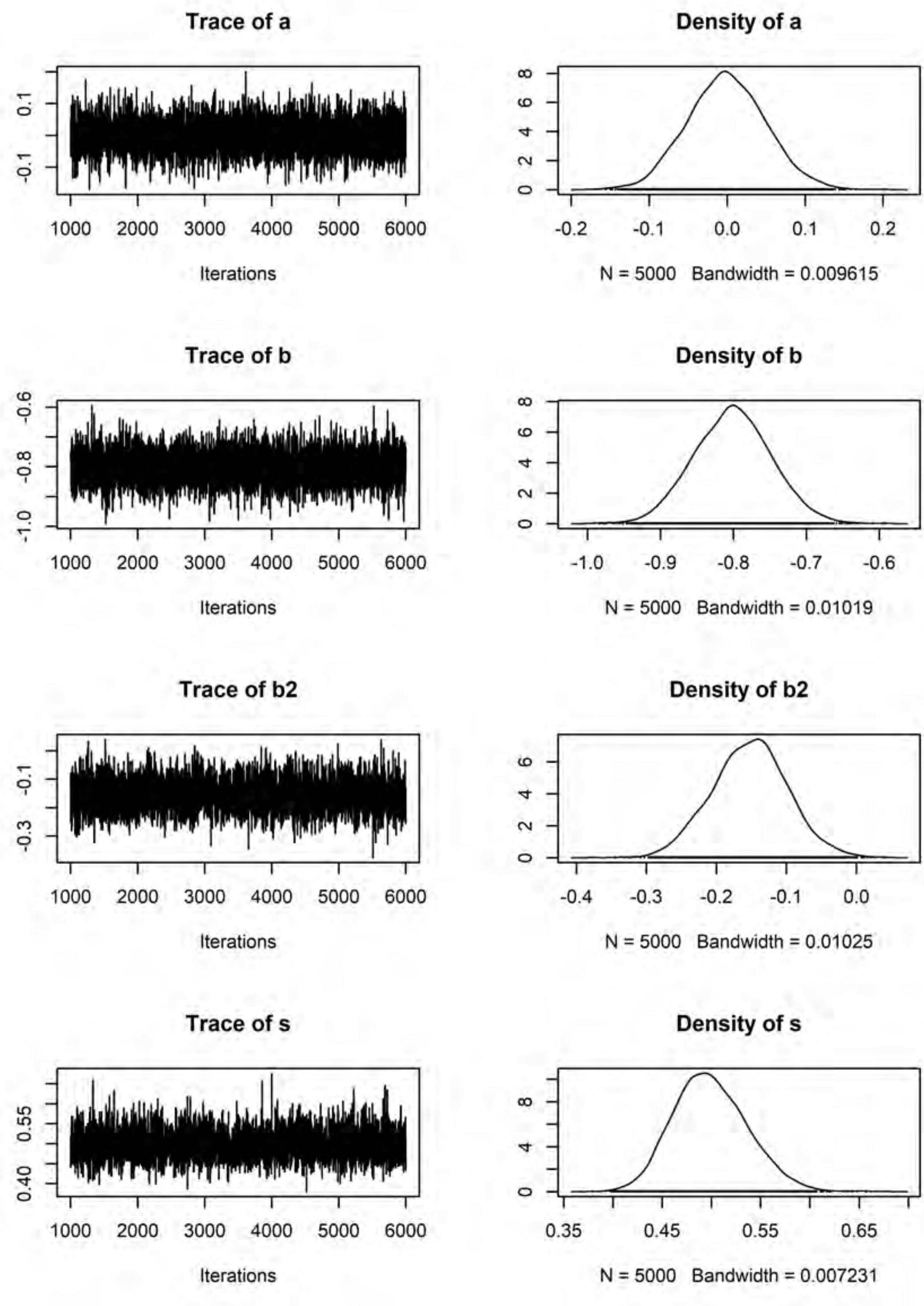


**Apx Figure B-7 Parameter MCMC trace and posterior parameter estimates for runoff coefficient regression model**

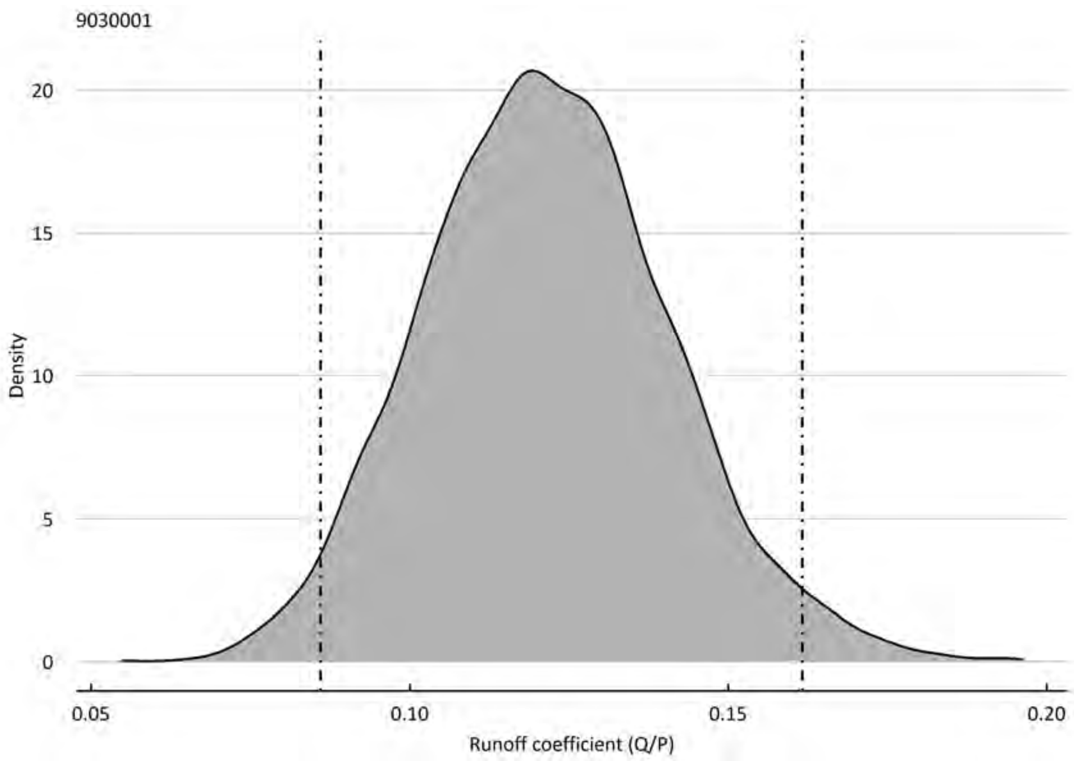


Apx Figure B-8 An example of posterior runoff coefficient estimates for a catchment independent of the training dataset. Vertical dashed lines bound the 95% prediction interval

## B.3 References

Bates D, Mächler M, Bolker B and Walker S (2015) Fitting linear mixed-effects models using lme4. Journal of Statistical Software 67(1), 1–48. DOI:10.18637/jss.v067.i01.

Beven K (1989) Changing ideas in hydrology - The case of physically-based models, Journal of Hydrology, 105(1–2), 157–172.

Blois JL, Williams JW, Fitzpatrick MC, Jackson ST and Ferrier S (2013) Space can substitute for time in predicting climate-change effects on biodiversity. PNAS 110(23), 9374–9379. DOI:10.1073/pnas.1220228110.

Bloschl G, Sivapalan M, Wagener T, Viglione A and Savenjie H (Eds.) (2013) Runoff Prediction in Ungauged Basins. Synthesis across Processes, Places and Scales, Cambridge University Press, April 2013, https://doi.org/10.1017/CBO9781139235761.

Booij MJ and Krol MS (2010) Balance between calibration objectives in a conceptual hydrological model. Hydrological Sciences Journal 55(6), 1017–1032. DOI: 10.1080/02626667.2010.505892.

Budyko M (1974) Climate and life. Academic Press, New York, 508.

Choudhury B (1999) Evaluation of an empirical equation for annual evaporation using field observations and results from a biophysical model. Journal of Hydrology 216(1–2), 99–110. DOI:10.1016/S0022-1694(98)00293-5.

Grundy MJ, Viscarra-Rossel RA, Searle RD, Wilson PL, Chen C and Gregory LJ (2015) Soil and Landscape Grid of Australia. Soil Research 53, 835–844.

Hooper RP, Stone A, Christophersen N, De Grosbois E and Seip HM (1988) Assessing the Birkenes Model of stream acidification using a multisignal calibration methodology, Water Resources Research, 24(8), 1308–1316.

Ibbit RP and O'Donnell TO (1971) Designing conceptual catchment models for automatic fitting methods, IASH Publication, 101, 461–475.

Jakeman AJ and Hornberger GM (1993) How much complexity is warranted in a rainfall-runoff model?, Water Resources Research, 29(8), 2637–2649.

Jeffrey SJ, Carter JO, Moodie KB and Beswick AR (2001) Using spatial interpolation to construct a comprehensive archive of Australian climate data. Environmental Modelling and Software 16(4), 309–330.

Koltermann CE and Gorelick SM (1992) Paleoclimatic signature in terrestrial flood deposits. Science 256, 1775–1782.

Kuczera G and Mroczkowski M (1998) Assessment of hydrologic parameter uncertainty and the worth of multipesponse data, Water Resources Research, 34(6), 1481–1489.

Morton FI (1983) Operational estimates of areal evapotranspiration and their significance to the science and practice of hydrology. Journal of Hydrology 66, 1–76.

Oudin L, Andréassian V, Perrin C, Michel C and Le Moine N (2008) Spatial proximity, physical similarity, regression and ungaged catchments: A comparison of regionalization approaches based on 913 French catchments, Water Resources Research, 44, W03413, DOI:10.1029/2007WR006240.

Nathan RJ and McMahon TA (1990) Identification of homogenous regions for the purposes of regionalisation, Journal of Hydrology, 121, 217–238.

Parajka A, Viglione A, Rogger M, Salinas JL, Sivapalan M and Bloschl G (2013) Comparative assessment of predictions in ungauged basins. Part 1 Runoff-hydrograph studies, Hydrology and Earth System Sciences, 17(5), 1783–1795.

Petheram C, McMahon T and Peel M (2008) Flow characteristics of rivers in northern Australia: implications for development. Journal of Hydrology 357 (1–2), 93–111. DOI: 10.1016/j.jhydrol.2008.05.008.

Petheram C, Rustomji P, Chiew F and Vleeshouwer J (2012) Rainfall–runoff modelling in northern Australia: a guide to modelling strategies in the tropics. Journal of Hydrology 462–463, 28–41. DOI:10.1016/j.jhydrol.2011.12.046.

Plummer M (2022) rjags: Bayesian Graphical Models using MCMC. R package version 4-13. https://cran.r-project.org/package=rjags

Post DA (2009) Regionalizing rainfall-runoff model parameters to predict the daily streamflow of ungauged catchments in the dry tropics, Hydrology Research, 40, 433–444. https://doi.org/10.2166/nh.2009.036

R Core Team (2021) R: a language and environment for statistical computing. R Foundation for Statistical Computing, Vienna, Austria. Viewed 4December 2023, https://www.R-project.org/.

Razavi S and Tolson BA (2013) An efficient framework for hydrologic model calibration on long data periods. Water Resources Research 49(12), 8418–8431. DOI:10.1002/2012WR013442.

Sivapalan M (2003) Prediction in ungauged basins: a grand challenge for theoretical hydrology, Hydrological Processes, 17(15), 3163–3170.

Sorooshian S and Gupta HV (1983) Automatic calibration of conceptual rainfall-runoff models: the question of parameter observability and uniqueness, Water Resources Research, 19, 260–268

Vaze J, Post D, Chiew FHS, Perraud JM, Viney NR and Teng J (2010) Climate non-stationarity – validity of calibrated rainfall–runoff models for use in climate change studies. Journal of Hydrology 394, 3–4. DOI:10.1016/j.jhydrol.2010.09.018.

Wilford J, Searle R, Thomas M and Grundy M (2015) Soil and Landscape Grid National Soil Attribute Maps – Depth of Regolith (3″ resolution) – Release 2 [Dataset]. CSIRO.

Yang W, Xia R, Chen H, Wang M and Xu C (2022) The impact of calibration conditions on the transferability of conceptual hydrological models under stationary and nonstationary climatic conditions. Journal of Hydrology 613, 128310. DOI: 10.1016/j.jhydrol.2022.128310.

Zhang L, Dawes W and Walker G (2001) Response of mean annual ET to vegetation changes at catchment scale. Water Resources Research 37(3), 701–708.

## Apx Table B-1 Gauge data properties

| ID | NAME | LATITUDE | LONGITUDE | START DATE | END DATE | LENGTH (YEARS) | TOTAL DAYS AVAILABLE | TOTAL MISSING DAYS | TOTAL MISSING (%) |
|---|---|---|---|---|---|---|---|---|---|
| **3303** | Barcoo_R Blackall | -24.4268 | 145.4583 | 1969-09-01 | 2020-08-31 | 52 | 18622 | 6 | 0.03 |
| **105101** | Battle Camp | -15.2816 | 144.8387 | 1968-09-01 | 2020-08-31 | 53 | 18909 | 84 | 0.44 |
| **105102** | Laura_R Coal Seam Ck | -15.6137 | 144.4848 | 1968-09-01 | 2020-08-31 | 53 | 18773 | 220 | 1.17 |
| **108002** | Daintree_R Bairds | -16.1796 | 145.2819 | 1969-09-01 | 2020-08-31 | 52 | 18202 | 426 | 2.34 |
| **111005** | The Fisheries | -17.1832 | 145.7248 | 1967-09-01 | 2020-08-31 | 54 | 19277 | 82 | 0.43 |
| **111007** | Mulgrave_R Peets Br | -17.1334 | 145.7646 | 1972-09-01 | 2020-08-31 | 49 | 17528 | 4 | 0.02 |
| **112002** | Fisher_Ck Nerada | -17.5653 | 145.9062 | 1929-09-01 | 2020-08-31 | 92 | 33227 | 11 | 0.03 |
| **112101** | US Central Mill | -17.6089 | 145.9791 | 1975-09-01 | 2020-08-31 | 46 | 16360 | 77 | 0.47 |
| **112102** | Upper Japoonvale | -17.7147 | 145.9057 | 1970-09-01 | 2020-08-31 | 51 | 18256 | 7 | 0.04 |
| **113004** | Powerline | -17.7396 | 145.6301 | 1967-09-01 | 2020-08-31 | 54 | 19162 | 197 | 1.03 |
| **113006** | Tully_R Euramo | -17.9921 | 145.9425 | 1972-09-01 | 2020-08-31 | 49 | 17332 | 200 | 1.15 |
| **114001** | Murray_R Up Murray | -18.1069 | 145.8054 | 1970-09-01 | 2020-08-31 | 51 | 18256 | 7 | 0.04 |
| **116001** | Herbert_R Ingham | -18.6372 | 146.1411 | 1915-09-01 | 2020-08-31 | 106 | 38335 | 17 | 0.04 |
| **116004** | Herbert_R Cashmere | -18.1368 | 145.3395 | 1922-09-01 | 2020-08-31 | 99 | 35789 | 6 | 0.02 |
| **116006** | Abergowrie College | -18.4900 | 145.8936 | 1968-09-01 | 2020-08-31 | 53 | 18609 | 384 | 2.06 |
| **116010** | Blencoe_Ck Falls | -18.2042 | 145.5371 | 1961-09-01 | 2020-08-31 | 60 | 21369 | 181 | 0.85 |
| **116011** | Millstream Ravenshoe | -17.6046 | 145.4770 | 1960-09-01 | 2020-08-31 | 61 | 21558 | 357 | 1.66 |
| **116013** | Millstream Archer Ck | -17.6523 | 145.3409 | 1962-09-01 | 2020-08-31 | 59 | 21172 | 13 | 0.06 |
| **116014** | Wild_R Silver Valley | -17.6266 | 145.2959 | 1962-09-01 | 2020-08-31 | 59 | 21184 | 1 | 0.00 |
| **116015** | Blunder_Ck Wooroora | -17.7371 | 145.4363 | 1967-09-01 | 2020-08-31 | 54 | 19359 | 0 | 0.00 |
| **117002** | Black_R Bruce Hwy | -19.2377 | 146.6329 | 1973-09-01 | 2020-08-31 | 48 | 17165 | 2 | 0.01 |
| **117003** | Bluewater | -19.1833 | 146.5469 | 1974-09-01 | 2020-08-31 | 47 | 14331 | 2471 | 17.24 |
| **118106** | Alligator Allendale | -19.3866 | 146.9579 | 1975-09-01 | 2020-08-31 | 46 | 16437 | 0 | 0.00 |
| **119003** | Haughton_R Powerline | -19.6331 | 147.1103 | 1970-09-01 | 2020-08-31 | 51 | 18263 | 0 | 0.00 |
| **120102** | Keelbottom | -19.3714 | 146.3612 | 1967-09-01 | 2020-08-31 | 54 | 19279 | 80 | 0.41 |

| ID | NAME | LATITUDE | LONGITUDE | START DATE | END DATE | LENGTH (YEARS) | TOTAL DAYS AVAILABLE | TOTAL MISSING DAYS | TOTAL MISSING (%) |
|---|---|---|---|---|---|---|---|---|---|
| **120110** | Mt Fullstop | -19.2073 | 145.4950 | 1965-09-01 | 2020-08-31 | 56 | 20085 | 4 | 0.02 |
| **120301** | Mt. Douglas | -21.5192 | 146.8685 | 1949-09-01 | 2020-08-31 | 72 | 23366 | 2567 | 10.99 |
| **120304** | Suttor_R Eaglefield | -21.4504 | 147.7143 | 1967-09-01 | 2020-08-31 | 54 | 19294 | 65 | 0.34 |
| **121002** | Elliot_R Guthalunga | -19.9333 | 147.8407 | 1973-09-01 | 2020-08-31 | 48 | 17167 | 0 | 0.00 |
| **121003** | Don_R Reeves | -20.1493 | 148.1555 | 1984-09-01 | 2020-08-31 | 37 | 13149 | 0 | 0.00 |
| **122004** | Lower Gregory | -20.3004 | 148.5484 | 1973-09-01 | 2020-08-31 | 48 | 17157 | 10 | 0.06 |
| **124002** | St.Helens_Ck Calen | -20.9058 | 148.7597 | 1973-09-01 | 2020-08-31 | 48 | 17166 | 1 | 0.01 |
| **125005** | Blacks_Ck Whitefords | -21.3228 | 148.8351 | 1974-09-01 | 2020-08-31 | 47 | 16802 | 0 | 0.00 |
| **126003** | Carmila_Ck Carmila | -21.9157 | 149.3986 | 1974-09-01 | 2020-08-31 | 47 | 16798 | 4 | 0.02 |
| **129001** | Waterpark_Ck Byfield | -22.8350 | 150.6659 | 1952-09-01 | 2020-08-31 | 69 | 23995 | 842 | 3.51 |
| **130004** | Raglan_Ck Old Stn | -23.8191 | 150.8206 | 1964-09-01 | 2020-08-31 | 57 | 20452 | 2 | 0.01 |
| **130302** | Dawson_RTaroom | -25.6377 | 149.7896 | 1911-09-01 | 2020-08-31 | 110 | 39808 | 5 | 0.01 |
| **130324** | Dawson_R Utopia Dns | -25.7447 | 149.3299 | 1966-09-01 | 2020-08-31 | 55 | 19721 | 3 | 0.02 |
| **130403** | Connors Mt Bridget | -22.0357 | 149.1315 | 1966-09-01 | 2020-08-31 | 55 | 19711 | 13 | 0.07 |
| **130410** | Isaac R_Deverill | -22.1708 | 148.3842 | 1968-09-01 | 2020-08-31 | 53 | 18931 | 62 | 0.33 |
| **130413** | Denison Ck_Braeside | -21.7694 | 148.7866 | 1972-09-01 | 2020-08-31 | 49 | 17532 | 0 | 0.00 |
| **132001** | Calliope Castlehope | -23.9850 | 151.0976 | 1939-09-01 | 2020-08-31 | 82 | 29584 | 2 | 0.01 |
| **135002** | Kolan_R Springfield | -24.7533 | 151.5872 | 1966-09-01 | 2020-08-31 | 55 | 19724 | 0 | 0.00 |
| **135004** | Gin Gin_Ck Brushy Ck | -24.9686 | 151.8919 | 1966-09-01 | 2020-08-31 | 55 | 19723 | 1 | 0.01 |
| **136006** | Reid_C Mungy | -25.2731 | 151.5173 | 1966-09-01 | 2020-08-31 | 55 | 19719 | 5 | 0.03 |
| **136208** | Boonara_Ck Ettiewyn | -25.9028 | 151.8438 | 1968-09-01 | 2020-08-31 | 53 | 18993 | 0 | 0.00 |
| **137101** | Gregory River | -25.0862 | 152.2405 | 1966-09-01 | 2020-08-31 | 55 | 19235 | 489 | 2.54 |
| **137201** | Isis River Bruce Hwy | -25.2666 | 152.3684 | 1966-09-01 | 2020-08-31 | 55 | 19723 | 1 | 0.01 |
| **138903** | Tinana_C Bauple East | -25.8203 | 152.7222 | 1981-09-01 | 2020-08-31 | 40 | 14245 | 0 | 0.00 |
| **704193** | Fishy Pool | -24.9438 | 114.6404 | 1964-09-01 | 2020-08-31 | 57 | 20454 | 0 | 0.00 |
| **707002** | Yarraloola | -21.6162 | 115.9225 | 1972-09-01 | 2020-08-31 | 49 | 17532 | 0 | 0.00 |

| ID | NAME | LATITUDE | LONGITUDE | START DATE | END DATE | LENGTH (YEARS) | TOTAL DAYS AVAILABLE | TOTAL MISSING DAYS | TOTAL MISSING (%) |
|---|---|---|---|---|---|---|---|---|---|
| **708011** | Newman | -23.4014 | 119.7943 | 1980-09-01 | 2020-08-31 | 41 | 14608 | 2 | 0.01 |
| **710003** | Coolenar Pool | -20.3114 | 119.2490 | 1975-09-01 | 2020-08-31 | 46 | 15360 | 1077 | 7.01 |
| **802137** | Dimond Gorge | -17.6722 | 126.0278 | 1963-09-01 | 2020-08-31 | 58 | 20531 | 289 | 1.41 |
| **802198** | Me No Savvy | -18.4497 | 126.5935 | 1966-09-01 | 2020-08-31 | 55 | 18874 | 850 | 4.50 |
| **802202** | Mt Winifred | -18.0152 | 126.3106 | 1965-09-01 | 2020-08-31 | 56 | 17819 | 2270 | 12.74 |
| **802213** | Phillips Range | -16.8715 | 126.0511 | 1967-09-01 | 2020-08-31 | 54 | 19021 | 338 | 1.78 |
| **809310** | Bedford Downs | -17.4259 | 127.6001 | 1968-09-01 | 2020-08-31 | 53 | 17893 | 1100 | 6.15 |
| **809315** | Homestead | -17.1768 | 129.0924 | 1970-09-01 | 2020-08-31 | 51 | 17966 | 297 | 1.65 |
| **809316** | Old Ord Homestead | -17.3726 | 128.8546 | 1971-09-01 | 2020-08-31 | 50 | 17062 | 836 | 4.90 |
| **912105** | Riversleigh | -18.9694 | 138.8041 | 1968-09-01 | 2020-08-31 | 53 | 18030 | 963 | 5.34 |
| **913006** | Gunpowder | -19.6878 | 139.3607 | 1971-09-01 | 2020-08-31 | 50 | 17714 | 184 | 1.04 |
| **913010** | 16 Mile Waterhole | -18.8769 | 139.3605 | 1973-09-01 | 2019-08-31 | 47 | 16297 | 504 | 3.09 |
| **915003** | Walkers Bend | -18.1617 | 140.8582 | 1970-09-01 | 2020-08-31 | 51 | 17758 | 505 | 2.84 |
| **915013** | Flinders_R Glendower | -20.7105 | 144.5268 | 1973-09-01 | 2012-08-31 | 40 | 13514 | 731 | 5.41 |
| **915206** | Dugald_R Rail Xing | -20.2008 | 140.2247 | 1970-09-01 | 2020-08-31 | 51 | 17202 | 1061 | 6.17 |
| **915208** | Julia_Ck | -20.6561 | 141.7611 | 1971-09-01 | 2020-08-31 | 50 | 16986 | 912 | 5.37 |
| **917001** | Forest Home | -18.2538 | 143.0838 | 1967-09-01 | 2020-08-31 | 54 | 18259 | 1100 | 6.02 |
| **917104** | Etheridge_R Roseglen | -18.3064 | 143.5790 | 1967-09-01 | 2020-08-31 | 54 | 18148 | 1211 | 6.67 |
| **917106** | Einasleigh | -18.5002 | 144.0959 | 1967-09-01 | 2020-08-31 | 54 | 19040 | 319 | 1.68 |
| **917107** | Mt Surprise | -18.1336 | 144.3065 | 1968-09-01 | 2020-08-31 | 53 | 18103 | 890 | 4.92 |
| **919003** | Mitchell_R OK Br | -16.4708 | 144.2894 | 1968-09-01 | 2020-08-31 | 53 | 18192 | 801 | 4.40 |
| **919011** | Mitchell_R Gamboola | -16.5345 | 143.6772 | 1972-09-01 | 2020-08-31 | 49 | 17095 | 437 | 2.56 |
| **919201** | Palmer_R Goldfields | -16.1076 | 144.7777 | 1968-09-01 | 2020-08-31 | 53 | 17967 | 1026 | 5.71 |
| **919309** | Walsh_R Trimbles | -16.5469 | 143.7828 | 1968-09-01 | 2020-08-31 | 53 | 18429 | 564 | 3.06 |
| **919310** | Walsh_R Rookwood | -16.9823 | 144.2887 | 1968-09-01 | 2020-08-31 | 53 | 18872 | 121 | 0.64 |
| **922001** | Archer_R Tele Xing | -13.4176 | 142.9207 | 1969-09-01 | 2020-08-31 | 52 | 18235 | 393 | 2.16 |

| ID | NAME | LATITUDE | LONGITUDE | START DATE | END DATE | LENGTH (YEARS) | TOTAL DAYS AVAILABLE | TOTAL MISSING DAYS | TOTAL MISSING (%) |
|---|---|---|---|---|---|---|---|---|---|
| **923001** | Watson_R Jackin Ck | -13.1280 | 142.0526 | 1973-09-01 | 2020-08-31 | 48 | 15266 | 1901 | 12.45 |
| **925001** | Wenlock_R Moreton | -12.4540 | 142.6392 | 1958-09-01 | 2020-08-31 | 63 | 21481 | 1165 | 5.42 |
| **926002** | Dulhunty_R Dougs Pad | -11.8327 | 142.4220 | 1971-09-01 | 2020-08-31 | 50 | 17547 | 351 | 2.00 |
| **927001** | Jardine_R Tele Line | -11.1518 | 142.3549 | 1969-09-01 | 2020-08-31 | 52 | 18235 | 393 | 2.16 |
| **8110004** | East Baines US Hwy | -15.7651 | 130.0313 | 1963-09-01 | 2019-08-31 | 57 | 19039 | 1415 | 7.43 |
| **8140001** | Kath Railway Bg | -14.4623 | 132.2570 | 1957-09-01 | 2019-08-31 | 63 | 20503 | 2142 | 10.45 |
| **8140008** | Fergusson R | -14.0709 | 131.9774 | 1957-09-01 | 2019-08-31 | 63 | 20257 | 2388 | 11.79 |
| **8140040** | Daly R Mt Nancar | -13.8297 | 130.7352 | 1967-09-01 | 2019-08-31 | 53 | 17862 | 1131 | 6.33 |
| **8140063** | Douglas DS Hst | -13.7971 | 131.3400 | 1958-09-01 | 2019-08-31 | 62 | 21755 | 525 | 2.41 |
| **8140067** | Daly US Dorisvale X | -14.3654 | 131.5740 | 1957-09-01 | 2020-08-31 | 64 | 20549 | 2462 | 11.98 |
| **8140159** | Waterfall View | -14.2835 | 132.3994 | 1963-09-01 | 2019-08-31 | 57 | 19272 | 1182 | 6.13 |
| **8140161** | Green Ant C Tip | -13.7381 | 131.1023 | 1966-09-01 | 2019-08-31 | 54 | 16778 | 2580 | 15.38 |
| **8150098** | Blackmore R | -12.7736 | 130.9450 | 1959-09-01 | 2019-08-31 | 61 | 19485 | 2430 | 12.47 |
| **8150180** | Gitchams Xng | -12.9695 | 130.7624 | 1961-09-01 | 2019-08-31 | 59 | 20414 | 770 | 3.77 |
| **8170066** | Coomalie C | -13.0136 | 131.1229 | 1958-09-01 | 2019-08-31 | 62 | 20110 | 2170 | 10.79 |
| **8180026** | El Sherana Rd Xng | -13.6012 | 132.2201 | 1961-09-01 | 2010-08-31 | 50 | 16752 | 1145 | 6.84 |
| **8180035** | Mary R / Mt Bundey | -12.9061 | 131.6466 | 1957-09-01 | 2013-08-31 | 57 | 19648 | 806 | 4.10 |
| **8180069** | Burrundie Mckinlay R | -13.5319 | 131.7179 | 1958-09-01 | 2009-08-31 | 52 | 17545 | 1083 | 6.17 |
| **8200045** | South Gator River 2 | -13.5253 | 132.5218 | 1958-09-01 | 2009-08-31 | 52 | 17577 | 1051 | 5.98 |
| **9030089** | Waterhouse R Rd Bg | -14.5628 | 133.1059 | 1973-09-01 | 2019-08-31 | 47 | 14453 | 2348 | 16.25 |
| **9030176** | Roper R DS Mataranka | -14.9434 | 133.2075 | 1961-09-01 | 2019-08-31 | 59 | 19684 | 1500 | 7.62 |
| **9030250** | Roper R /Red Rock | -14.6968 | 134.4216 | 1966-09-01 | 2019-08-31 | 54 | 16775 | 2583 | 15.40 |

**Apx Table B-2 Catchment mean aridity, regolith depth, regional group, observed runoff coefficient and mean predicted runoff coefficient with standard deviation calculated from Bayesian posterior estimates**

| ID | ARIDITY | REGOLITH DEPTH (m) | REGION | OBSERVED QCOEF | MEAN PREDICTED QCOEF | PREDICTED STANDARD DEVIATION |
|---|---|---|---|---|---|---|
| **3303** | 3.13 | 14.40 | qld | 0.030 | 0.096 | 0.0087 |
| **105101** | 1.26 | 6.04 | hqld | 0.223 | 0.335 | 0.0118 |
| **105102** | 1.77 | 7.27 | qld | 0.262 | 0.238 | 0.0087 |
| **108002** | 0.79 | 3.00 | hqld | 0.479 | 0.508 | 0.0228 |
| **111005** | 0.50 | 1.92 | hqld | 0.500 | 0.690 | 0.0360 |
| **111007** | 0.56 | 1.94 | hqld | 0.523 | 0.647 | 0.0328 |
| **112002** | 0.49 | 4.66 | hqld | 0.654 | 0.679 | 0.0353 |
| **112101** | 0.53 | 2.97 | hqld | 0.673 | 0.660 | 0.0336 |
| **112102** | 0.48 | 2.36 | hqld | 0.605 | 0.710 | 0.0375 |
| **113004** | 0.69 | 1.99 | hqld | 0.821 | 0.561 | 0.0268 |
| **113006** | 0.59 | 8.67 | hqld | 0.838 | 0.572 | 0.0296 |
| **114001** | 0.88 | 4.51 | hqld | 0.615 | 0.457 | 0.0189 |
| **116001** | 1.53 | 9.83 | hqld | 0.374 | 0.262 | 0.0092 |
| **116004** | 1.80 | 11.76 | hqld | 0.225 | 0.213 | 0.0090 |
| **116006** | 1.55 | 10.01 | hqld | 0.315 | 0.257 | 0.0091 |
| **116010** | 1.22 | 6.60 | hqld | 0.442 | 0.341 | 0.0119 |
| **116011** | 0.99 | 13.38 | hqld | 0.422 | 0.366 | 0.0198 |
| **116013** | 1.13 | 8.80 | hqld | 0.406 | 0.351 | 0.0130 |
| **116014** | 1.44 | 5.22 | hqld | 0.265 | 0.301 | 0.0113 |
| **116015** | 1.02 | 4.22 | hqld | 0.456 | 0.412 | 0.0165 |
| **117002** | 1.51 | 9.68 | hqld | 0.339 | 0.267 | 0.0093 |
| **117003** | 1.20 | 2.12 | hqld | 0.579 | 0.373 | 0.0169 |
| **118106** | 1.36 | 2.96 | hqld | 0.465 | 0.330 | 0.0146 |
| **119003** | 1.92 | 8.24 | qld | 0.268 | 0.213 | 0.0081 |
| **120102** | 1.34 | 3.79 | hqld | 0.456 | 0.330 | 0.0135 |
| **120110** | 2.43 | 8.16 | qld | 0.156 | 0.162 | 0.0084 |
| **120301** | 3.07 | 27.27 | qld | 0.036 | 0.064 | 0.0157 |
| **120304** | 2.86 | 15.05 | qld | 0.088 | 0.108 | 0.0093 |
| **121002** | 2.22 | 7.50 | qld | 0.291 | 0.183 | 0.0086 |
| **121003** | 2.00 | 6.16 | qld | 0.196 | 0.213 | 0.0095 |
| **122004** | 1.06 | 3.22 | qld | 0.524 | 0.406 | 0.0170 |
| **124002** | 0.88 | 3.02 | qld | 0.615 | 0.470 | 0.0204 |
| **125005** | 1.14 | 3.71 | qld | 0.290 | 0.380 | 0.0153 |
| **126003** | 1.20 | 3.34 | qld | 0.373 | 0.365 | 0.0152 |
| **129001** | 1.06 | 14.76 | qld | 0.355 | 0.336 | 0.0199 |
| **130004** | 1.95 | 5.97 | qld | 0.111 | 0.220 | 0.0096 |
| **130302** | 2.62 | 7.68 | qld | 0.040 | 0.149 | 0.0089 |
| **130324** | 2.58 | 6.29 | qld | 0.034 | 0.157 | 0.0098 |
| **130403** | 1.54 | 4.04 | qld | 0.411 | 0.289 | 0.0123 |
| **130410** | 2.90 | 15.54 | qld | 0.070 | 0.104 | 0.0095 |
| **130413** | 1.64 | 5.31 | qld | 0.245 | 0.266 | 0.0105 |

| ID | ARIDITY | REGOLITH DEPTH (m) | REGION | OBSERVED QCOEF | MEAN PREDICTED QCOEF | PREDICTED STANDARD DEVIATION |
|---|---|---|---|---|---|---|
| **132001** | 1.93 | 7.22 | qld | 0.153 | 0.217 | 0.0086 |
| **135002** | 1.66 | 3.23 | qld | 0.150 | 0.274 | 0.0132 |
| **135004** | 1.81 | 3.26 | qld | 0.144 | 0.250 | 0.0129 |
| **136006** | 1.99 | 3.16 | qld | 0.135 | 0.228 | 0.0130 |
| **136208** | 2.03 | 4.61 | qld | 0.061 | 0.217 | 0.0111 |
| **137101** | 1.67 | 6.73 | qld | 0.136 | 0.254 | 0.0092 |
| **137201** | 1.67 | 6.13 | qld | 0.146 | 0.257 | 0.0097 |
| **138903** | 1.25 | 6.94 | qld | 0.200 | 0.332 | 0.0114 |
| **704193** | 7.97 | 14.20 | nw | 0.049 | 0.006 | 0.0039 |
| **707002** | 4.77 | 10.77 | nw | 0.040 | 0.049 | 0.0080 |
| **708011** | 5.62 | 13.50 | nw | 0.050 | 0.028 | 0.0068 |
| **710003** | 5.13 | 13.14 | nw | 0.070 | 0.036 | 0.0073 |
| **802137** | 2.44 | 10.84 | nw | 0.207 | 0.151 | 0.0079 |
| **802198** | 3.52 | 9.39 | nw | 0.182 | 0.092 | 0.0087 |
| **802202** | 2.91 | 3.51 | nw | 0.225 | 0.144 | 0.0127 |
| **802213** | 2.09 | 14.86 | nw | 0.176 | 0.167 | 0.0106 |
| **809310** | 2.60 | 6.50 | nw | 0.166 | 0.155 | 0.0097 |
| **809315** | 2.95 | 8.29 | nw | 0.118 | 0.125 | 0.0089 |
| **809316** | 3.16 | 6.98 | nw | 0.153 | 0.117 | 0.0098 |
| **912105** | 3.83 | 11.51 | qld | 0.125 | 0.074 | 0.0082 |
| **913006** | 3.61 | 5.44 | qld | 0.128 | 0.100 | 0.0110 |
| **913010** | 3.35 | 3.67 | qld | 0.130 | 0.118 | 0.0126 |
| **915003** | 3.65 | 23.38 | qld | 0.062 | 0.052 | 0.0115 |
| **915013** | 2.67 | 7.42 | qld | 0.112 | 0.146 | 0.0091 |
| **915206** | 3.48 | 3.18 | qld | 0.170 | 0.113 | 0.0130 |
| **915208** | 4.00 | 18.95 | qld | 0.053 | 0.051 | 0.0091 |
| **917001** | 2.43 | 4.73 | qld | 0.164 | 0.176 | 0.0112 |
| **917104** | 2.11 | 5.83 | qld | 0.245 | 0.202 | 0.0098 |
| **917106** | 2.42 | 7.31 | qld | 0.168 | 0.166 | 0.0089 |
| **917107** | 2.22 | 6.81 | qld | 0.139 | 0.187 | 0.0091 |
| **919003** | 1.93 | 4.36 | qld | 0.276 | 0.230 | 0.0114 |
| **919011** | 1.98 | 7.13 | qld | 0.208 | 0.211 | 0.0087 |
| **919201** | 1.48 | 2.87 | qld | 0.269 | 0.307 | 0.0142 |
| **919309** | 2.04 | 6.49 | qld | 0.202 | 0.207 | 0.0092 |
| **919310** | 1.99 | 4.15 | qld | 0.252 | 0.223 | 0.0117 |
| **922001** | 1.32 | 12.53 | hqld | 0.426 | 0.286 | 0.0131 |
| **923001** | 1.16 | 17.38 | qld | 0.374 | 0.298 | 0.0217 |
| **925001** | 1.17 | 13.61 | hqld | 0.286 | 0.316 | 0.0166 |
| **926002** | 1.06 | 12.32 | hqld | 0.403 | 0.351 | 0.0170 |
| **927001** | 1.01 | 12.92 | hqld | 0.500 | 0.362 | 0.0187 |
| **8110004** | 2.27 | 5.55 | nw | 0.146 | 0.187 | 0.0102 |
| **8140001** | 1.63 | 13.39 | nt | 0.248 | 0.228 | 0.0113 |
| **8140008** | 1.56 | 13.56 | nt | 0.247 | 0.239 | 0.0120 |

| ID | ARIDITY | REGOLITH DEPTH (m) | REGION | OBSERVED QCOEF | MEAN PREDICTED QCOEF | PREDICTED STANDARD DEVIATION |
|---|---|---|---|---|---|---|
| **8140040** | 1.73 | 15.99 | nt | 0.163 | 0.203 | 0.0134 |
| **8140063** | 1.44 | 14.39 | nt | 0.220 | 0.256 | 0.0140 |
| **8140067** | 1.92 | 16.70 | nt | 0.150 | 0.178 | 0.0131 |
| **8140159** | 1.63 | 21.23 | nt | 0.217 | 0.194 | 0.0205 |
| **8140161** | 1.38 | 12.96 | nt | 0.167 | 0.273 | 0.0129 |
| **8150098** | 1.20 | 10.02 | nt | 0.417 | 0.327 | 0.0125 |
| **8150180** | 1.23 | 8.98 | nt | 0.319 | 0.325 | 0.0116 |
| **8170066** | 1.33 | 8.97 | nt | 0.298 | 0.304 | 0.0105 |
| **8180026** | 1.44 | 19.87 | nt | 0.172 | 0.229 | 0.0209 |
| **8180035** | 1.39 | 8.97 | nt | 0.273 | 0.292 | 0.0100 |
| **8180069** | 1.44 | 2.14 | nt | 0.299 | 0.317 | 0.0154 |
| **8200045** | 1.40 | 7.23 | nt | 0.351 | 0.298 | 0.0100 |
| **9030089** | 1.74 | 12.30 | nt | 0.179 | 0.218 | 0.0097 |
| **9030176** | 1.94 | 16.71 | nt | 0.123 | 0.175 | 0.0130 |
| **9030250** | 2.20 | 18.53 | nt | 0.084 | 0.143 | 0.0135 |

Page deliberately left blank

# Appendix C  Stream gauge data plots

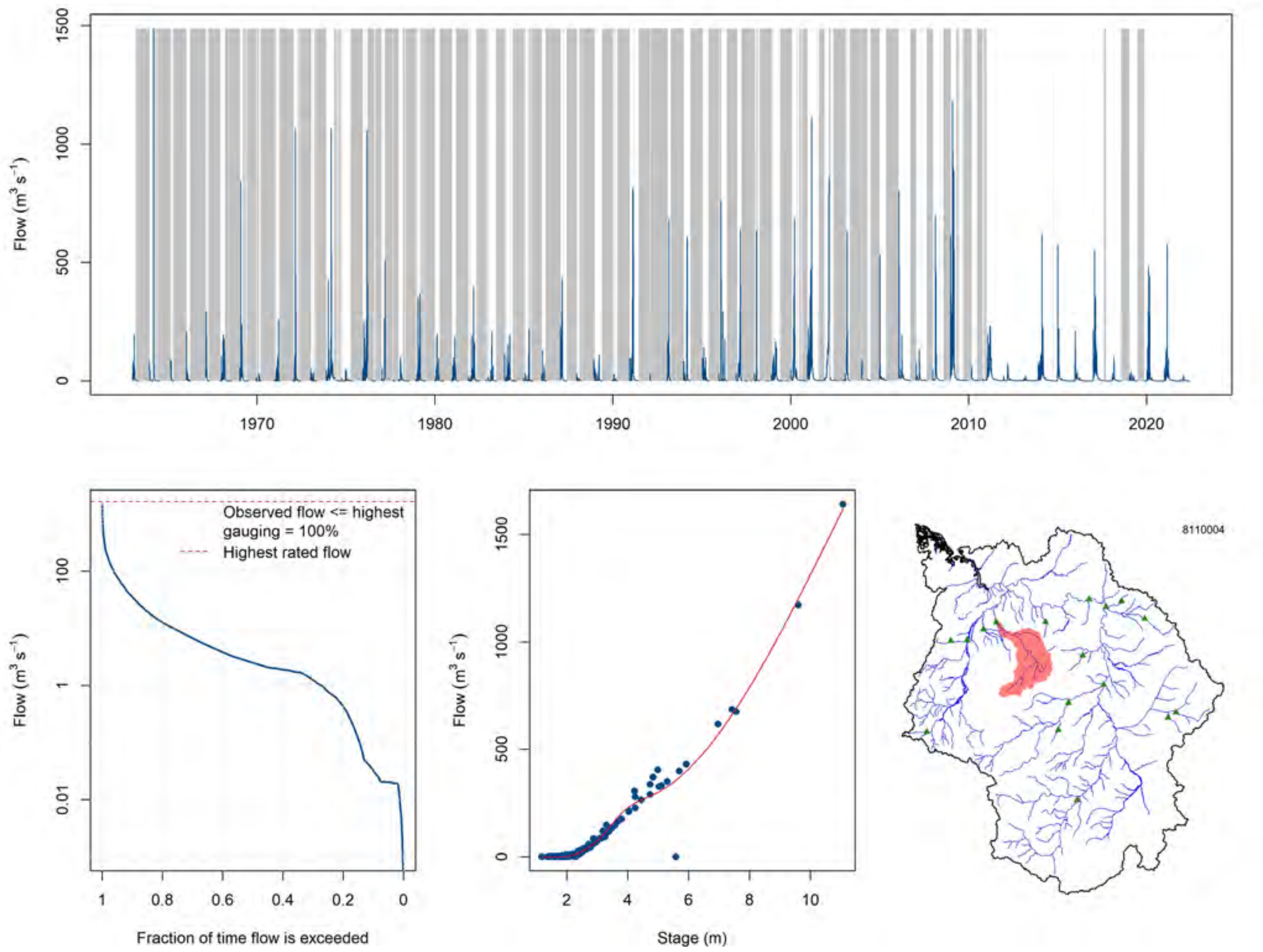


**Apx Figure C-1 Stream gauge data for site 8110004 (East Baines River at Victoria Highway). The dashed red line in the top and bottom left panel shows highest gauged point. Grey vertical lines indicate missing data**

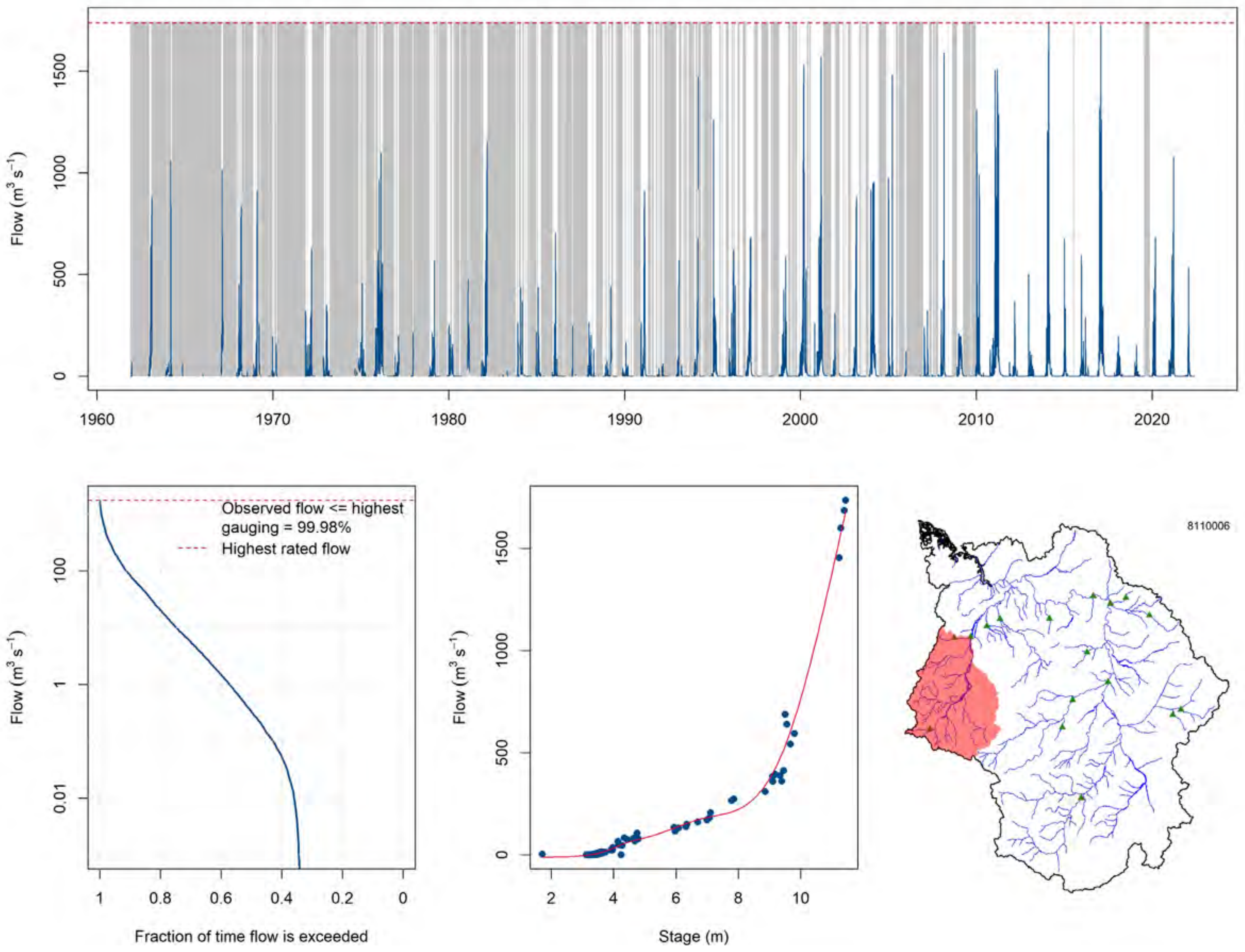


**Apx Figure C-2 Stream gauge data for site 8110006 (West Baines River at Victoria Highway). The dashed red line in the top and bottom left panel shows highest gauged point. Grey vertical lines indicate missing data**

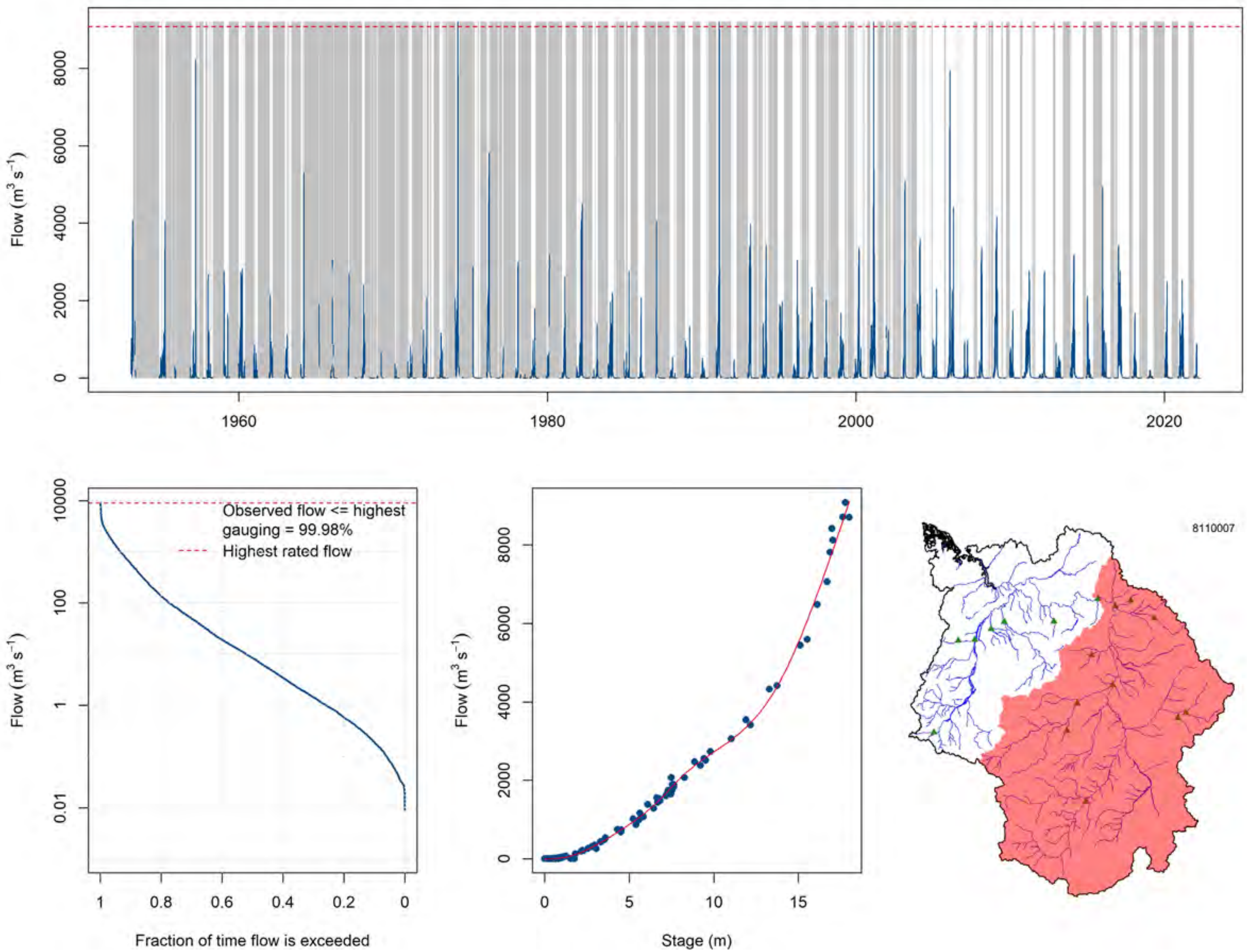


**Apx Figure C-3 Stream gauge data for site 8110007 (Victoria River at Coolibah Homestead). The dashed red line in the top and bottom left panel shows highest gauged point. Grey vertical lines indicate missing data**

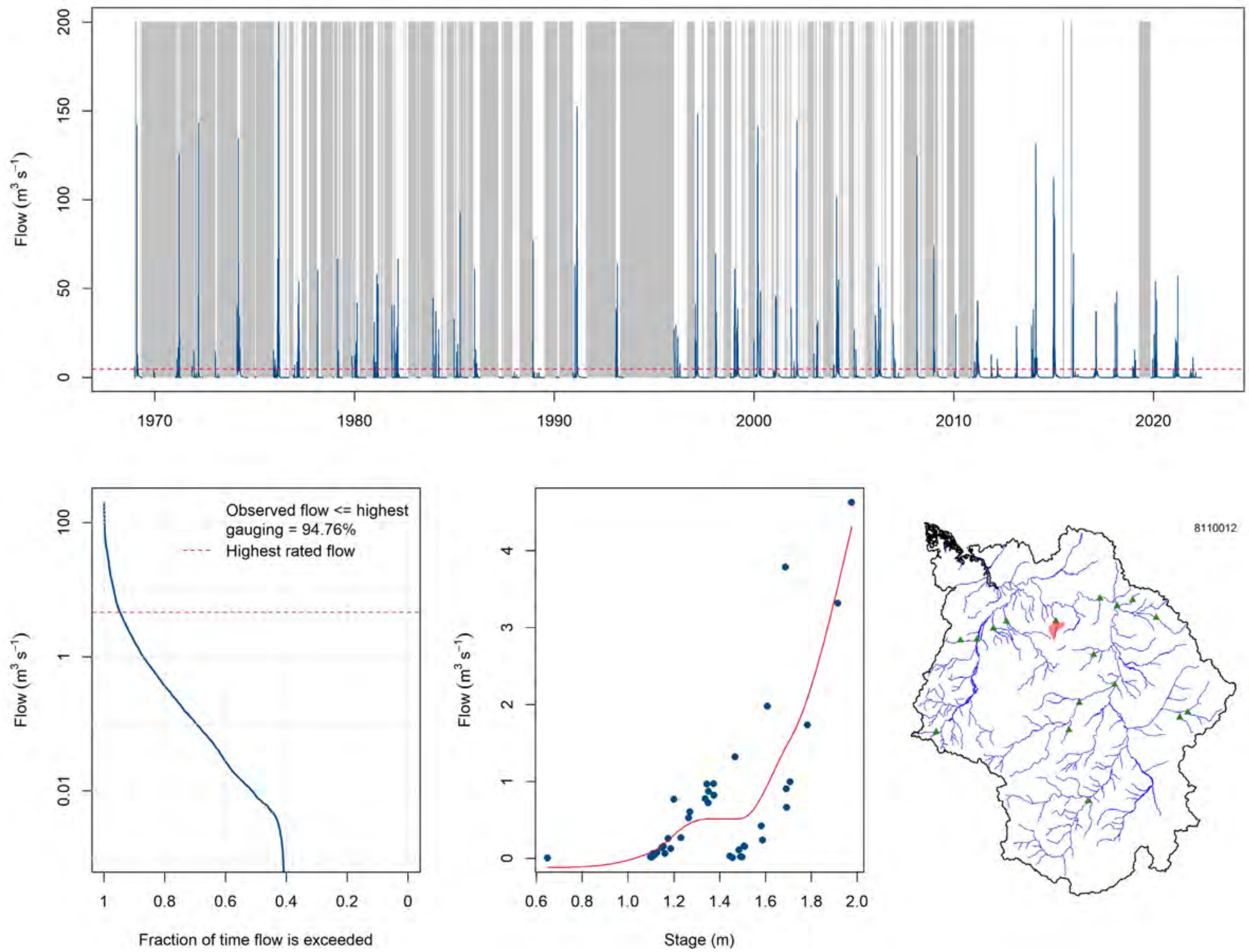


Apx Figure C-4 Stream gauge data for site 8110012 (Timber Creek upstream of Victoria Highway). The dashed red line in the top and bottom left panel shows highest gauged point. Grey vertical lines indicate missing data

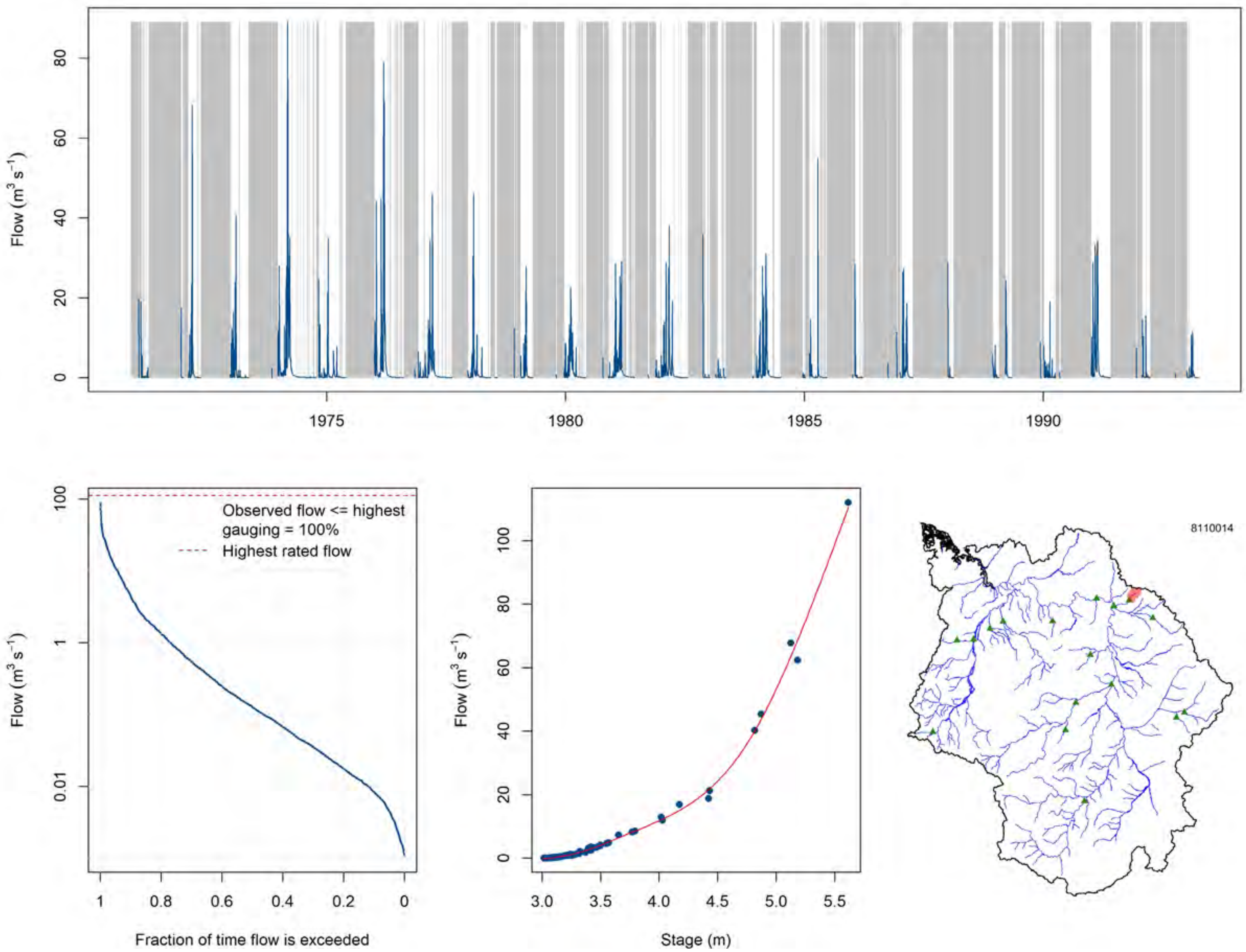


Apx Figure C-5 Stream gauge data for site 8110014 (Sullivans Creek upstream of Fig Tree Yard). The dashed red line in the top and bottom left panel shows highest gauged point. Grey vertical lines indicate missing data

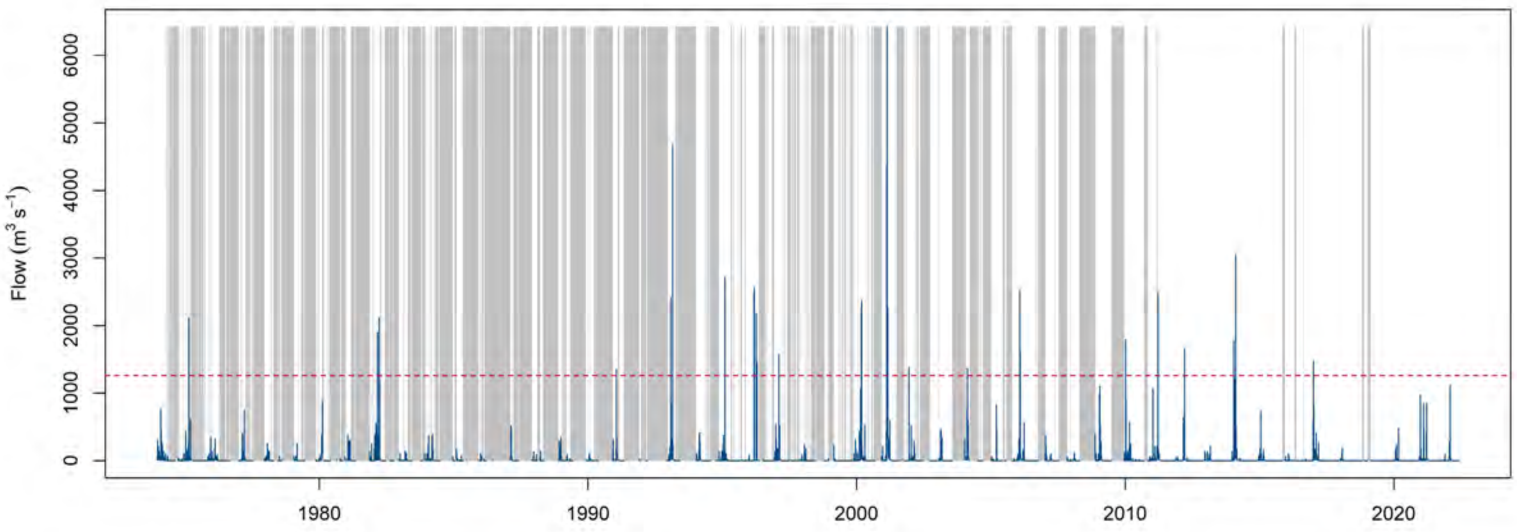


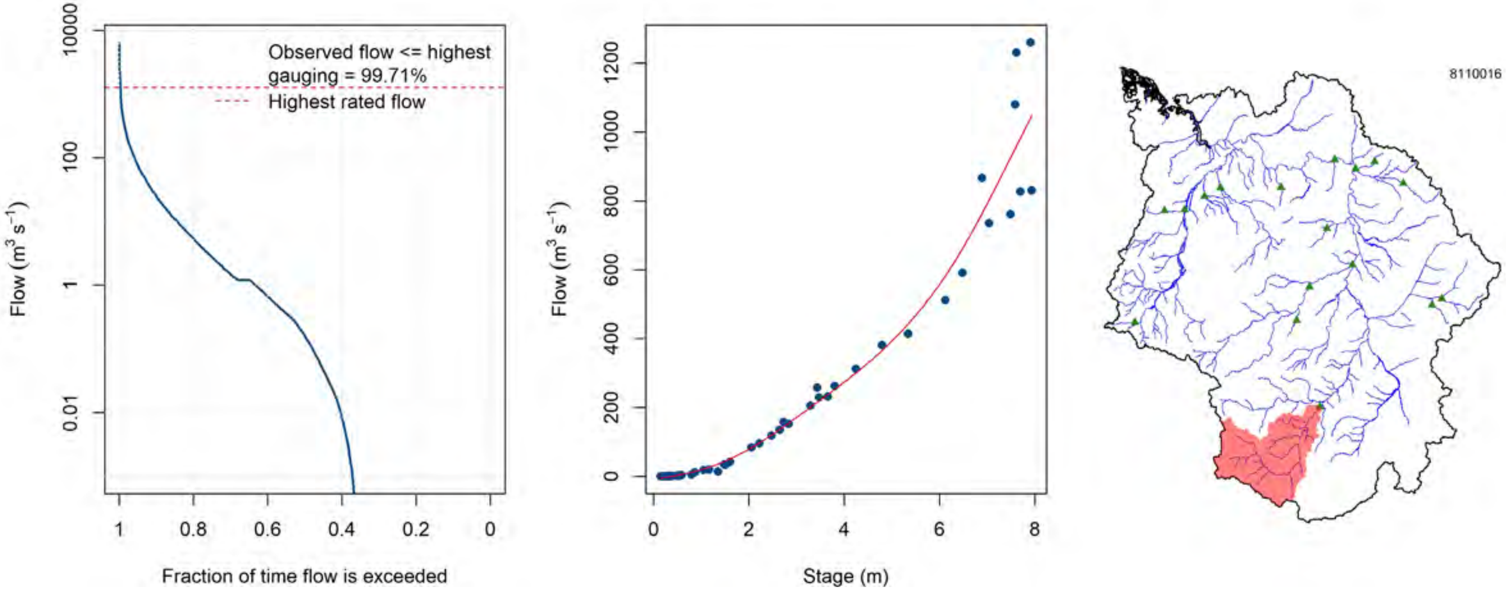


**Apx Figure C-6 Stream gauge data for site 8110016 (Victoria River at Wave Hill Police Station). The dashed red line in the top and bottom left panel shows highest gauged point. Grey vertical lines indicate missing data**

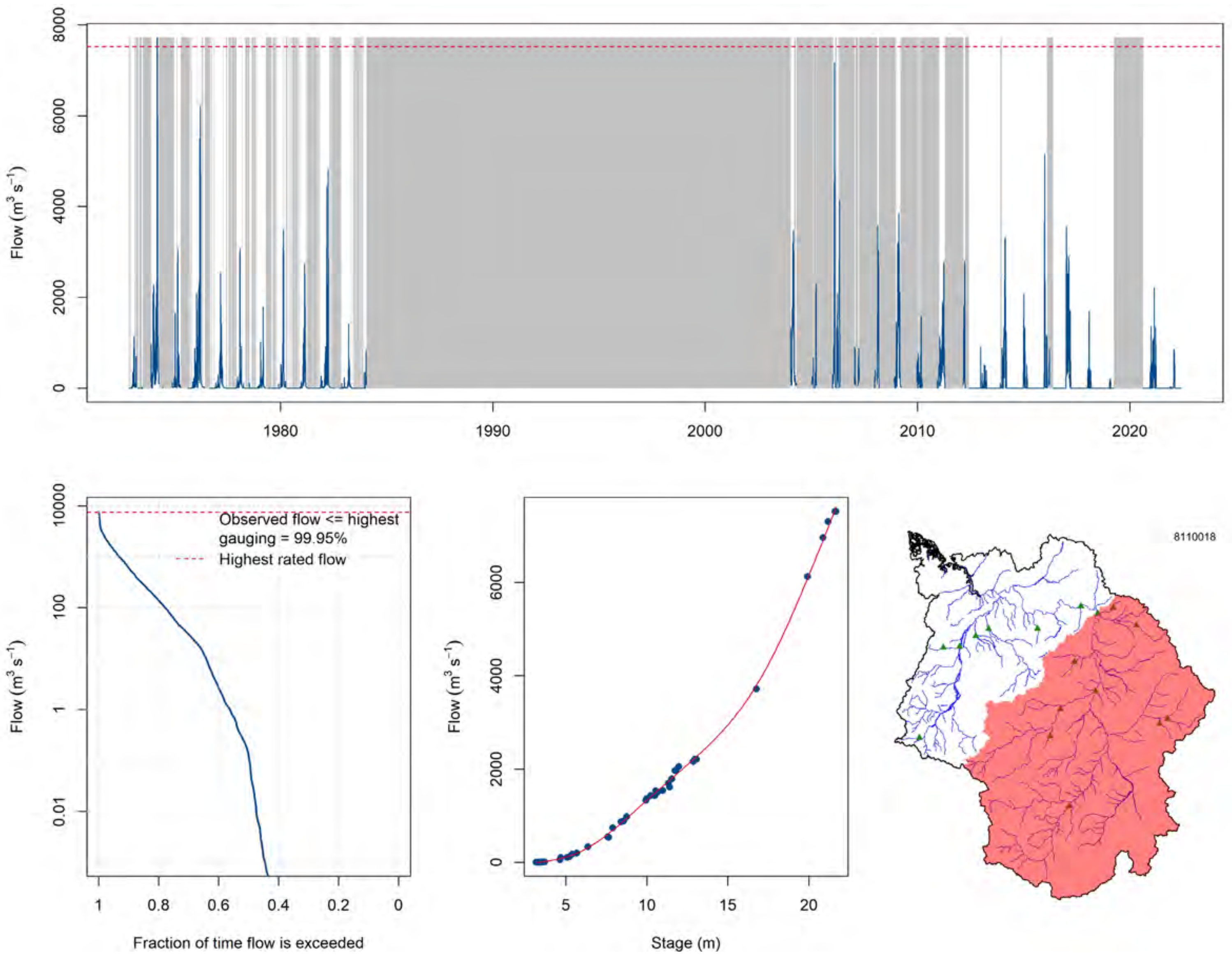


**Apx Figure C-7 Stream gauge data for site 8110018 (Victoria River at Victoria Highway). The dashed red line in the top and bottom left panel shows highest gauged point. Grey vertical lines indicate missing data**

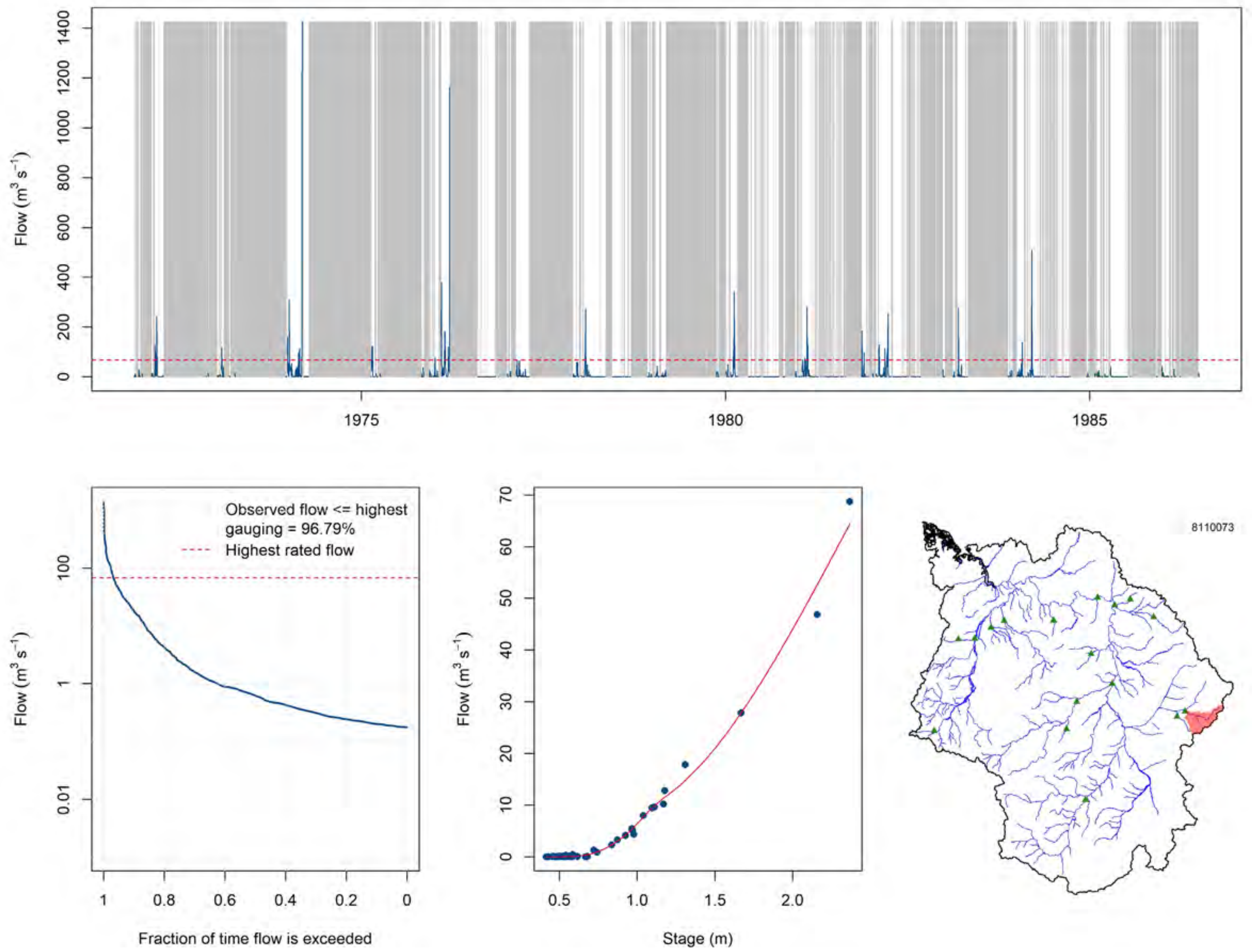


Apx Figure C-8 Stream gauge data for site 8110073 (Armstrong River near Top Springs). The dashed red line in the top and bottom left panel shows highest gauged point. Grey vertical lines indicate missing data

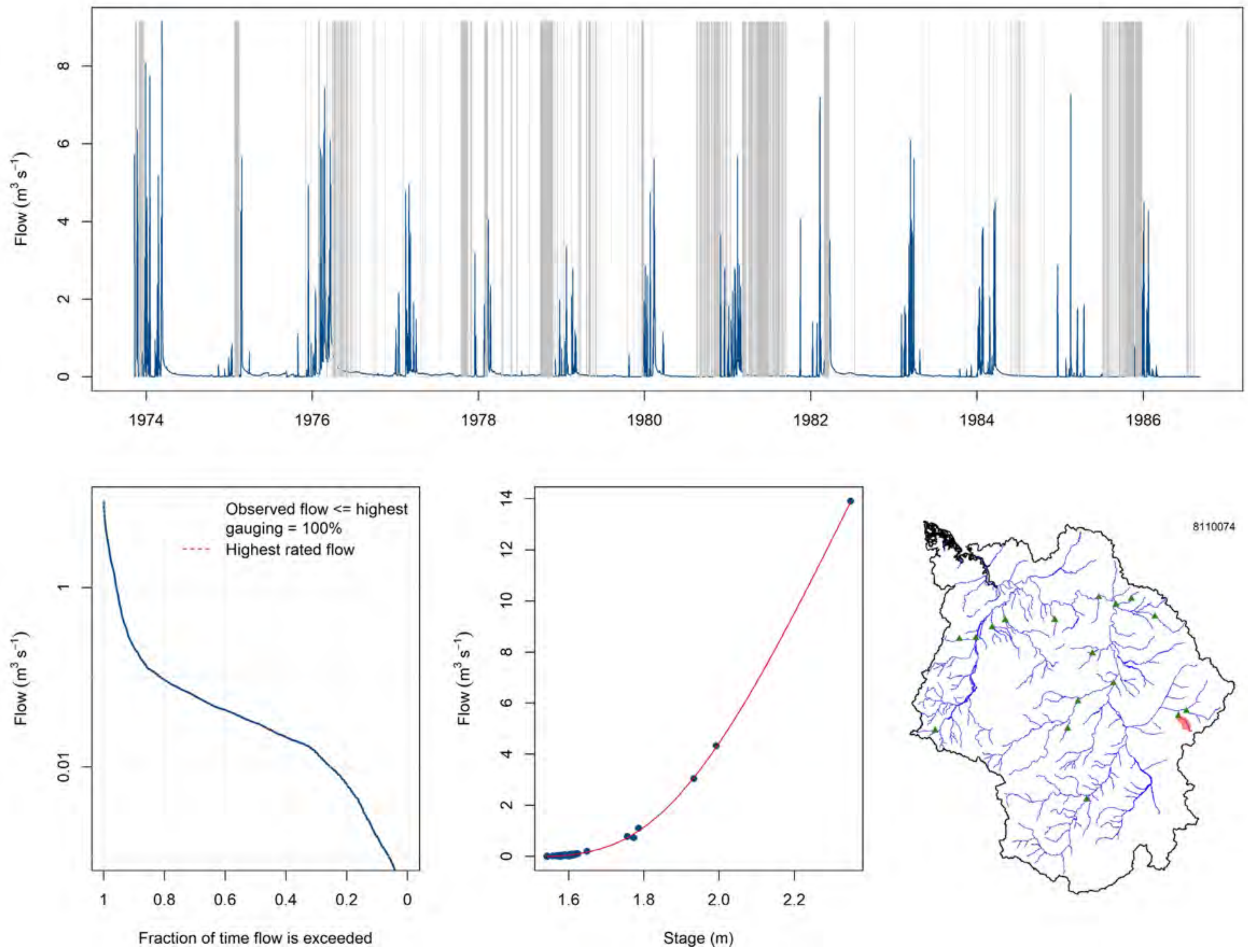


Apx Figure C-9 Stream gauge data for site 8110074 (Montejinnie Creek at Montejinni Homestead). The dashed red line in the top and bottom left panel shows highest gauged point. Grey vertical lines indicate missing data

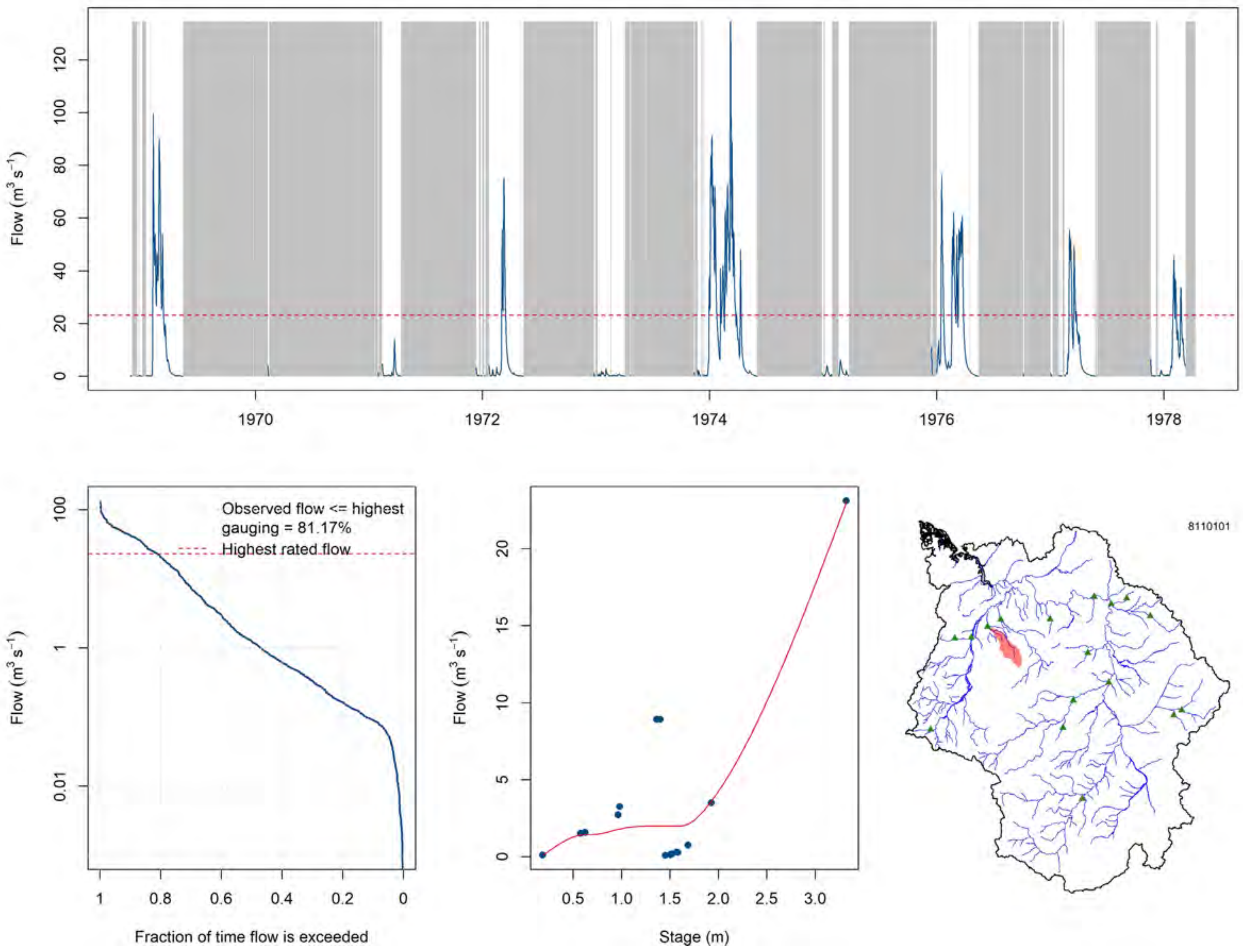


Apx Figure C-10 Stream gauge data for site 8110101 (Dick Creek at Victoria Highway). The dashed red line in the top and bottom left panel shows highest gauged point. Grey vertical lines indicate missing data

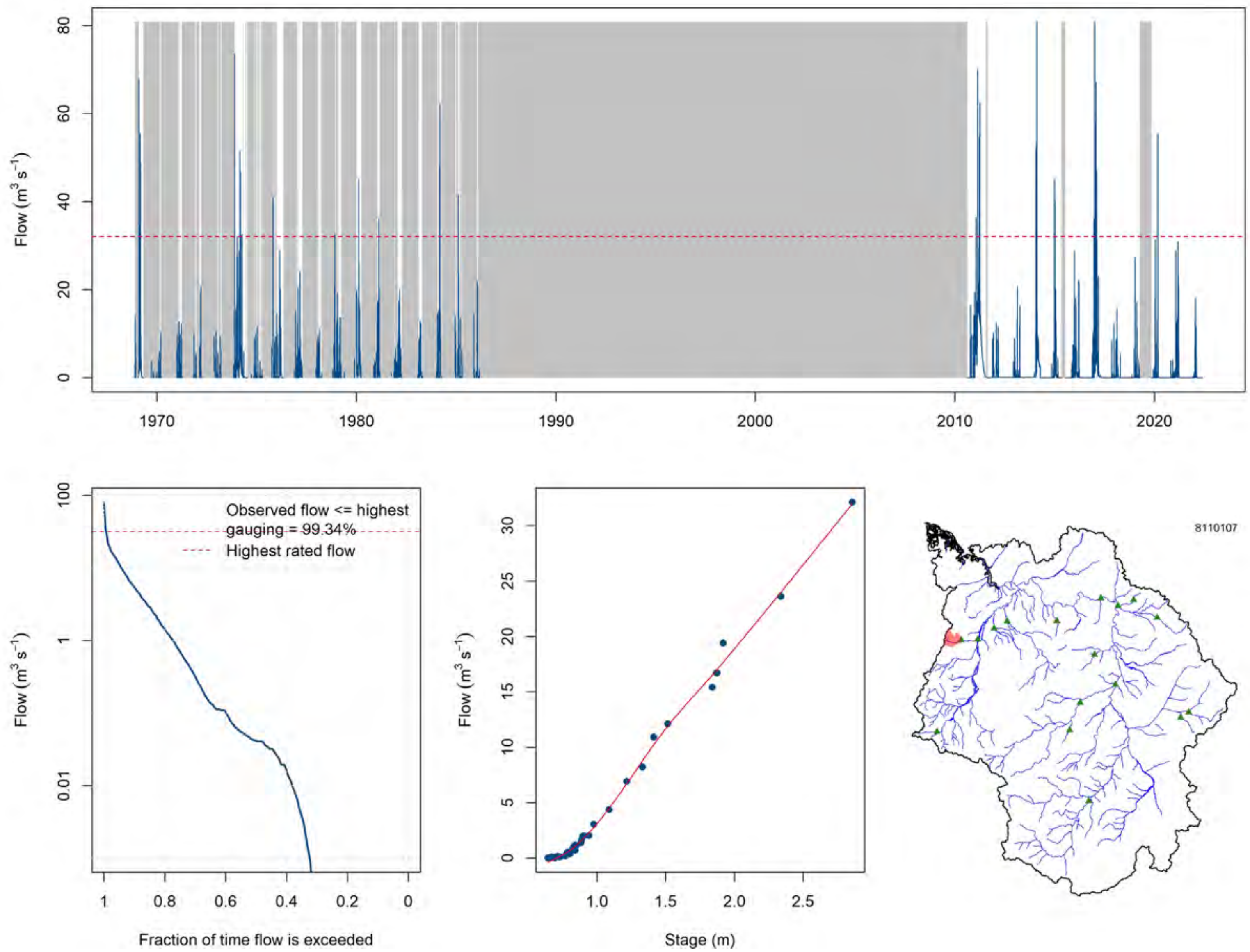


**Apx Figure C-11 Stream gauge data for site 8110107 (Saddle Creek at Victoria Highway). The dashed red line in the top and bottom left panel shows highest gauged point. Grey vertical lines indicate missing data**

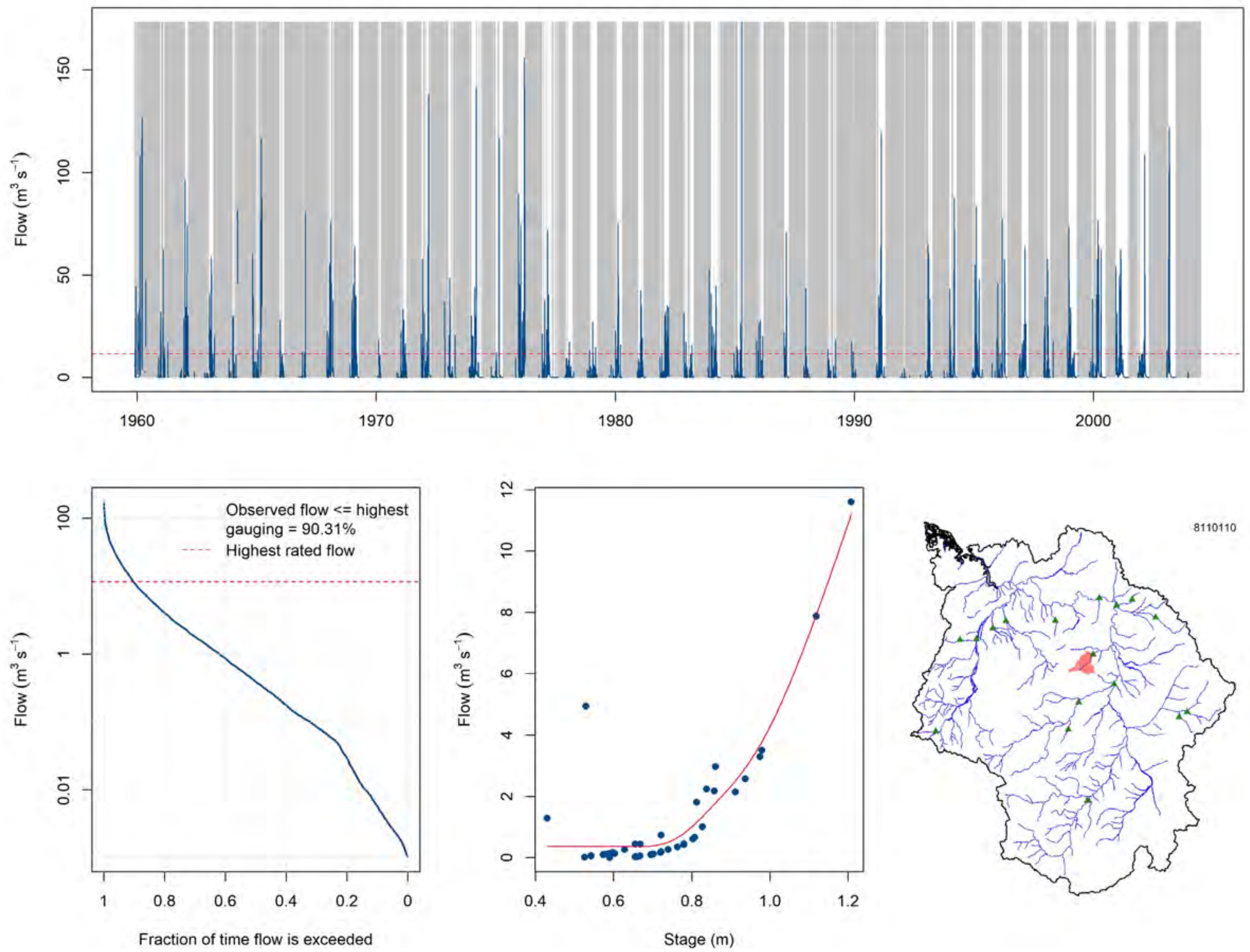


**Apx Figure C-12 Stream gauge data for site 8110110 (Surprise Creek at VRD Road crossing). The dashed red line in the top and bottom left panel shows highest gauged point. Grey vertical lines indicate missing data**

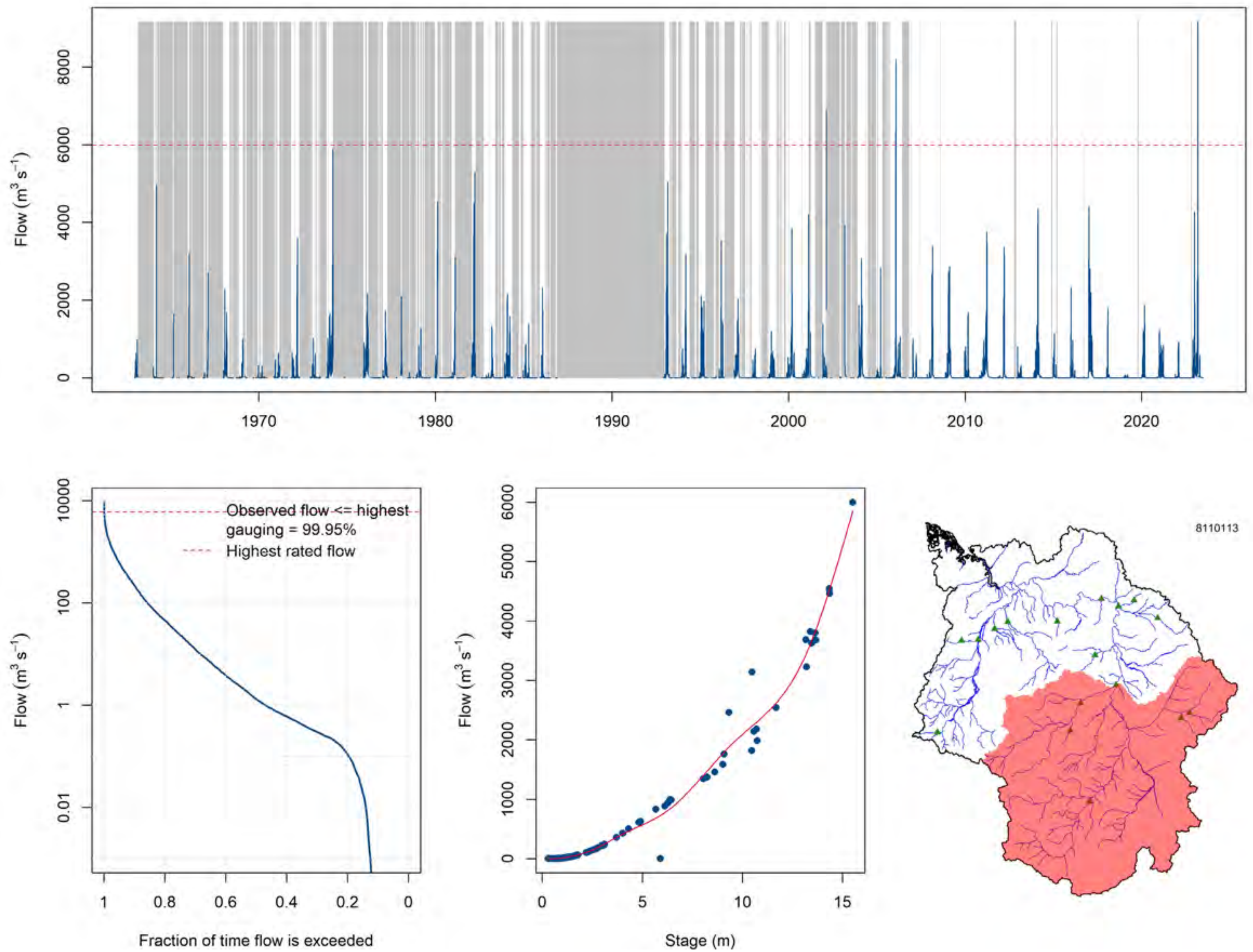


Apx Figure C-13 Stream gauge data for site 8110013 (Victoria River at Dashwood Crossing). The dashed red line in the top and bottom left panel shows highest gauged point. Grey vertical lines indicate missing data

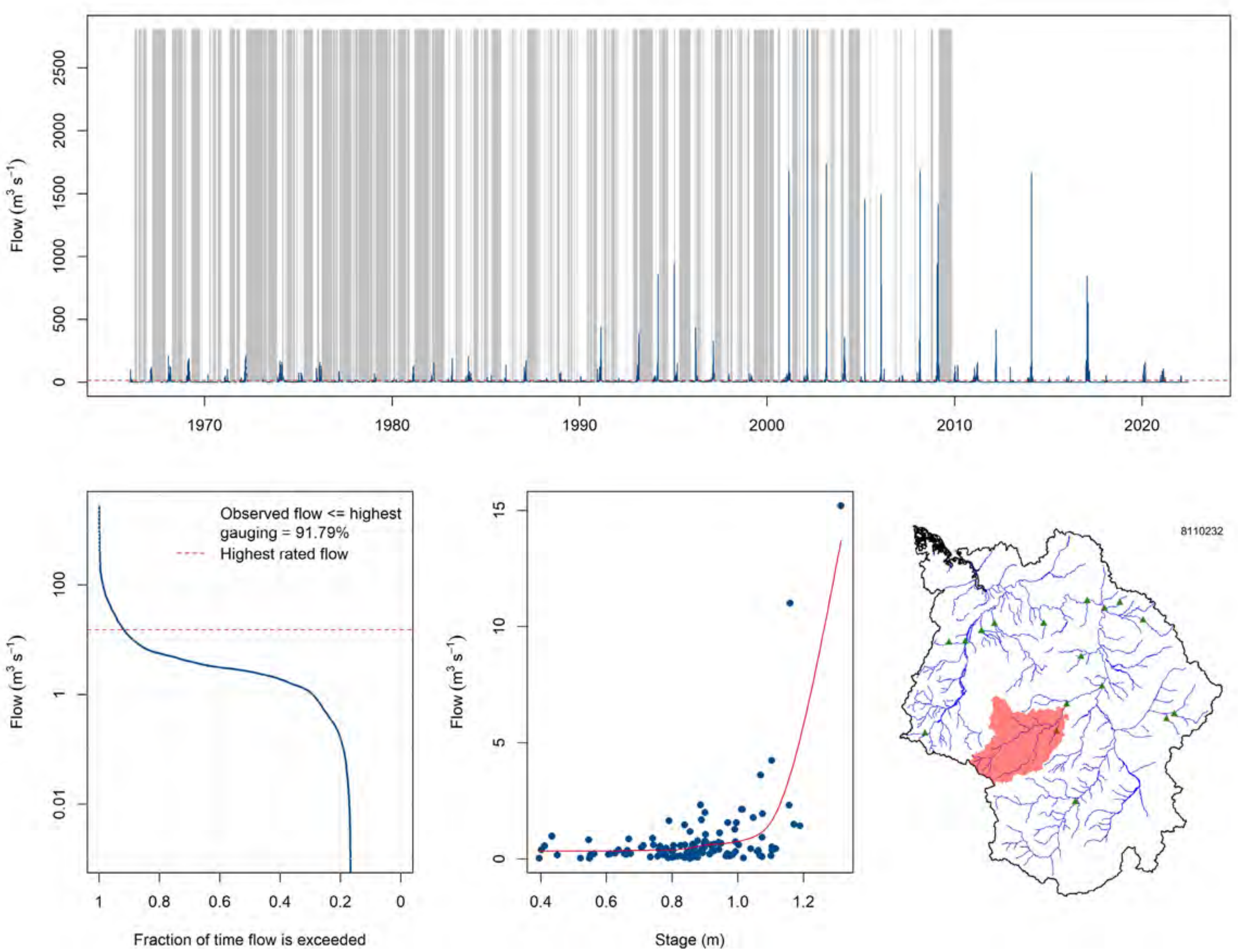


**Apx Figure C-14 Stream gauge data for site 8110232 (Wickham River at Williams Crossing). The dashed red line in the top and bottom left panel shows highest gauged point. Grey vertical lines indicate missing data**

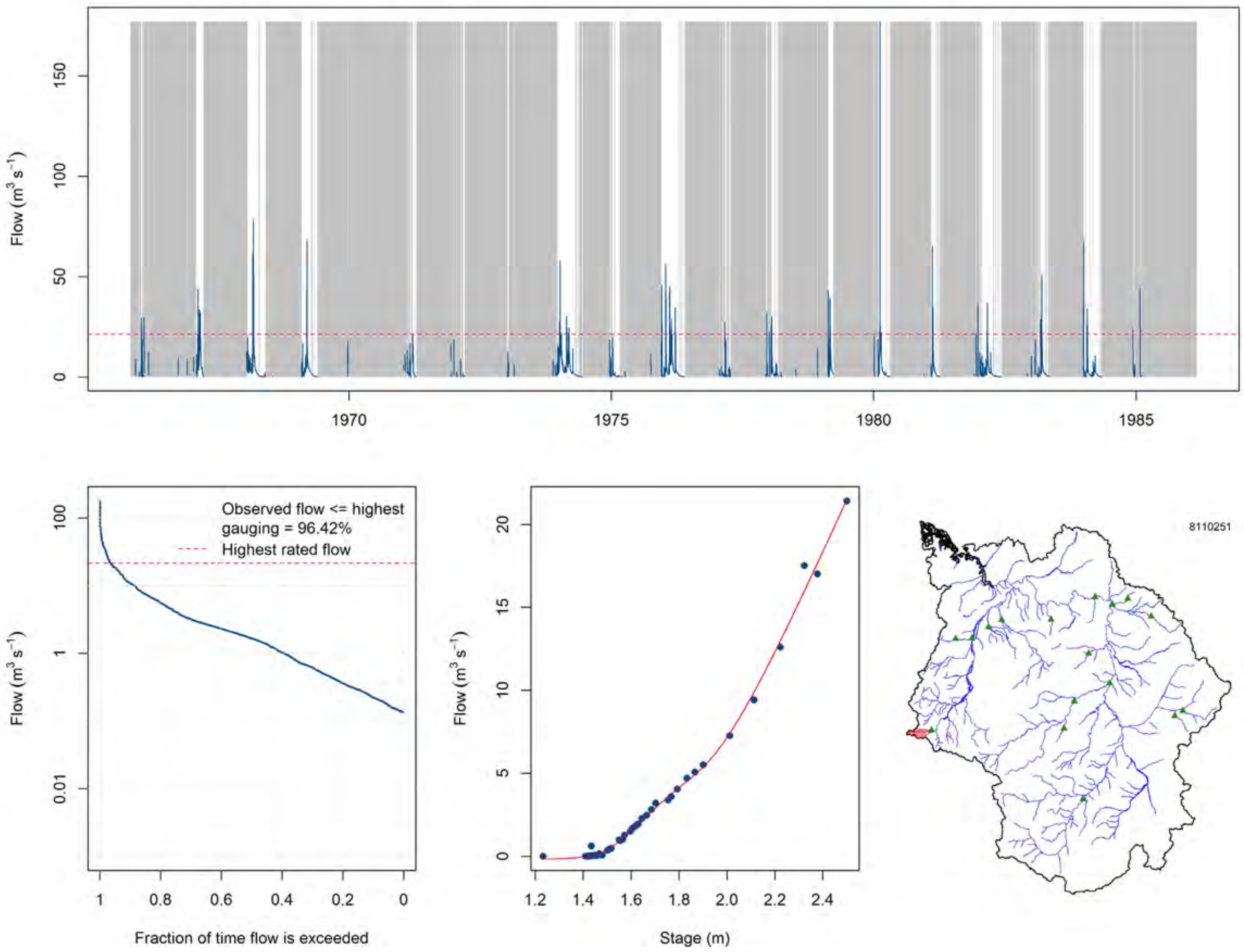


**Apx Figure C-15 Stream gauge data for site 8110251 (West Baines River at Brumby Hill). The dashed red line in the top and bottom left panel shows highest gauged point. Grey vertical lines indicate missing data**

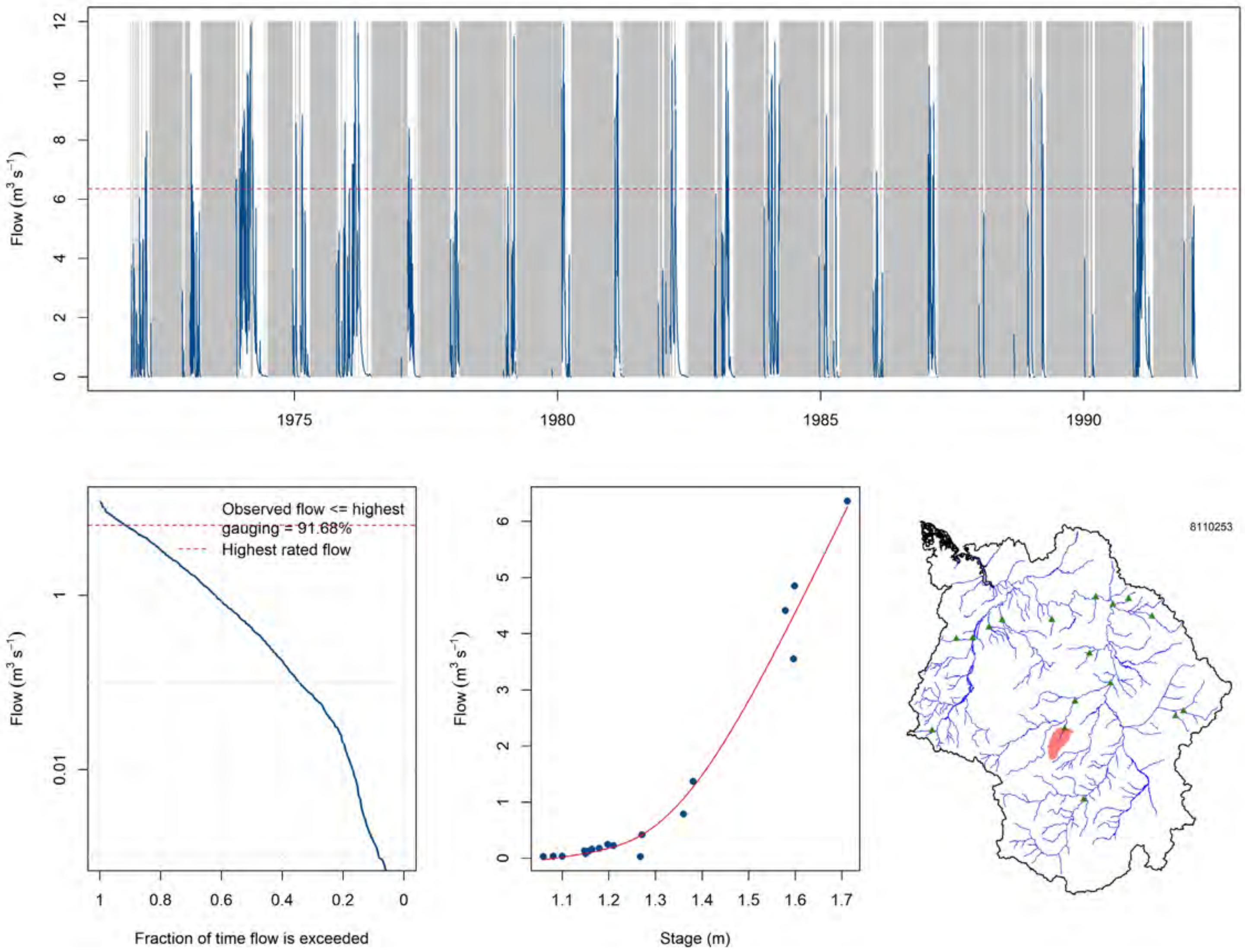


**Apx Figure C-16 Stream gauge data for site 8110253 (Gribble Creek at Wagon Wheel Hole). The dashed red line in the top and bottom left panel shows highest gauged point. Grey vertical lines indicate missing data**

# Appendix D River model benchmark plots

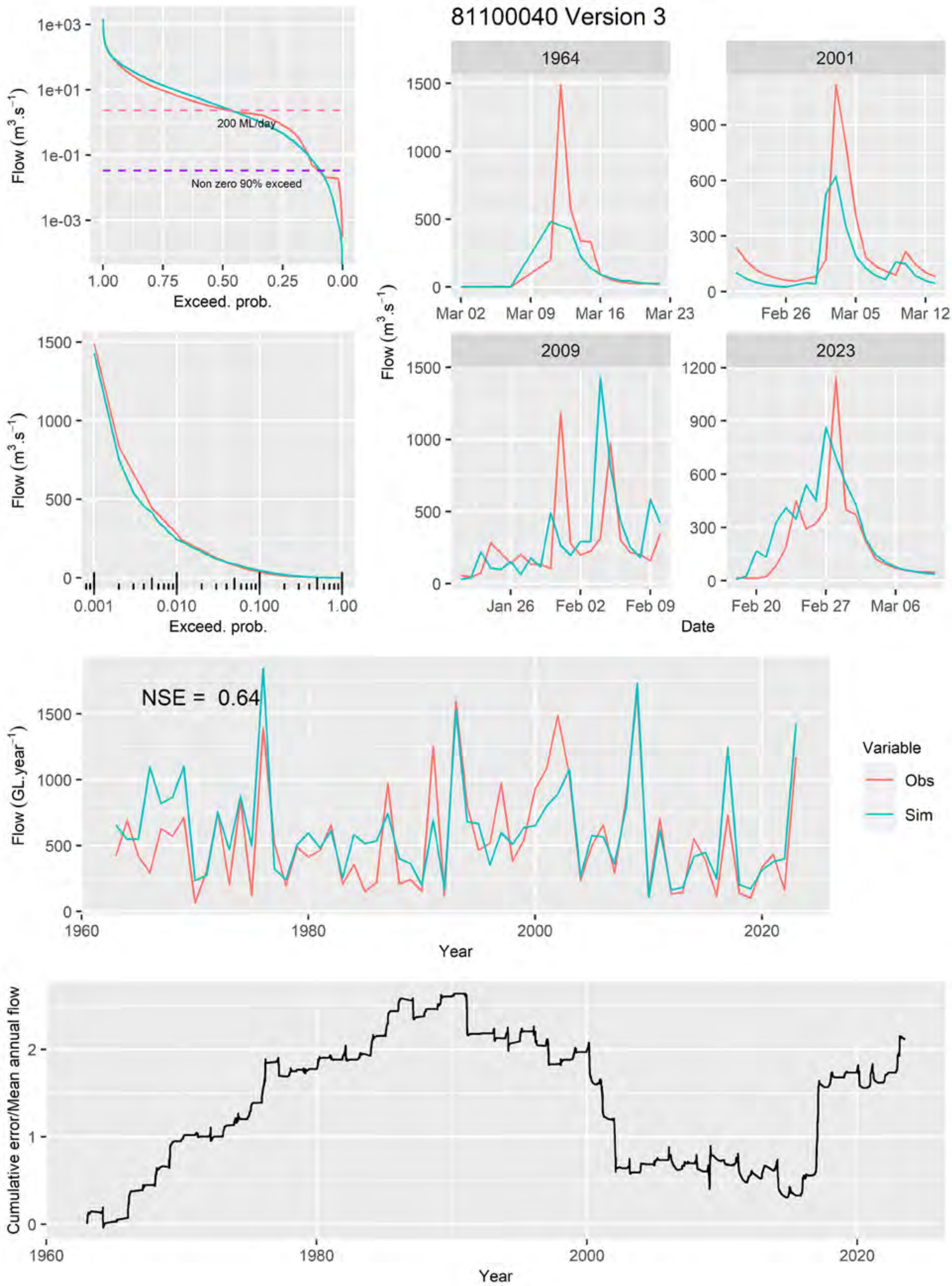


**Apx Figure D-1 Goodness-of-fit plots for node 81100040, model version 3**

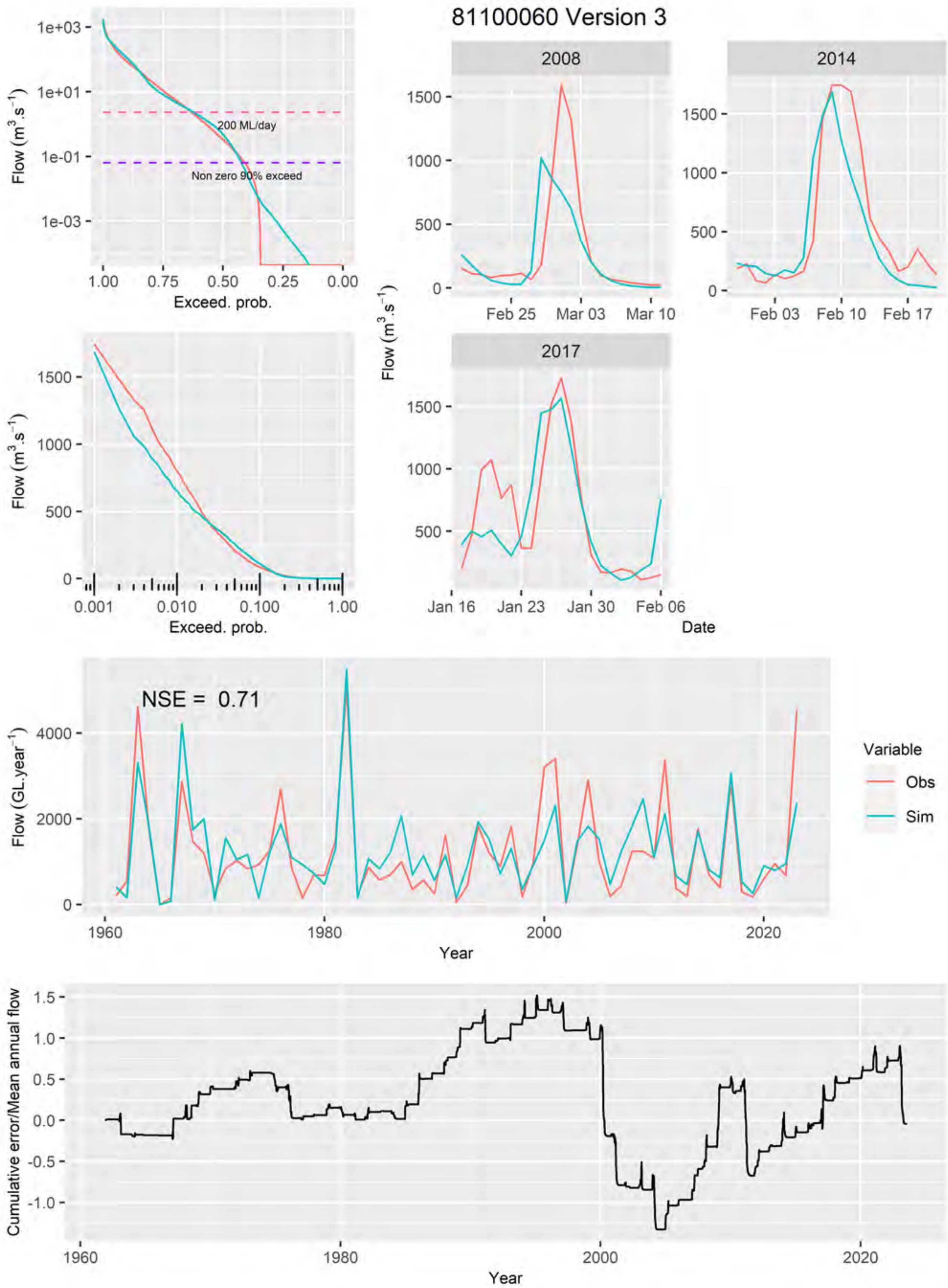


**Apx Figure D-2 Goodness-of-fit plots for node 81100060, model version 3**

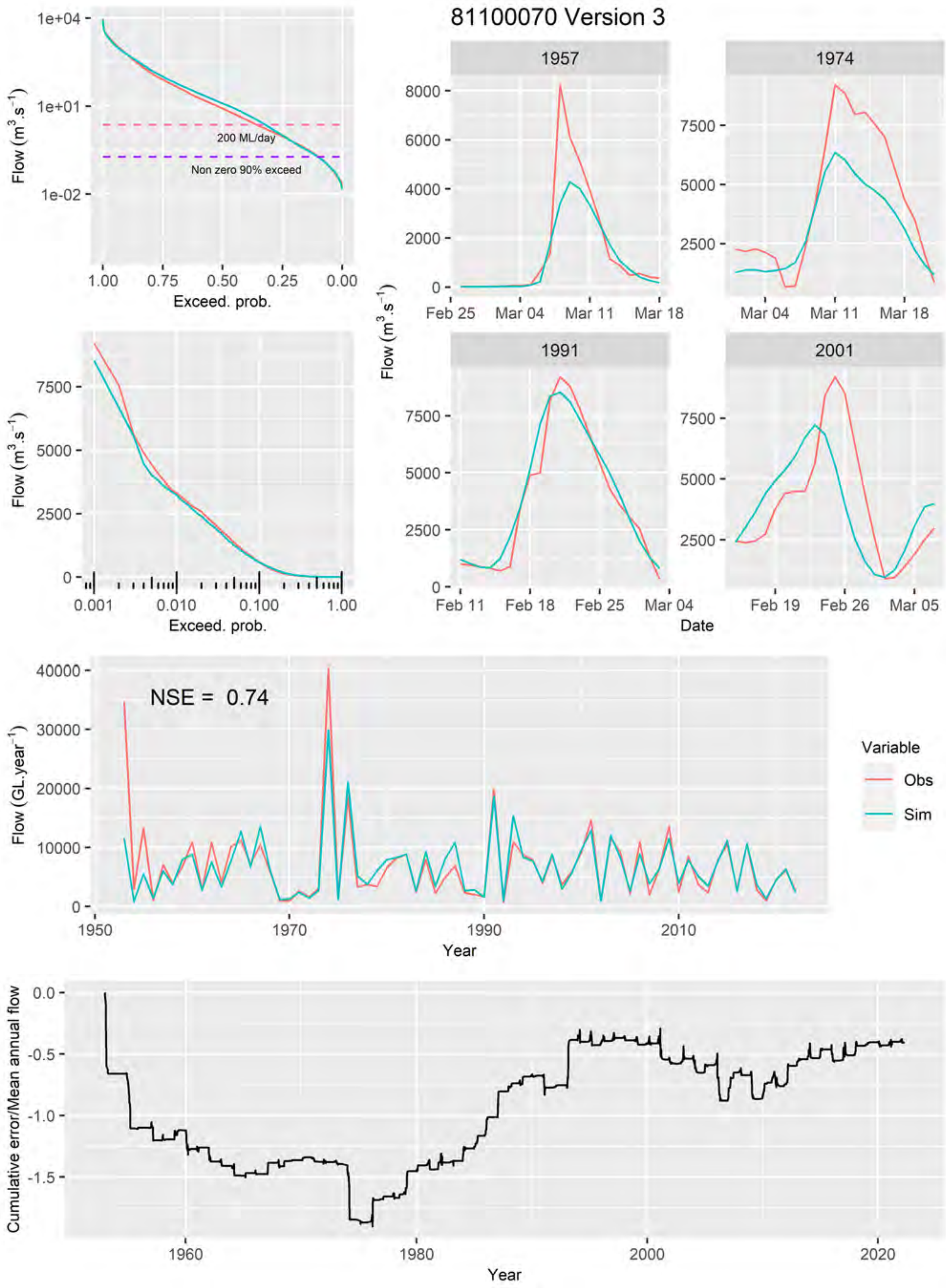


Apx Figure D-3 Goodness-of-fit plots for node 81100070, model version 3

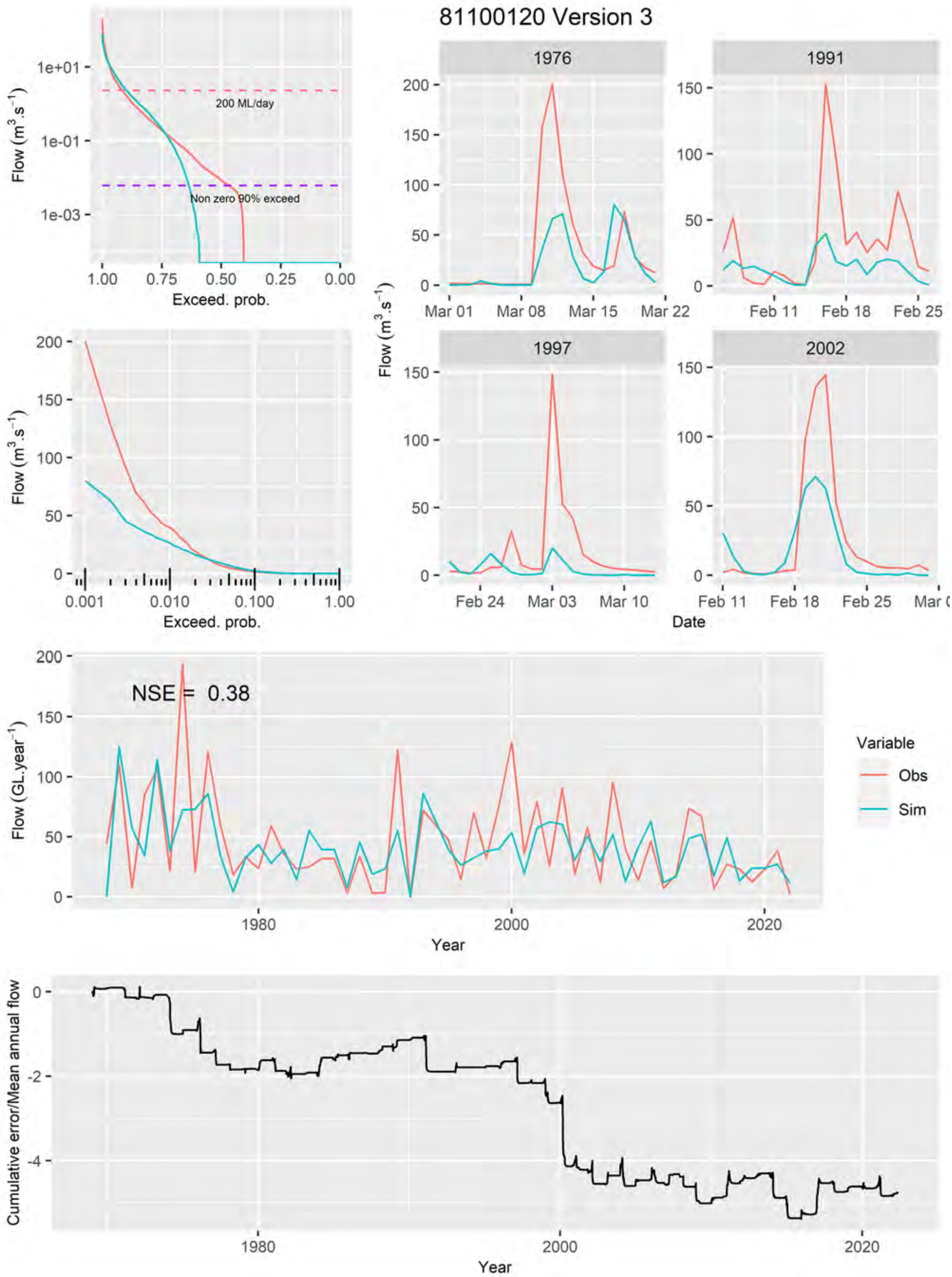


Apx Figure D-4 Goodness-of-fit plots for node 81100120, model version 3

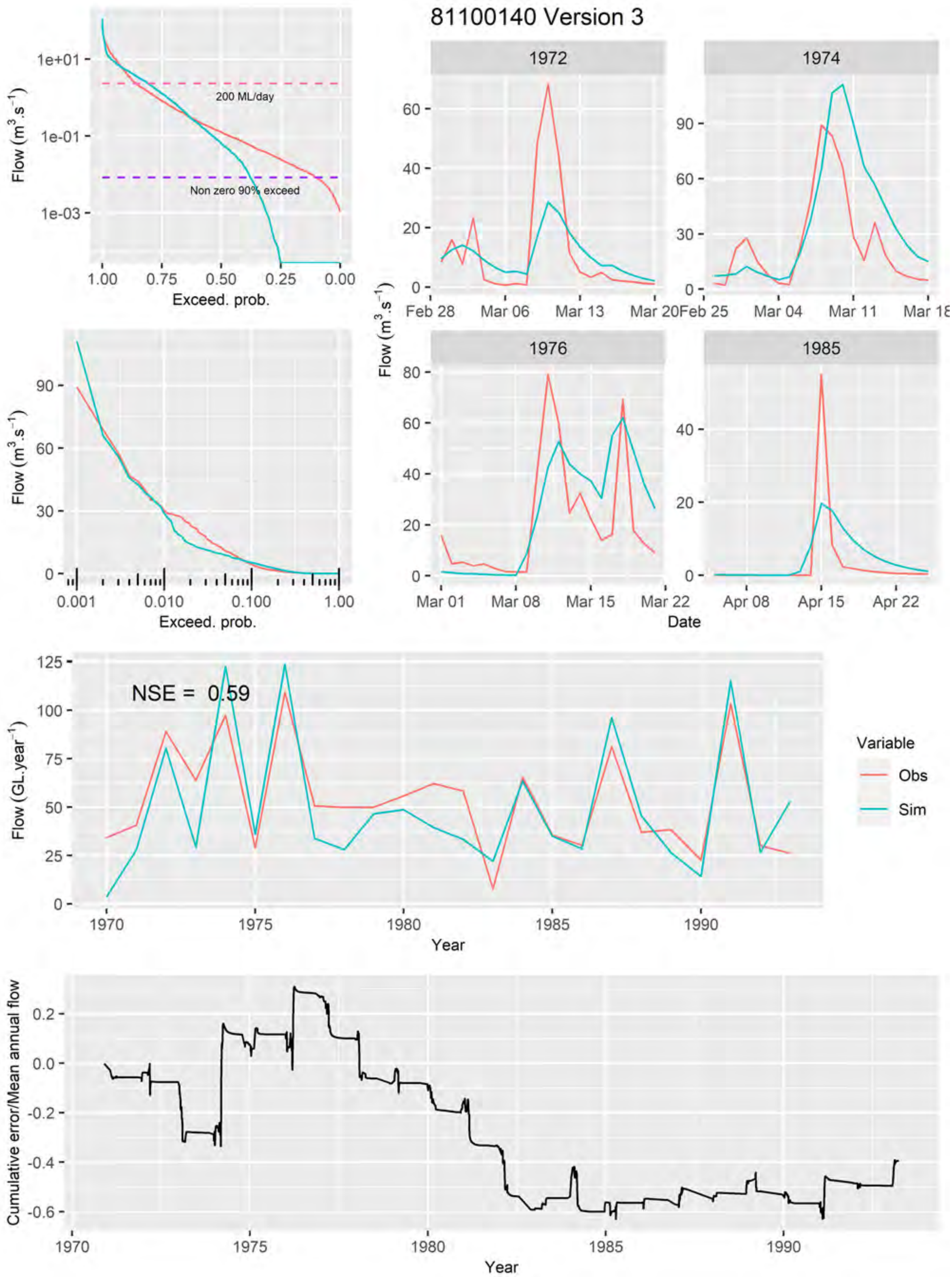


**Apx Figure D-5 Goodness-of-fit plots for node 81100140, model version 3**

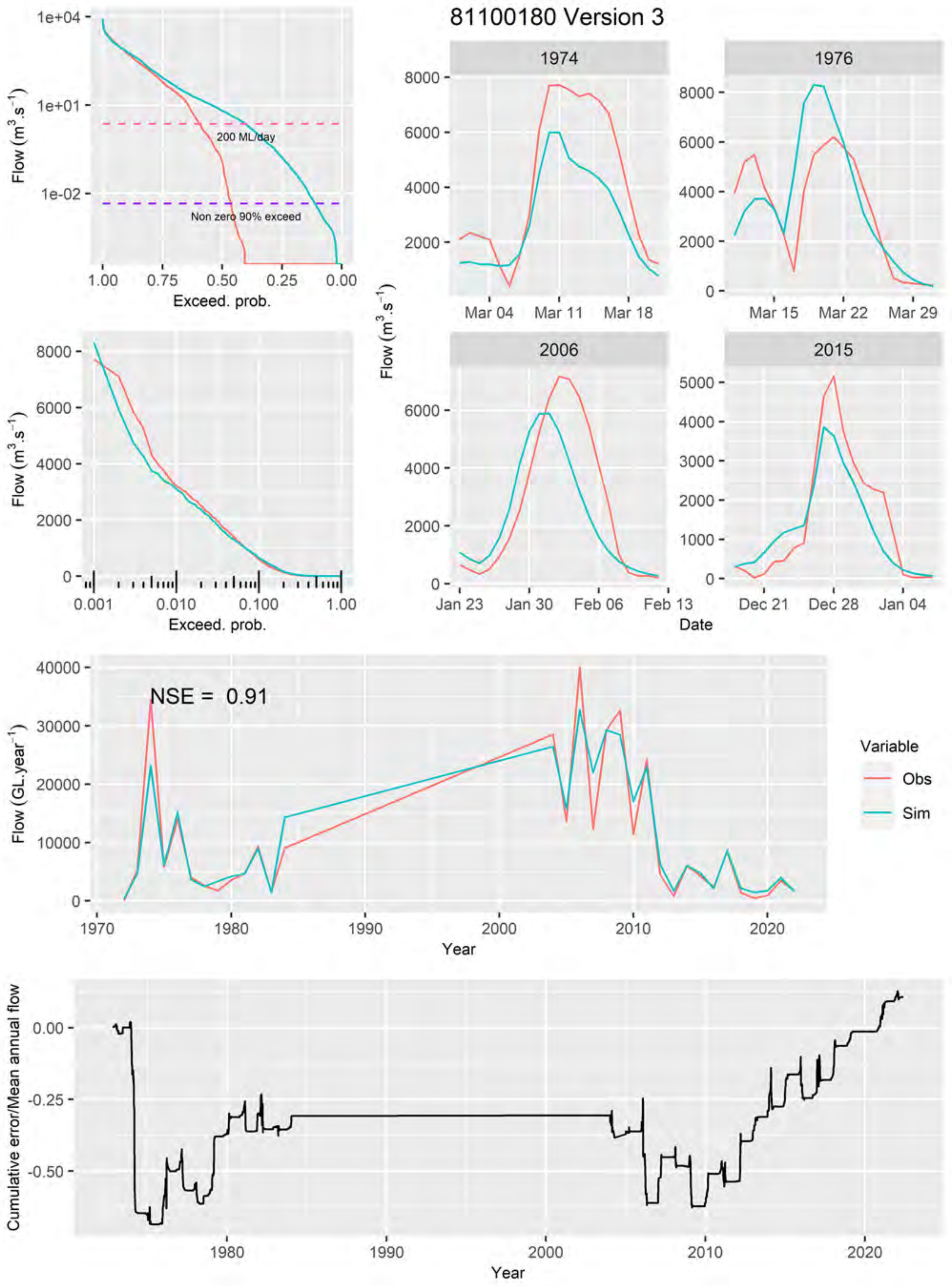


Apx Figure D-6 Goodness-of-fit plots for node 81100180, model version 3

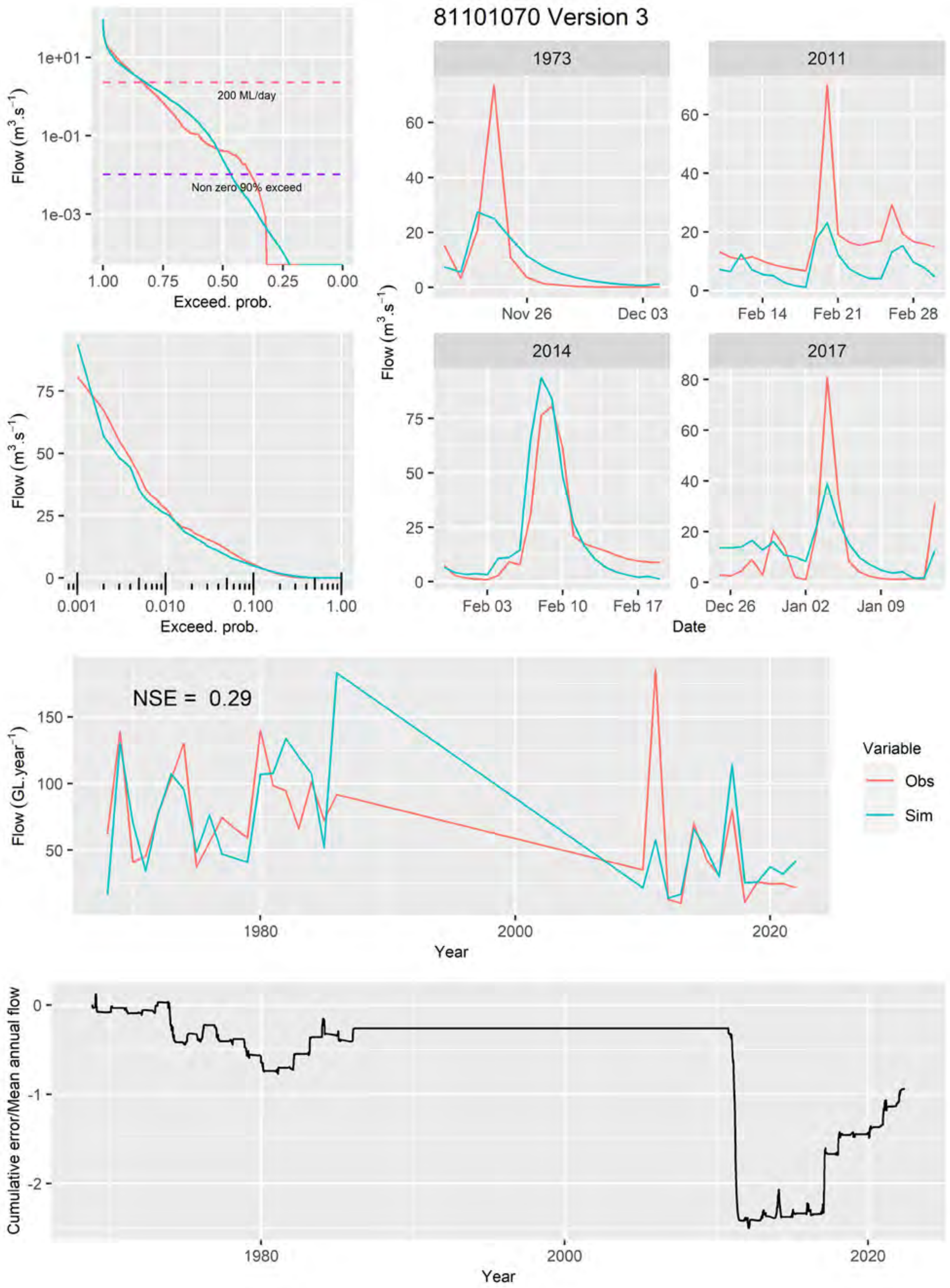


**Apx Figure D-7 Goodness-of-fit plots for node 81101070, model version 3**

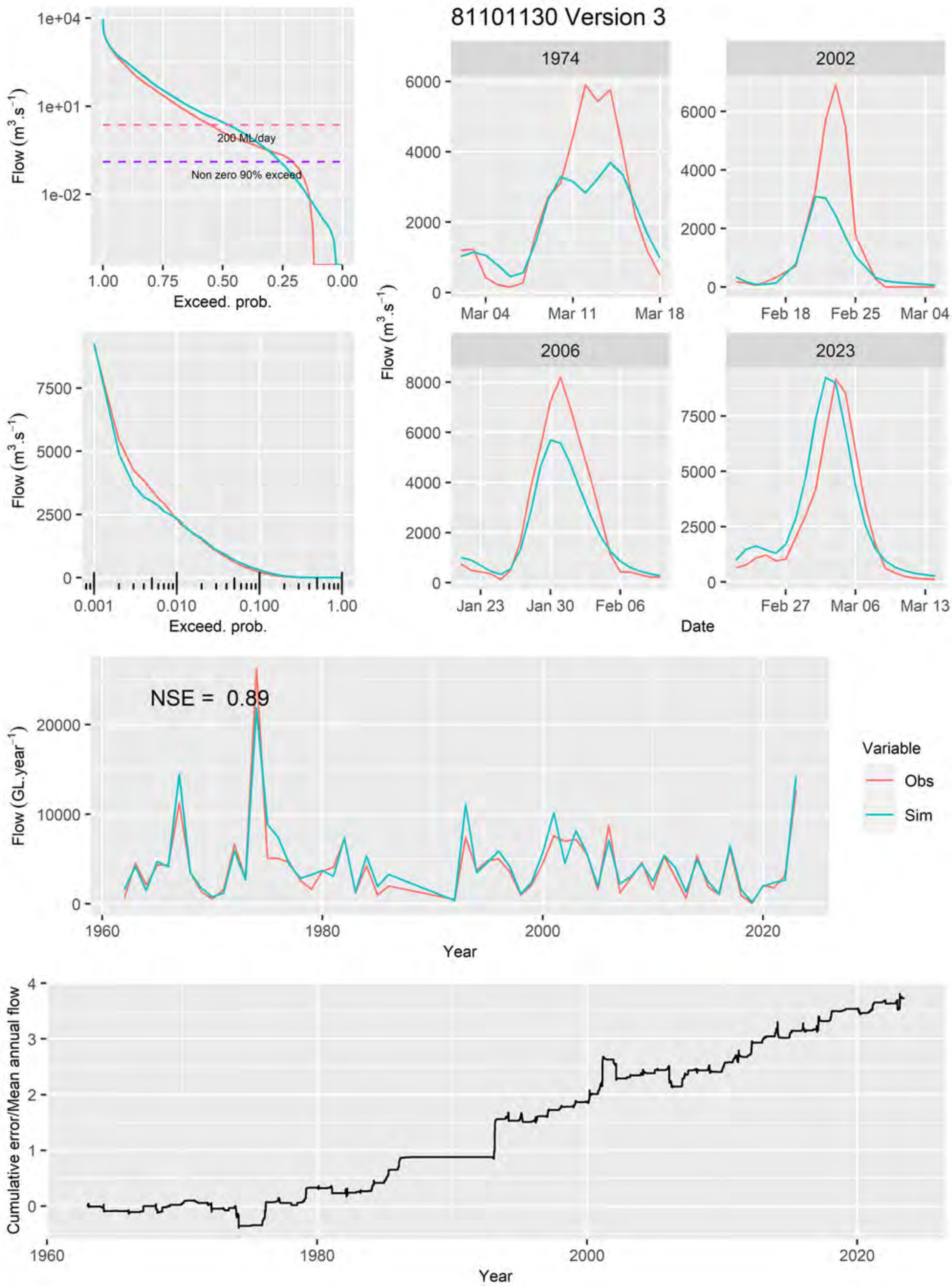


**Apx Figure D-8 Goodness-of-fit plots for node 81101130, model version 3**

**As Australia's national science agency and innovation catalyst, CSIRO is solving the greatest challenges through innovative science and technology.**

CSIRO. Unlocking a better future for everyone.


**Contact us**

1300 363 400
+61 3 9545 2176
csiroenquiries@csiro.au
csiro.au

**For further information**

**Environment**
Dr Chris Chilcott
+61 8 8944 8422
chris.chilcott@csiro.au

**Environment**
Dr Cuan Petheram
+61 3 6237 5669
cuan.petheram@csiro.au

**Agriculture and Food**
Dr Ian Watson
+61 7 4753 8606
Ian.watson@csiro.au